

METHODICAL RESEARCH AND FURTHER
DEVELOPMENT OF CAESIUM MAGNETOMETRY
FOR THE INVESTIGATION OF GEOGLYPHS
OF PALPA/NASCA, SOUTHERN PERU

Dissertation
zur Erlangung des Doktorgrades
der Fakultät für Geowissenschaften der
Ludwig – Maximilians – Universität München

vorgelegt von
Tomasz Górka

am
19. Mai 2009

Erster Berichterstatter: Prof. Dr. Valerian Bachtadse
Zweiter Berichterstatter: Prof. Dr. Heinrich C. Soffel

Tag der mündlichen Prüfung: 21. Oktober 2009

Abstract

The geoglyphs of Palpa and Nasca in southern Peru have been considered one of the greatest mysteries of archaeology (Aveni 1990). Thousands of lines, cleared fields and figures were carved on flat plateaus in the desert, the so-called pampas, during the Paracas and Nasca cultures (800 BC - 650 AD). The geoglyphs of Palpa have been studied in detail with archaeological methods since 1997 by the Nasca - Palpa Project (Reindel and Grün 2006). In the framework of this project, the first prospection with geophysical methods in the pampa was conducted in 2003 (Fassbinder and Reindel 2005). During the following field seasons five geoglyph sites in the vicinity of Palpa were chosen that had previously been documented through a combined field survey and analysis of high resolution aerial images (Lambers 2006). Since the geoglyphs of Palpa and Nasca have been declared the UNESCO World Heritage, the best non-destructive technique of site exploration to detect and map possible features beneath the trapezoids, turned to be the magnetic prospecting.

So far, magnetometry has rarely been used for archaeological surveying in South America. As the magnetic inclination in Palpa is less than 3° and the intensity of the total Earth's magnetic field hardly exceeds 25.000 Nanotesla, the highly sensitive total field caesium magnetometer (Scintrex SmartMag SM4G-Special), to be used during fieldwork, needed to be adapted to these conditions. In addition, geochemical processes forming iron oxides in soil, which usually cause clear magnetic anomalies, could not be expected there because of the lack of precipitation. On the contrary, due to the shallow inclination of the Earth's magnetic field, simple anomalies created more complicated patterns, which were difficult to interpret. To overcome this problem and to enhance the visibility of magnetic data, two sensors were arranged in a horizontal gradiometer configuration. The application of the magnetometer in such an arrangement, in combination with magnetic total field data, allowed to enhance the visibility of archaeological features in a region close to the magnetic

equator. This enabled to trace the older geoglyphs that had been obliterated during the gradual surface clearing carried out on the same sites in Nasca times.

The present study reports on the results of the magnetic prospecting on five large geoglyph complexes located on the pampas to the north, east, west and south of Palpa. Most of these places were in use during several centuries and developed in time (Lambers 2006). The sites were enlarged or remodelled, which led to the destruction of older lines by the trapezoids. During their construction the stones between the existing lines were removed, which efficiently wiped out the older lines from the surface. The magnetic images clearly revealed the course of those lines on all five investigated sites.

It is believed that the older lineal geoglyphs are visible in the magnetograms due to their heavily compacted surface, which was caused by people frequently walking over them in the course of ritual activity taking place on geoglyph sites. This compaction destroyed the vesicular horizon of exposed loess sediments and its remanent magnetization. On the contrary, the large trapezoids constructed later did not confine movement of people over them, so their surface is generally less compacted. For this reason, the older lines are visible in the magnetograms even though their cleared surface resembles that of the trapezoids.

Apart from the geoglyphs, the magnetic measurements showed anomalies that may be interpreted as traces of buildings, postholes, pits or other man-made structures. The relation of these features to the geoglyphs has been also investigated.

In conclusion, the magnetic surveying not only shed new light on the development of large geoglyph complexes over time but also on the understanding of the Paracas and Nasca cultures and the history of the region in general. Without destruction and excavation, magnetometry has thus proven to be a powerful method for studying geoglyph stratigraphy.

Contents

Abstract	<i>I</i>
Contents	<i>III</i>
Chapter 1 Introduction	<i>1</i>
1.1 Preface	<i>1</i>
1.2 Foreword to project	<i>2</i>
1.3 Objectives and main tasks	<i>3</i>
Chapter 2 Palpa Geoglyphs and Their Archaeological Setting	<i>5</i>
Chapter 3 Area of Research	<i>10</i>
2.1 Location	<i>10</i>
2.2 Climatic conditions of coastal Peru and their influence on Pre-Columbian cultures	<i>13</i>
2.3 Geographical and Geological Setting	<i>15</i>
Chapter 4 Basics of Magnetism in Reference to Archaeological Prospecction	<i>17</i>
4.1 Magnetic field of the Earth	<i>17</i>
4.2 Magnetic susceptibility and magnetic minerals	<i>18</i>
4.3 Magnetic remanence	<i>20</i>
4.4 Magnetic anomalies on archaeological sites	<i>21</i>
4.5 Soil magnetism on archaeological sites	<i>25</i>
4.5.1 Magnetic enhancement mechanisms	<i>26</i>
4.5.2 Soil magnetism on geoglyph sites	<i>27</i>
4.6 Time variations in the Earth's magnetic field	<i>28</i>
Chapter 5 Methodology	<i>30</i>
5.1 Instrumentation and sampling procedure	<i>30</i>
5.2 Data acquisition and processing	<i>35</i>
5.3 Presentation and interpretation of results	<i>39</i>
5.3.1 Presentation of results	<i>39</i>
5.3.2 Interpretation of results	<i>40</i>
5.4 Common laboratory procedures in this work	<i>42</i>
Chapter 6 Results of geophysical prospecting on site PP01-36 "Llipata"	<i>43</i>
Chapter 7 Results of geophysical prospecting on site PV67A-15/16 "Yunama"	<i>56</i>
Chapter 8 Results of geophysical prospecting on site PV67A-47 "Sacramento"	<i>69</i>
Chapter 9 Results of geophysical prospecting on site PV67B-55 "Carapo"	<i>86</i>
Chapter 10 Results of geophysical prospecting on site PP01-49 "San Ignacio"	<i>96</i>
Chapter 11 Synopsis	<i>104</i>
Chapter 12 Last Word and Conclusions	<i>107</i>
References	<i>109</i>
List of figures	<i>117</i>
List of tables	<i>123</i>
Acknowledgments	<i>124</i>
Curriculum Vitae	<i>126</i>

Chapter 1

Introduction

1.1. PREFACE

Magnetic investigations have long been a source of productive interaction between archaeology and geophysics (Aitken 1974). Together with resistivity survey they are one of the earliest applications of geophysical prospecting and are nowadays well established as a standard method for archaeology (Linington 1970). Although numerous techniques of geophysical surveying have been applied to site exploration, it was magnetometry that happened to be the most important way in which physics has been involved in archaeological research. Such fusion formed a new scientific area, which essentially grew out of the numerous interdisciplinary studies involving highly sophisticated technical methods for detecting and mapping otherwise not accessible archaeological features. This relatively new science, frequently termed as *archaeological prospecting*, has well developed into a separate scientific discipline with its own specialities, in which almost all the techniques were initially derived from methods used in geological geophysical prospecting and conventional aerial survey (Scollar et al. 1990). This combination of archaeology, aerial photography, remote sensing, and geophysics has been accurately described by Anthony Clark (1990):

[...] archaeological prospecting, which can be uncomfortable and tedious, is the romance and enduring excitement of this peculiarly civilized detective work – restoring to visibility the settlements of long-forgotten people who also knew our lands, by means of technology beyond their dreams. (Clark 1996)

1.2. FOREWORD TO THE PROJECT

The geoglyphs of Palpa/Nasca are the geometrical and biomorphic figures drawn on the desert surface by pre-Columbian cultures in Southern Peru (Figure 1.1; compare Chapter 2). They have been studied in detail with archaeological methods since 1997 by the Nasca - Palpa Project (Reindel and Grün 2006) supported by the Swiss-Lichtenstein Foundation for Archaeological Research Abroad (SLSA) and the German Federal Ministry of Education and Research (BMBF). In the framework of the sponsoring program “NTG – New Scientific Methods and Technologies in Humanities”, the first prospecting with geophysical methods has been conducted in the year 2003 (Fassbinder and Reindel 2005) as a result of the cooperation between Bavarian State Department of Monument and Sites (BLfD Munich) and the German Archaeological Institute, Commission for Archaeology of Non-European Cultures (KAAK DAI Bonn).



Figure 1.1. Reloj Solar (Sun Dial) - geoglyph complex located on the southern slope of Cresta de Sacramento, north of Palpa; source – DAI: http://www.dainst.org/index_593_de.html

Since the geoglyphs of Palpa and Nasca have been declared a UNESCO World Heritage site, the geophysical prospecting was the only none-destructive technique of site exploration apart from aerial archaeology, and the main tool to detect and map possible unknown features beneath the lines and trapezoids. Therefore, during the following field

seasons, in joint effort with BLfD, geophysicists from the Department of Earth and Environmental Sciences of the Ludwig Maximilian University Munich, have measured approximately 60 Ha of studied project territory covering entirely five foremost geoglyph complexes.

1.3. OBJECTIVES AND MAIN TASKS

The general aim of the Nasca – Palpa project was the study of the cultural and palaeoenvironmental history of the Palpa region on the Peruvian southern coast. By means of surveying, mapping, excavations and geoarchaeological research, a systematic documentation of the cultural heritage (among others geoglyphs) was pursued to establish a basis for scientific investigation of the cultural history. Various survey and dating methods and technologies were developed, enhanced, as well as tested under different conditions. Through the applications of these methods, archaeologists and natural scientists cooperated closely working on the reconstruction of life and environment of the past cultures of the region (http://www.dainst.org/index_593_de.html on 21.03.2008).

Most of the geoglyph complexes were in use during several centuries and grew considerably over time, new drawings were frequently added and existing ones enlarged or remodelled. In this process, large trapezoids often covered older lines. During their construction the stones of the desert pavement between the existing lines were removed, making the older lines invisible on the surface. Therefore, the major objective was:

- the detection and interpretation of obliterated archaeological structures within the trapezoidal figures, in particular the disclosure of the course of the previous linear patterns.

The enhancement of the magnetic sensitivity of the measuring device in relatively unfavourable geophysical conditions on Peruvian sites, in addition to the improvement of the fieldwork methods for further application in Europe, became the main technical aim. It was based on the identification of the differences in the measurements of the archaeological anomalies on the example of these two unlike environments. From the archaeological point of view, the most important reason of geophysical contribution was the assistance in systematic documentation of cultural heritage and recognition of the complete

chronology of the Peruvian southern coast. This was coupled with the primary goal of the project – the preservation of one of the most important South American archaeological monument complexes.

In order to achieve the given objectives, a number of tasks had to be completed in due course of the considered research activities. The most important ones are briefly summarized as follows:

- Improvement of the new magnetometer system for archaeological prospecting, which implied the further development of the commercial geophysical device (Scintrex Smartmag SM4G) for data collection in the field. It was combined with the adjustment of the instrument to the archaeological applications in the region of geomagnetic inclination close to the limits of operating zone of the apparatus (2° to 86° based on the specifications of CS3 sensor, Scintrex, Ltd.).
- Development of new digital image processing techniques for the more precise and accurate interpretation of magnetic anomalies (for information on magnetic anomalies see Chapter 4.4).
- Assessment of the specific measurement conditions in Peru (in comparison to Europe) and resulting dissimilarities in the size and shape of anomalies due to the shallow inclination of the local geomagnetic field.
- Application of the caesium magnetometer to the geoglyphs and execution of series of measurements on site, covering most significant complexes in the vicinity of Palpa, during several annual field campaigns.
- Study of the archaeological setting of Paracas and Nasca cultures and the geoglyphs background, for the better understanding of archaeological structures on site and resulting variations in magnetic images.
- Data processing and visualisation work on the collected data set using series of highly developed computer programs.
- Interpretation by the combination of geophysical results with the archaeological knowledge.

Chapter 2

Palpa Geoglyphs and Their Archaeological Setting

The Geoglyphs of Nasca and Palpa in southern Peru have been considered one of the greatest mysteries of archaeology (Aveni 1990). Over an area of several hundred square-kilometers, on flat plateaus called "pampas", ancient civilizations have carved an array of over thousand geometrical and biomorphic figures of varying size and precision into the earth. Lines several kilometers long, rectangles and trapezoids several hectares large, human figures on hillsides, and huge depictions of animals and plants were drawn on the desert surface already in prehispanic times during the Paracas and Nasca cultures (800 BC - 650 AD) (Grün et al. 2000; Sauerbier and Lambers 2003; Lambers 2006) (Table 2.1).

Unfortunately, the understanding of geoglyphs has been hindered for a long time by the lack of an accurate documentation (Sauerbier and Lambers 2003). Ever since the first report in 1927 by Peruvian archaeologist Toribio Mejía Xesspe, serious archaeological investigations have by far been outnumbered by unscientific interpretations. Additionally, the whole Palpa area of the Nasca basin and the geoglyphs located in its close proximity have been largely ignored by archaeological researchers, although they are comparable in quality and complexity to the better known ones on the Nasca pampa. There has also been a lack of public interest in them and little or no protection, although they are part of the same cultural phenomenon (Lambers 2006). For those reasons as well as for the fact that in this area geoglyphs are located close to densely settled zones along the valley floors, which makes it an easier place to study the relationships between two classes of cultural remains (Lambers 2006), the Palpa region was chosen as the new area of interdisciplinary geoglyph investigation.

The Nasca drainage provide many suitable spots to place geoglyphs. It is restricted by the foothills of the Andes to the northeast and by the coastal mountain range to the southwest. This unique topographic feature which led to the development of a large basin and later a vast sediment plain (Chapter 3.3 – Geographical and Geological Setting), proved to be crucial for the creation of these remarkable drawings.

In order to construct a geoglyph on flat plateaus, darkly oxidized stones of the natural desert pavement were removed and heaped along the border of the cleared area, thereby revealing a bright layer of sand and silt standing out in strong contrast to the surrounding undisturbed surface. Piling the dark stones up at another place considerably enhanced the contrast in color and brightness between the original and altered surface (Lambers 2006).

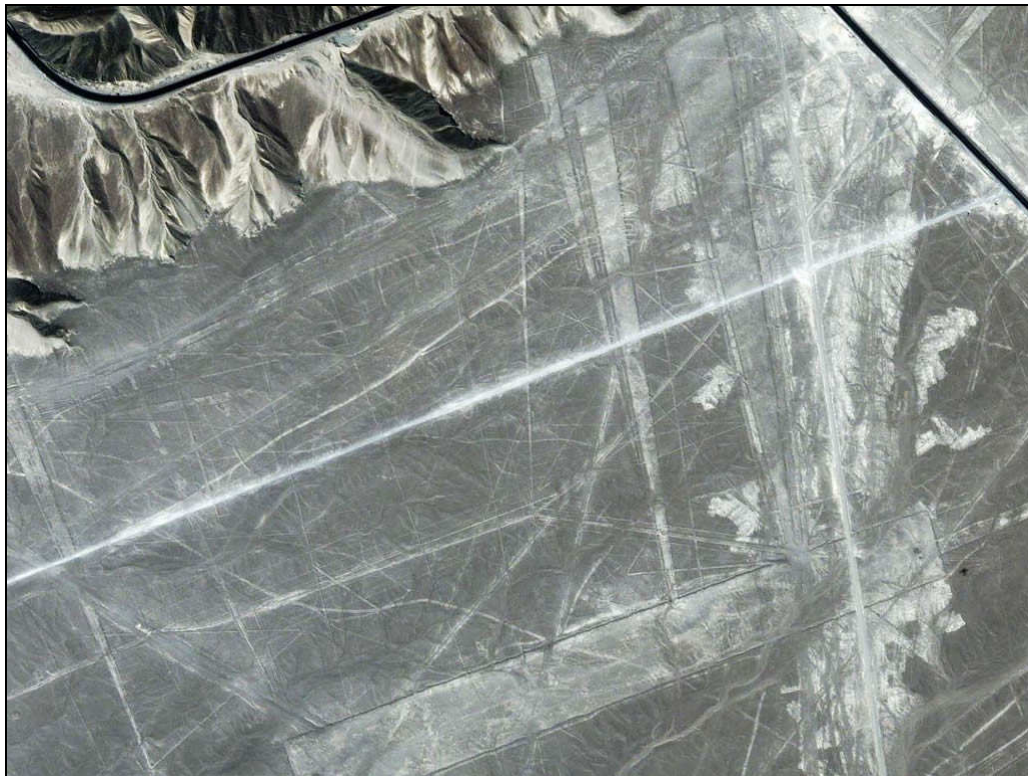


Figure 2.1. Geoglyph complex along the northern edge of the Nasca pampa (black line – Panamerican Highway); source NASA

When geoglyphs were constructed, the underlying sandy deposits were exposed allowing the silty elements together with humidity to develop a thin crust on top of the layer. It prevented a wind erosion and permitted the preservation of the geoglyphs. Moreover, as the Atacama Desert between northern Chile and southern Peru is one of the driest areas of the Earth (see Chapter 3.2 – Climatic Conditions), hardly any precipitation reaches the

desert floor, thus erosion by water runoff has been rare for centuries. For that reason and due to the development of the crusty layer, the enigmatic Nasca Lines have survived almost unaltered and are easily visible today.

The predominant kind of prehispanic geoglyph found on the large flat plateaus is a cleared area often in trapezoidal or rectangular form (Figure 2.1). It is usually accompanied by lines running straight or bending several times, forming zig-zags, meanders or spirals. Biomorphic figures constitute the smallest fraction of the whole corpus, but at the same time they are the most famous designs. A common feature of the geoglyphs is that they occur together in complexes, often crosscutting each other, with older geoglyphs obliterated by more recent ones. The new drawings were added to existing ones in such a way that older geoglyphs were not build over, but rather incorporated into the group. They are therefore the result of several working steps: lateral enlargements, repeated surface clearing and redrawing on the same place (Lambers 2006). This makes the older geoglyphs not visible for majority of the ground archaeological techniques as well as for the aerial imaging. Thus, a powerful geophysical method had to be applied in order to trace previously obliterated patterns (see Chapter 5 – Methodology).

Date	Period	Archaeological culture	Phase
1532 AD	Late Horizon	Inca	
1400 AD	Late Intermediate Period	Ica/Chincha	
1000 AD	Middle Horizon	Wari	
600 AD 450 AD 250 AD	Early Intermediate Period	Nasca	Late Middle Early
1 BC		Initial Nasca	
200 BC 400 BC 600 BC	Early Horizon	Paracas	Late Middle Early
800 BC	Initial Period		
1800 BC	Archaic		

Table 2.1. Chronology and the cultural history of the Nasca basin (dates based on preliminary results of the Nasca – Palpa Project); after Lambers (2006).

Although it is commonly assumed that most of these earth drawings have been produced by the Nasca people that emerged out of the preceding Paracas culture (Table 2.1), the purpose of the geoglyphs for a long time has remained unclear. Many hypotheses

have been put forward by reputable Nasca researches like: Paul Kosok (1965), Maria Reiche (1976), Anthony Aveni (1990), Peris Clarkson (1990), Gary Urton (1990), Heleine Silverman (1990), David Johnson (1990), David Browne (1992), Maria Rostworowski (1993), Johan Reinhard (1996), Aurelio Rodriguez (1999), as well as by those less renowned. As a result there exist more than twenty of theories offering explanations. Those acceptable ones may be classified into the following categories (Aveni 1990):

- Solar, star or moon calendar and astronomy,
- Indicators for underground water, irrigation and agriculture.
- Ceremonial practices, mountain or fertility cult,
- Geometry and artistic expression,
- Movement, communication, transportation.

The variety of different patterns and figures is so large that it is hard to believe that these drawings did serve just one specific purpose (Aveni 1990). Nevertheless, as the archaeological excavations uncovered broken pottery and ample evidence of offerings and sacrifices, including guinea pigs, corn, crayfish and *Spondylus* seashells from thousand kilometres away, it seems that the sites had mainly a religious function (Reindel et al. 2003; Curry 2007). As some of the project archaeologists declare: “they were locations, not pictures”. Concerning the chronology of the geoglyphs, they are believed of having been created in a period of 1000 years (Table 2.1). Over such a long time, cultural change can be expected to affect their construction, use, perception and physical manifestation. Thus, the presented theories have to be improved by adding the time depth (Lambers 2006).

The geoglyph chronology from Palpa region relies mainly on the relative datings using the stratigraphic relationships of specified geoglyphs along with the classification of associated ceramics, as well as direct chronometric datings obtained using scientific methods (e.g. optically stimulated luminescence measurements or accelerator mass spectrometry radiocarbon dating) (Greilich et al. 2004, Kadereit et al. 2007). Available chronological evidence from Palpa suggests that the earliest geoglyphs date to the Early Horizon (Table 2.1), although the precise starting date remains unclear. Geoglyph related activity is in any case present in Late Paracas and increases in Initial Nasca, reaching its peak in the Early Nasca period. Afterwards it decreases continuously through Middle and Late Nasca, and finally ceases during the Middle Horizon (Lambers 2006).

Unfortunately, the most frequent geoglyph types on which geophysical prospecting was performed, the straight lines and trapezoids, have no chronological relevance since they cover the whole time span of the geoglyph phenomenon (Lambers 2006). In general, geoglyph variety was greatest in the Early Nasca period when all kinds of geoglyphs were made and used. Antropomorphic figures, probably the earliest ones, were typical until Early Nasca, when spirals, biomorphic figures, and different line types coexisted with trapezoids and rectangles. Later diversity was reduced to certain line types and areal forms. By Late Nasca times, only straight and meandering lines and large areal geoglyphs had survived. Thus, these types were not only common forms throughout all phases of geoglyph creation, but represented also the standard to which the geoglyph repertoire was finally reduced (Lambers 2006).

The construction and use of the geoglyphs and their associated structures were not separated, but were considered as parts of an integrated whole. Many groups of people were involved in geoglyph related activity over a long period of time. The following kinds of activity, summarized by Lambers (2006), could be recognized on the geoglyphs of Palpa:

- Construction and remodelling of geoglyphs and stone structures,
- Walking on lineal geoglyphs and around stone structures,
- Placing and breaking of pots on or along borders of lines and trapezoids,
- Placing of vessels, field crops, shells, and other objects on stone structures,
- Erection of wooden posts on trapezoids close to the stone structures, sometimes accompanied by placing of offerings in the excavated pit.
- Food consumption and placing,
- Cleaning and maintenance of geoglyphs,
- Burying of stone structures at the end of their use.

The precise documentation of these well defined activities related to geoglyphs is particularly important for the correct understanding of the origin of anomalies measured by geophysical means. As indicated in due course of this study (see Chapter 4.5), the repetitive geoglyph walking resulting in heavy compaction of line surfaces, as well as vessel and pot placing along with erection of wooden posts, could have been the crucial activities for later applicability of magnetic methods on site.

Chapter 3

Area of Research

3.1. LOCATION

The Palpa and Nasca geoglyphs are located in the Peruvian coastal plain, which is high arid plateau that stretches around 50 km between the towns of Nasca and Palpa on the Pampas de Jumana in Peru. The geoglyphs are situated approximately 400 km south of the capital Lima and cover about 450 km² of the desert territory (see figures 3.1, 3.2 and 3.3).



Figure 3.1. Map of the Ica Region (Southern Peru) (SLSA Zürich; DAI Bonn)

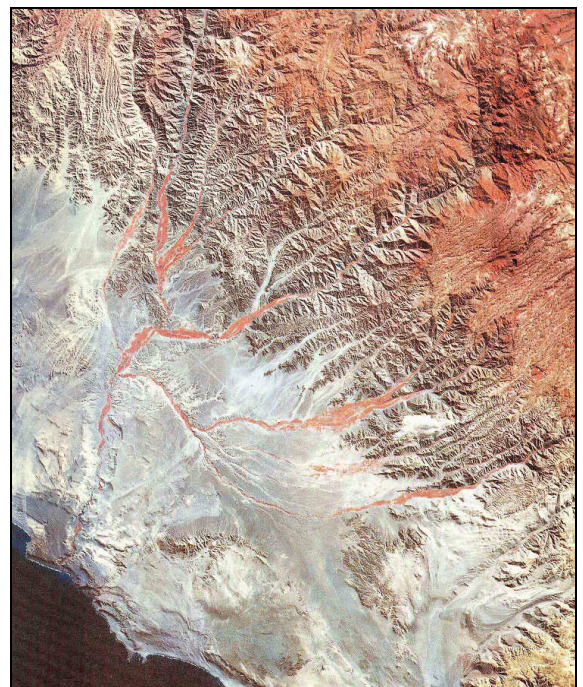


Figure 3.2. Satellite photograph of the Provinces of Palpa and Nasca (Southern Peru) (SLSA Zürich; DAI Bonn)

The desert itself occupies a strip along the southern Pacific coast of Peru extending from the shoreline 20-100 km inland to the secondary ridges of the Andes Mountains. There, in the Provinces of Palpa and Nasca, the world's largest concentration of ground drawings is located. For the purposes presented in Chapter 2, the area of research was carefully selected in the close surroundings of the city of Palpa (Figure 3.4).



Figure 3.3. Shaded relief map of Peru (source: <http://www.lib.utexas.edu/maps/peru.html> on 15.02.2008); changed by the author; green circle – area of research.

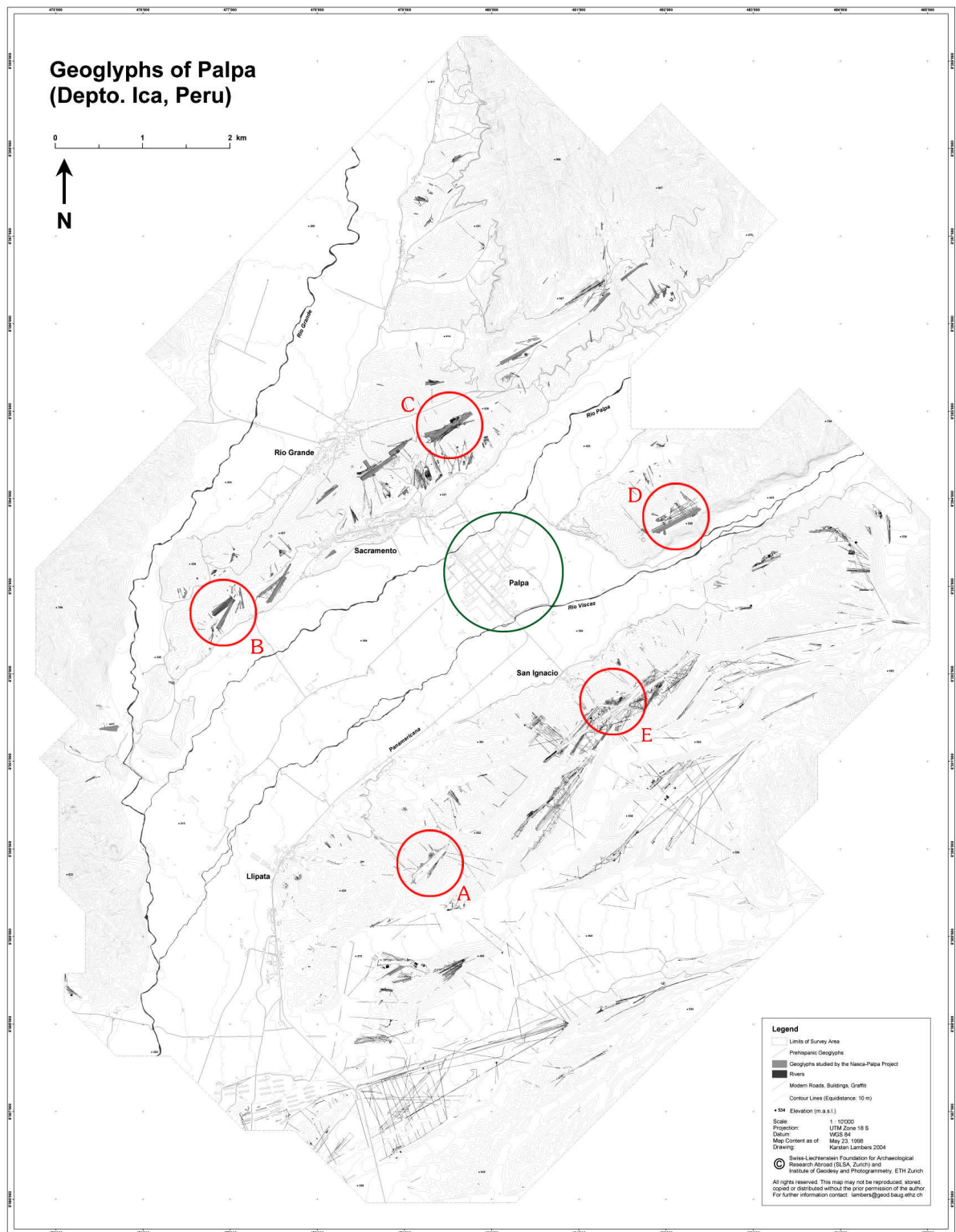


Figure 3.4 Area of research; red circles represent 5 measured geoglyph complexes surrounding the modern city of Palpa (green circle): A – PP01-36 Llipata, B – PV67A-15/16 Yunama, C – PV67A-47 Sacramento, D – PV67B-55 Carapo and E – PP01-49 San Ignacio; source Depto. Ica, Peru; SLSA Zürich, ETH Zürich; K. Lambers (2006); changed by the author.

Palpa itself is a modern settlement situated in the broad valley formed by Rio Palpa and Rio Viscas. Both rivers flow to the southeast until their junction with Rio Grande shortly thereafter, which is the only waterway of the whole drainage system having its perennial runoff to the Pacific Ocean. On the slopes and plateaus stretching along the rivers a vast geoglyph concentration can be found. In the present study a thorough investigation of five main complexes was made. During the several field campaigns within the years 2003 and 2007, the main geoglyph plateaus, which are presented in chronological order below, were covered by means of geophysical prospecting (see Figure 3.4 and Table 3.1):

- *PP01-36* (PAP379) located on Pampa de Llipata (to the south of Palpa),
- *PV67A-15/16* (PAP64) laying on Cresta de Sacramento (to the north),
- *PV67A-47* (PAP51A) situated on Cresta de Sacramento (to the north),
- *PV67B-55* (PAP283A) placed on Cerro Carapo (to the east),
- *PP01-49* (PAP365) being part of Pampa de San Ignacio (to the south).

	Site name	Project name	Official name
A.	Llipata	PAP379	PP01-36
B.	Yunama	PAP64	PV67A-15/16
C.	Sacramento	PAP51A	PV67A-47
D.	Carapo	PAP283A	PV67B-55
E.	San Ignacio	PAP365	PP01-49

Table 3.1. *The geoglyph nomenclature within the area of research.*

3.2 CLIMATIC CONDITIONS OF COASTAL PERU AND THEIR INFLUENCE ON PRE-COLUMBIAN CULTURES

The combination of tropical latitude, various mountain ranges, topography variations, Humboldt – cold ocean current that flows north-west along the western coast of South America and El Nino – temperature fluctuations in surface waters of the eastern Pacific Ocean, give Peru a large diversity of climatic conditions. One of the most significant climatic factors is El Nino. In normal circumstances, when El Nino does not occur, winds blowing in a westerly direction along the equator concentrate a warm surface water in the western part of the Pacific with the sea surface temperatures about 8°C higher and cool temperatures near South America. The diminishing of easterly winds during El Nino and weakening of the Humboldt current allows the temperatures of waters along the coast of

Peru to raise, what creates warmer than usual conditions along the whole coast of South America (Enfield 1987; Trenberth 1997; <http://www.pmel.noaa.gov/tao/elnino/nino-home.html> on 28.02.2009). This fact have important consequences for weather not only in Peru but around the whole globe as well.

For the reason of Peruvian climatic diversity, only the geographical region of the country, in which the geoglyphs are located, will be briefly summarized.

The study area near Palpa belongs to the hyperarid northern Atacama desert (Mächtle et al. 2009). The desert is influenced by two climatic systems. The cold upwelling of the Peruvian coast causes the coastal desert, and produces fog. In the austral winter months the fog often crosses the Cordillera de la Costa, covers the Ica – Nasca Depression and reaches the Andean footzone at 600 – 1200 m above sea level. The aridity can be briefly interrupted by prominent El Nino events in the austral summer months, when the upwelling activity is reduced or interrupted. However, for the study area, even in the case of El Nino rains, the Pacific influence mainly affects the coastal range and not the basin, where geoglyphs are located (Eitel et al. 2005, Mächtle et al. 2009).

In contrary to these claims, Hesse and Baade (2007) argue that there are Nasca lines that do show signs of water flowing over them or that have even been dissected by run-off. They presume that the reason why most of the lines and figures remain virtually unaffected is that they are placed 'high and dry'. They were carved to the flattest and highest parts of the pediment plains – in places where they are not affected by run-off from higher catchments and upslope areas, where run-off is not concentrated and does not reach destructive shear stress. It is believed that as recently as in 1998, El Nino related rainfall caused damage to some geoglyphs (Aveni 2000), thus, according to Hesse and Baade (2007), El Nino is the only known phenomenon that has been shown to cause pronounced rainfall in the study area.

However, as research of Eitel et al. (2005) confirm, to the east, the coastal desert merges into the semi arid ecosystem of the Andes. During the humid season (November – May), Amazonian monsoonal thunderstorms can cross the Cordillera Occidental and reach the uppermost catchments of the rivers. Even if El Nino rains should occur along the coast of southern Peru, it should be kept in mind that the Paracas – Nasca civilization was settled in the footzone of the Andes – in the eastern Atacama, leeward of the Cordillera de la Costa. This mountain range protected the settlement area of the Pre-Columbian cultures

from catastrophic El Nino rains. Thus, in the Nasca – Ica region, the deep cultural changes of Pre-Columbian civilizations were not caused by catastrophic run-off of El Nino events, but by a shifting eastern desert margin due to the changing monsoonal influence (Eitel et al. 2005, Mächtle et al. 2006; Mächtle et al. 2009).

3.3 GEOGRAPHICAL AND GEOLOGICAL SETTING

In southern Peru (at Palpa latitude) the desert zone is much broader than further north and reaches 90km in width. This is caused by an existence of coastal mountains – Cordillera de la Costa. This unique range is 170 km long and reaches 1500 m in altitude. To the east, a 20 km broad basin, the Ica – Nasca Depression, with heights between 150 and 500 m, separates the Cordillera de la Costa from the Andean Cordillera Occidental, which exceeds 4000 m above sea level. The footzone of the Andes together with the large Pleistocene pediments belong to the eastern part of the desert as well (Eitel et al. 2005, Mächtle 2007; Eitel et al. 2009).

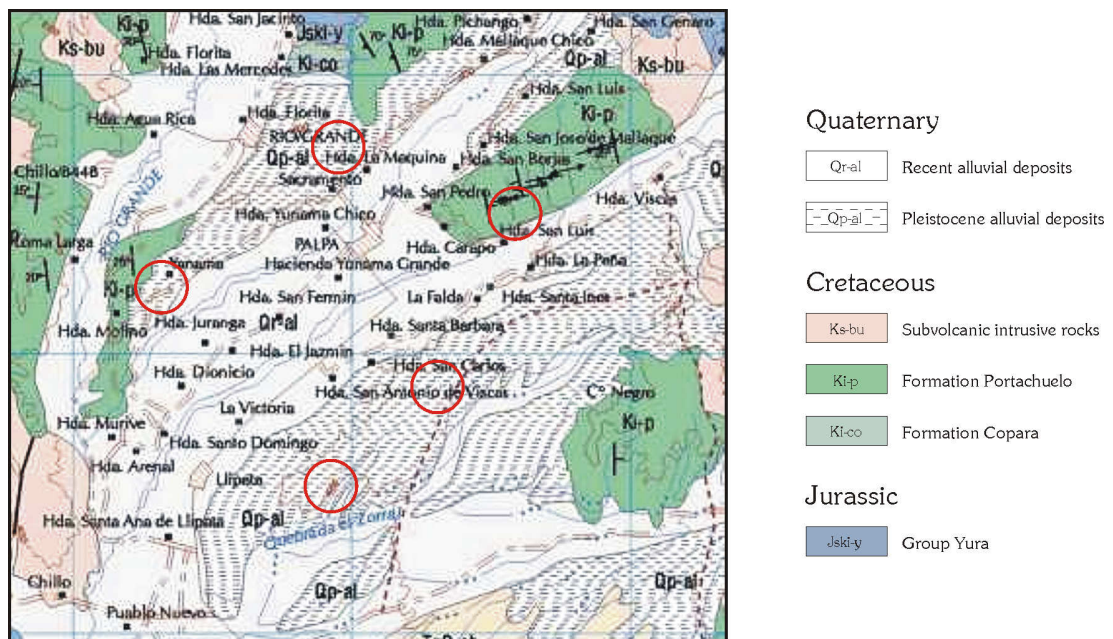


Figure 3.5. Geological map of the study area; red circles – prospected geoglyph locations; Carta Geologica del Peru (Mapa Geológico del Caudrángulo de Palpa) Ministerio de Energia y Minas, Instituto Geológico Minero y Metalúrgico, 1994 (source: <http://www.ingemmet.gob.pe/form/plantilla01.aspx?opcion=27> on 24.04.2007); modified by the author.

The Cordillera de la Costa is formed by Palaeozoic igneous rocks and Mesozoic to Tertiary sedimentary layers. The geomorphology there is dominated by large scarplands and

steep rocky cliffs. The Ica – Nasca Depression, formed by Tertiary and Quaternary tectonics is a NW – SE oriented rift, which contains Tertiary terrigenous and marine sediments. The eastern part contains large Pleistocene pediments, which form the transition zone to the Cordillera Occidental. The pediments are alluvial deposits (Figure 3.5) composed of sands of different grain size, small to middle-sized stones and rocks, and large boulders. On their surfaces, where the geoglyphs are created, the loose sand between the stones has been blown away by wind erosion, leaving behind a thin, but dense layer of gravels called desert pavement. Its stones are dark-coloured due to oxidised weathering crusts. The pavement is underlain by a silty yellow layer of roughly 30 cm thickness, with a weakly cemented vesicular horizon. It contains significantly much carbonate (4,2%) and sulphur (0,8%), which comes together with the weak calcareous and gypseous cementation of the vesicular layer. The sulphur originates from marine sources, transported as an aerosol to the Atacama. Together with dissolved terrigenous carbonate, it infiltrated with fog and sporadic rains into the uppermost sections of the soil. The silt layer belongs to the upper part of the pediments and represents, together with the desert pavement, the final pedimentation process. The succeeding dissection of the pediments led to the formation of the river oases and the *quebradas*, which are autochthonous dry valley systems. With the formation of river oases the pediments became relic forms (Eitel et al. 2005; Mächtle 2007; Lambers 2006; Eitel et al. 2009).

Chapter 4

Basics of Magnetism in Reference to Archaeological Prospection

In due course of this work various topics of geo- and rock magnetism in regard to archaeological research have been presented. Thus, the explanation of several conceptions of Earth's and rock magnetism have had to be given. Chapter 4 briefly reviews those which are crucial for understanding the functionality of magnetic method for archaeology.

4.1. MAGNETIC FIELD OF THE EARTH

Iron constitutes about six percent of the Earth's crust, but little of it is readily apparent. Most of it is dispersed through soils, clays and rocks as chemical compounds which are very weakly magnetic. Redistributions of some of these compounds and transformations of others into more magnetic forms, created patterns of anomalies in the Earth's magnetic field, invisible to a compass but detectable with sensitive magnetometers (Clark 1990). Those magnetic anomalies, caused among others by archaeological structures, are localised effects superimposed on the normal magnetic field of the Earth. Consequently, knowledge of the behaviour of the geomagnetic field is necessary both in the reduction of magnetic data to a suitable datum and in the interpretation of the resulting anomalies.

The geomagnetic field is caused by a westward current flowing in the liquid outer core of the Earth, organized by the Earth's spin, and generated by a gravitational accretion process at the core-mantle boundary (Campbell 1997). When represented by the field of a theoretical magnetic dipole at the centre of the Earth inclined at about $11,5^\circ$ to the axis of rotation, it is geometrically not complex, however, it exhibits irregular variations in both

orientation and magnitude with latitude, longitude and time. In order to illustrate the magnetic field vector, the use is made of descriptors known as the geomagnetic elements. The magnitude of the magnetic vector is given by the field strength “ F ”. It has a vertical component “ Z ” and a horizontal component “ H ” in the direction of the magnetic north and its direction is defined by two angles (Figure 4.1 left): the *declination* “ D ” is the angle between the magnetic meridian while the *inclination* “ I ” is the angle at which the magnetic vector dips below the horizontal (Lowrie 1997). In the northern hemisphere the magnetic field generally dips downward towards the north and becomes vertical at the north magnetic pole (Figure 4.1 right). In the southern hemisphere the dip is generally upwards towards the north. The line of zero inclination approximates the geographic equator, and is known as the magnetic equator. The field varies in strength from about 30000 nT in equatorial regions to about 60000 nT at the poles (see on-line magnetic field values of NGDC for more detail – <http://www.ngdc.noaa.gov/geomagmodels/IGRFWMM.jsp>).

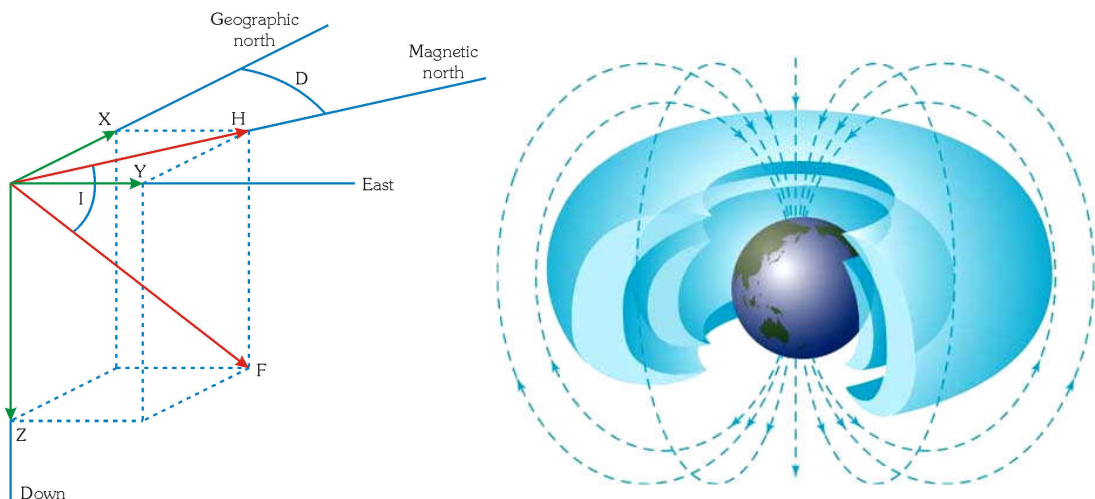


Figure 4.1. The elements of the Earth's magnetic field (left) and the dipole approximation of the geomagnetic field (right) (source <http://radbelts.gsfc.nasa.gov/outreach/Radbelts0.html> on 15.02.2009).

4.2 MAGNETIC SUSCEPTIBILITY AND MAGNETIC MINERALS

Magnetic susceptibility is a measure of the ease with which the material can be magnetized (Thompson and Oldfield 1986). It is a very convenient parameter for the simple non-destructive measurement which may be performed fast in the field. Therefore it is often ideal in reconnaissance studies before magnetic surveying is applied on site. It helps to

identify the type of material and the amount of iron-bearing minerals present (Evans and Heller 2005). Most common rock-forming minerals exhibit a very low values of this physical parameter, thus rocks and sediments owe their magnetic character to the generally small proportion of magnetic minerals that they contain. There are several geochemical groups which provide such minerals:

- Iron oxides – possess solid solution series of magnetic minerals from magnetite (Fe_3O_4) to ulvöspinel (Fe_2TiO_4). Hematite ($\alpha\text{Fe}_2\text{O}_3$), another iron oxide, is common in soils and sediments of environmental significance. Another important mineral of this group which widely occurs in soils is maghemite ($\gamma\text{Fe}_2\text{O}_3$). Its chemical formula is identical to that of hematite, but the crystal structure is different (Cornell & Schwertmann 1996; Evans & Heller 2005).
- Iron oxyhydroxides – only goethite (αFeOOH) is magnetically significant. Some of the others, such as ferrihydrite ($5\text{Fe}_2\text{O}_3 \cdot 9\text{H}_2\text{O}$) or lepidocrocite (γFeOOH) are noteworthy because they may undergo chemical changes to produce hematite and maghemite (Cornell & Schwertmann 1996; Dunlop & Özdemir 1997; Evans & Heller 2005) (see Chapter 4.5).
- Iron sulphides – provide among others the magnetic mineral pyrrhotite which is a minor constituent of rocks and whose magnetic susceptibility is dependent on its actual composition. The second significant mineral of this group is greigite (Fe_3S_4) which is known to occur widely in many sedimentary environments (Berner 1967, Dell 1972, Stanjek et al. 1994; Evans & Heller 2005).
- Iron carbonate – this group has one iron mineral, siderite (FeCO_3), which is common in carbonate sediments. It often forms by direct precipitation from water, and by oxidation processes may form magnetite, maghemite and hematite. Once created, these magnetic minerals play a significant role in the carbonate-rich environments, like silty layers of Peruvian pediment deposits (Ellwood et al. 1986; Dunlop & Özdemir 1997; Okrusch & Matthes 2005) (see Chapters 3.3 and 4.5).

The most important terrestrial magnetic minerals are iron oxides (Dunlop and Özdemir 1997). By far the most common is magnetite, however, by oxidation, it frequently forms maghemite. Although it is the size, shape and dispersion of grains that affect its magnetic character, it is reasonable to classify the magnetic behaviour of rocks and sediments according to their overall magnetite/maghemite content. Sedimentary deposits, like those in which Peruvian geoglyphs were carved, are considered as non-magnetic unless they contain a significant amount of iron oxides in the heavy mineral fraction (Linnington 1970; Dunlop and Özdemir 1997).

From a geological viewpoint, where magnetic anomalies are observed over sediment covered areas, the anomalies are generally caused by an underlying igneous or metamorphic basement, or by intrusions. Sometimes the anomalies of igneous geology itself may be strong enough to mask the anomalies from archaeological features (Aitken 1974). Nevertheless, by the use of gradiometer mode of the magnetometer system (Chapter 5.2), geological input can be easily eliminated and the archaeological contribution emphasized. However, the chance of detection of this archaeological contribution at Palpa and Nasca may to the large extent depend on the geology, present in the form of fanglomeratic deposits of the pediment plains (Chapter 3.3).

4.3 MAGNETIC REMANENCE

The small concentration of ferrimagnetic minerals in a rock or sediment gives it the ability to acquire a remanent magnetization. The unprocessed remanence of a rock is called its natural remanent magnetization (NRM) (Dunlop and Özdemir 1997) and it refers to a natural sample before any laboratory experiments have been conducted on it. As this term reflects unawareness concerning the sample history (Evans and Heller 2005), being more specific, it is useful to employ detailed types of remanent magnetization. Lowrie (1997) differentiates remanence to the one acquired at or close to the time of the rock formation and calls it primary magnetization, and the one acquired at a later time, which is a secondary magnetization. A remanence acquired by cooling from an elevated temperature is known as a thermoremanent magnetization (TRM) (Thellier and Thellier 1959), and is the most important type of the former group concerning remanence of igneous and high-grade metamorphic rocks (Lowrie 1997). The other type falling into the same group is called a depositional remanent magnetisation (DRM) and is due to the

alignment of magnetic particles during sedimentation and eventual lithification in the presence of the Earth's magnetic field (Dunlop and Özdemir 1997; Evans and Heller 2005). As the latter mostly contributes to the general understanding and interpretation of magnetic anomalies on studied Peruvian sites, which is described in due course of this work, this type of remanence will be explained in more detail.

In DRM the alignment of the magnetic particles starts when they are suspended in the water column and ends at the stage of dewatering and consolidation of the sediment. During settling the particles are oriented by the ambient magnetic field, however, water currents disturb this alignment, giving rise to a declination error. Elongated particles tend to be oriented horizontally producing too shallow inclination, while the pressure of overlying sediments results in compaction, which can cause further directional errors. The DRM is finally fixed in sedimentary rocks during diagenesis (Telford et al. 1976; Dunlop and Özdemir 1997; Lowrie 1997; Evans and Heller 2005). A modified form of DRM is the post-depositional remanent magnetization (pDRM). It relies on the fact that small grains of magnetic minerals in pores in the sediment are in the water suspension and may be also oriented by the magnetic field (Telford et al. 1976; Lowrie 1997).

In the secondary magnetization group are chemical remanent magnetization (CRM) and isothermal remanent magnetization (IRM). The former occurs when the magnetic minerals undergo chemical changes or when new minerals are formed (Telford et al. 1976; Dunlop and Özdemir 1997; Lowrie 1997). Some examples for this phenomenon are presented in Chapter 4.5. The latter (IRM) is induced in a rock sample by placing it in a magnetic field at constant temperature and usually refers to laboratory procedures. It can also arise in nature, for example in the lightning strikes (Maki 2005), producing rare, high-amplitude anomalies in magnetometer readings, which are illustrated in the following chapters of this work.

4.4. MAGNETIC ANOMALIES ON ARCHAEOLOGICAL SITES

The successful application of magnetometers to archaeological exploration depends on the existence of a distinguishable magnetic anomaly associated with a site of archaeological importance (Breiner 1965). However, the existence of contrasts in the magnetic properties of materials forming an archaeological site, is only one factor in the production of magnetic anomalies. Additionally, there are also problems of the consistency

of materials, of the correlation of contrasts with archaeological features, of size, shape and depth of the features and of the overall distribution and complexity of the features and deposits (Linington 1970). Thus, the origin of magnetic anomalies in archaeological settings is rather complex. The main possibilities, summarized by Evans and Heller (2005) and complemented by the author are presented below:

- Enhanced susceptibility by burning and fermentation (Le Borgne 1955; Le Borgne 1960; Tite and Mullins 1971; Mullins 1977),
- Bacterial magnetite from magnetotactic bacteria (Fassbinder et al. 1990),
- Residual, magnetically enhanced ash (McClellan and Kean 1993),
- Thermoremanent magnetization of in situ material (Canti and Linford 2000),
- Mechanical destruction of NRM of the sediment (Fassbinder 1994),
- Other manmade differences of magnetic susceptibility (Le Borgne 1955),
- Different pedogenic processes (insignificant on the geoglyphs of Palpa and Nasca) (Fassbinder and Gorke 2007),
- Lightning magnetization (Maki 2005; Fassbinder and Gorke 2007).
- Wind separation of magnetic minerals (Fassbinder and Gorke 2009).

While the range of magnetic properties is important, actual variations in the measured field only occur if sufficiently large contrasts are present. Therefore, the types of archaeological features, in which the contrast is likely to occur, have been summarized after the classification of Linington (1970) and supplemented by the author :

1. Features formed of material that is more magnetic than its surroundings:
 - Features cut down into the natural rock – pits and ditches cut in sedimentary rocks and filled with soil or occupation debris,
 - Areas of intense heating – kilns, furnaces, ovens and hearths where the bulk of material is undisturbed,
 - Constructional features – formed from bricks, tiles, volcanic rocks or any other magnetic material.
 - Areas of ritual activity – deposits with enhanced susceptibility, the primary structure of which has been compacted.

2. Features formed of material that is less magnetic than its surroundings:
 - Features cut out of magnetic deposits – tombs and in certain cases soil filled features in volcanic and other highly magnetic rocks,
 - Constructional features – built of sedimentary rocks or other non-magnetic material, especially if the adjacent deposits contain a fair proportion of occupation soil and debris.
 - Areas of ritual activity – deposits, the natural remanence of which has been destroyed (i.e. by intensive and multiple walking).

3. Features where the confusion is likely:
 - Features cut in soil layers or entirely within other archaeological deposits.
 - Complex constructional features especially on sites having several periods.
 - Features refilled with the same material that was removed during the excavation.
 - Features the material of which is physically the same as the surroundings.

The shape and nature of any anomaly depends on the value of the Earth's field at the concerned geographical location. In archaeological surveying two aspects of the field are important: its magnitude and direction. The magnitude is often needed in connection with the use of the surveying instrument, and the direction of the field is more important in determining the anomaly shape. Normally this direction is referred to the inclination "I". Because of this directional property of the Earth's field all anomalies tend to be asymmetrical. This asymmetry is most marked in a magnetic north – south direction while it disappears for the magnetic east – west profiles across the anomaly. Thus, although profiles in both direction usually need thorough consideration, that in magnetic north – south course is of more practical value (Linington 1970).

The anomaly for an inclination equal to 60° is a typical for the regions of greatest present interest. The north – south profile of the anomaly is shown in Figure 4.2 (left) and the main points summarized after Aitken (1974) are presented below:

- The maximum of the anomaly lies to the south of the source (northern hemisphere), the displacement is approximately one third of the depth of the source.

- The separation between two points at which the anomaly has half its maximum value, is equal to the depth of the source.
- The extreme of the reverse anomaly is 10% of the maximum, and lies one depth unit to the north of the source (northern hemisphere).
- The anomaly is very small (less than 2%) at distances greater than 3 times the source distance.

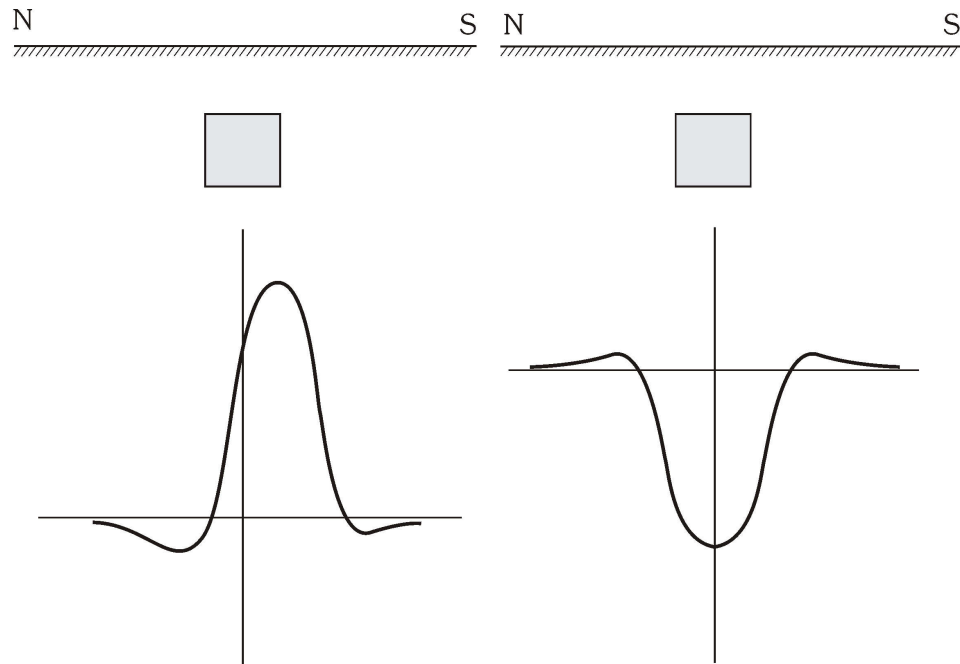


Figure 4.2. Idealized shape of anomaly in the total magnetic field intensity from a dipole source at different geomagnetic latitudes; left in Europe – the angle of dip is taken to be approx. 60° ; right in Palpa at up to 3° , idealized to magnetic equator 0° . The horizontal scale represents a north – south traverse through the centre of anomaly in units of burial depth (violet square – anomaly source), vertical scale – anomaly strength as a deviation from the normal field strength (horizontal line of the coordinate system).

This description of the simple magnetic anomaly is limited to the situation existing in Europe and other northern areas where the inclination lies between 50° and 80° (Lington 1970) or $60^\circ - 70^\circ$ according to Aitken (1974). Moving from the north magnetic pole to the equator, changes occur in the shape of the anomalies as the field direction ranges from vertical at the pole to horizontal at the magnetic equator (Clark 1996). Such situation may be observed in Peru, where at the latitude of Palpa and Nasca, the angle of dip hardly exceeds 3° (Figure 4.2 right). It gives entirely different shape of the anomaly, which could be compared to the west – east anomaly profile of $50^\circ - 80^\circ$ zone, but with the polarity reversed. It means that the whole anomaly appears to be mostly negative with no

displacement in any direction. There are two positive peaks of the size of up to 10% of the reverse anomaly, which in this case is dominant and has its maximum directly above the source. This can seem rather confusing for interpretation at first, as the feature of higher magnetic material than its surroundings appears to give an anomaly corresponding to a decrease in magnetism (Linnington 1970), but bearing in mind reversed polarity, the interpretation of anomalies should not be too difficult. However, the complexity arises with two maxima, which in case of dense linear structures, which are common for studied Peruvian sites, produce additional 'shade lines' and make the analyses much more problematical (compare Chapter 5.3).

4.5. SOIL MAGNETISM ON ARCHAEOLOGICAL SITES

The changes in magnetic intensity across an archaeological site are due to natural variations in thickness of topsoil and the activities of man (Aitken 1974). Topsoil is normally more magnetic than the underlying subsoil or bedrock (Le Borgne 1965), from which it has been derived, so that excavated features silted or backfilled with topsoil produce a well-defined positive magnetic signal. Conversely, less magnetic material intruding into the topsoil can be detectable by a subtractive effect which gives a negative signal (Aitken 1974; Clark 1996). That suggests that any intervention in soil produces a magnetic anomaly which can be measured above ground. As already stated before, the contrast in magnetic susceptibility and remanent magnetization between the structure and the adjacent undisturbed soil enables the detection of single archaeological features such as posts, palisades, stone structures, ditches, pits, kilns or fireplaces. Depending on the type of the soil, the enrichment of magnetic minerals in a trace of a post or palisade may enhance the magnetic susceptibility by 2 – 50 times and increase the magnetic remanence by 5 – 20 times (Fassbinder and Stanjek 1993). Man made fire or natural fire may produce a much higher increase. The caesium magnetometer enables the detection of anomalies caused by each single post in the adjacent soil, but the detectability of an archaeological anomaly is a rather complicated function of the sensitivity of the instrument, sampling density and soil properties (Fassbinder and Irlinger 1999).

Under moderate conditions humus and plough soils are normally fairly magnetic especially where long periods of cultivation have occurred. Occupation soils and deposits are normally even more magnetic. Under tropical and very humid conditions it is possible

that the magnetisation will be smaller which can be also true for uncultivated soils and those where serious leaching or soil exhaustion has occurred. In this cases the soil magnetism may become very small (Linington 1970).

4.5.1 MAGNETIC ENHANCEMENT MECHANISMS

The higher magnetic susceptibility of the uppermost centimetres of soils is due to the enrichment of ferromagnetic minerals in topsoil (Le Borgne 1955; Tite & Mullins 1971; Mullins 1977). The enhancement is due to the formation of maghemite and magnetite by different processes (Le Borgne 1955; Tite and Mullins 1971, Mullins 1977; Loveley et al. 1987; Maher & Taylor 1989; Fassbinder et al. 1990). The explanation given is in terms of the conversion of iron oxide in the soil from the very weakly magnetic hematite, which exists in “raw” soils and rocks, to the form of maghemite, which has a susceptibility greater by two orders of magnitude. The conversion proceeds by reduction to magnetite and subsequent re-oxidation. Two possible mechanisms have been proposed (Mullins 1977):

- Fermentation (Le Borgne, 1955) – which occurs at ordinary temperatures and is favoured by humid anaerobic conditions suitable for oxidation,
- Burning (Le Borgne, 1960) – which is an effect of fire ground clearing by burning as a part of ancient methods of cultivation.

Of the two enhancement mechanisms, it is assumed that the burning is predominant. However, as the research of Fassbinder and Stanjek (1993) showed, hematite does not have to be present in soils or it is not always likely that natural or anthropogenic fires would achieve soil temperatures able to reduce it to magnetite (Evans & Heller 2005). Instead, four alternative maghemite-forming processes have been proposed:

- Oxidation of magnetite inherited from parent material (Mullins 1977),
- Dehydration of lepidocrocite (Mullins 1977),
- Dehydration of goethite (Longworth and Tite 1977; Yapp 1983),
- Oxidation of siderite (Housen et al. 1996).

The magnetic enhancement can also occur in the lack of fires and without any lithogenic magnetite inherited from the parent material due to the occurrence of ultrafine magnetite grains of the bacterial origin (Loveley et al. 1987; Fassbinder and Stanjek 1993).

4.5.2 SOIL MAGNETISM ON GEOGLYPH SITES

For the reason that the areas were never subjected to any irrigation systems and because of the deficiency in precipitation, no geochemical processes resulting in the new formation of iron oxides in soil could have been expected there. Given that the extreme aridity (see Chapter 3.2) is unfavourable for the fermentation processes as well as for other magnetic enhancements of surface soils (Thompson and Oldfield 1986), and due to the absence of burning activities on geoglyphs, most of the processes producing magnetic minerals in soil seem not to be substantial there (Fassbinder and Reindel 2005).

The exception, however, could be the oxidation of siderite to maghemite, which favoured by high temperatures, is common for carbonate-rich sediments (Mullins 1977; Evans and Heller 2005). It is followed by the general fact that calcareous soils (see Chapter 3.3) are conducive to maghemite formation (Mullins 1977), therefore, the magnetic signal from the pediment desert soil could be explained by the oxidation of this mineral, as well as by the presence of magnetic components of parental material which was brought in as a part of the original airfall loess (Evans and Heller 2005).

Even if those processes indeed occurred, the soil conditions are still understood to be unfavourable for geophysical prospecting. Fortunately, the lack of interfering effects of extraneous iron on site, such as horseshoes, power lines, buried pipes, wire-netting and iron fencing, allowed the studied lineal geoglyphs to become perfectly visible in the resulting magnetograms.

It is believed that the visibility is due to the delicate structure of the vesicular desert subsoil, which was destroyed on the exposed lines by people frequently walking over them in the course of ritual activity taking place on geoglyph sites (Gorka et al. 2007). It is unlike the horizon below the desert pavement, the intact structure of which shows that people avoided walking outside the figures (Eitel et al. 2005). Furthermore, the large trapezoids constructed later did not confine movement of people over them either, so their surface is generally less compacted. This is why the older lines are visible in the magnetograms even though their cleared surface resembles that of the trapezoids (Gorka et al. 2007).

In conclusion, it is assumed that the heavily compacted vesicular layer under the lines led to the total destruction of remanent magnetization of deposits, giving the measurable signal in the shape of the magnetic anomaly. However, in some cases, the same

intensive and multiple walking process might have led to the susceptibility enhancement, acquired by the denser concentration of magnetic particles in the compacted deposit's structure. Additionally, the enrichment of magnetic minerals by wind separation might have contributed to the detection of magnetic anomalies on lines as well.

4.6. TIME VARIATIONS IN THE EARTH'S MAGNETIC FIELD

In the discussion of magnetic anomalies the Earth's magnetic field was taken as being constant. Unfortunately this is not true as small scale time variations occur both in intensity and direction. These variations are often of the same order of size as the measured anomalies produced by archaeological features, and thus cannot be ignored. From the point of view of practical surveying two elements are of importance: diurnal variations and the effect of magnetic storms (Linington 1970). In addition, there is a variety of much faster types of variations usually referred to as micropulsations. These can introduce an uncertainty in individual instrument readings and are a serious difficulty on sites for which the soil properties permit detection of very weak anomalies, and for which a high sensitive instrument, like caesium magnetometer is being used (Aitken 1974).

The effect that must be compensated in the first place is diurnal variation. In a simple form it is the variation in the intensity of the geomagnetic field at the Earth's surface during the course of a day, and is found to vary depending on the geographical latitude. The change in the field is normally most rapid during the early morning and late afternoon when the magnetic field intensity decreases soon after sunrise, reaching a minimum at noon, and increases during the afternoon and night. However, especially on magnetically disturbed days, the pattern can show a wide range of behaviour. Whereas throughout the winter the overall variation may amount to only 5 nT, which is barely significant, during the summer it may reach 50 nT and cannot be ignored. This variation is too irregular to allow readings to be corrected by some generalized formula. The best solution is to make simultaneous measurement at the fixed reference point or to use a gradiometer type of an instrument. A simpler alternative is to complete the survey of each area in a time short enough for a variation to be negligible. However, there are magnetic storm days, associated with strong sunspot activity, on which surveying is only possible if a reference detector or a gradiometer is used. Such storms differ both in duration and size. While changes of 1000 nT have been recorded, especially towards the equator, normal storms reach about 100 nT. The most

intensive ones may last for several days, the smaller storms are normally shorter and usually last a few hours (Linnington 1970; Aitken 1974; Lowrie 1997; <http://www.geophysik.uni-muenchen.de/observatory/geomagnetism>).

For the measurements in Peru, the linear changes in the daily variation of the geomagnetic field were reduced to the mean value of the 40 m sampling profile and alternatively to the mean value of all data of a 40 m grid. Here it was assumed that the variation of the Earth's magnetic field during one profile length of 40 meters (approximately 25 – 30 seconds of measuring time) follows a linear increase or decrease of the intensity. Therefore, it is possible to eliminate this variation for each profile line simply by a reduction to the mean line value. Alternatively, in magnetically quiet periods, it is also useful to calculate the mean value of the whole 40 x 40 m square. This avoids the disappearance of linear structures parallel to one profile. To create discrete field values a resampling program (see Chapter 5.2) setting data to 25 x 25 cm was used. By the whole procedure the difference between the measurement of magnetometer probes and the theoretically calculated mean value of the Earth's magnetic field was obtained. The intensity difference gave the apparent magnetic anomaly, which was influenced by the magnetic properties of the archaeological structure, soil magnetism and geology. In order to cancel the natural micro-pulsations and high frequency disturbances of the Earth's magnetic field, a band pass filter in the hardware of the magnetometer processor was used (Fassbinder and Irlinger 1999; Becker 1999; Fassbinder et al. 2007, Gorka et al. 2007; Fassbinder and Gorka 2009) (see Figure 5.8 and compare Chapter 5.2).

Chapter 5

Methodology

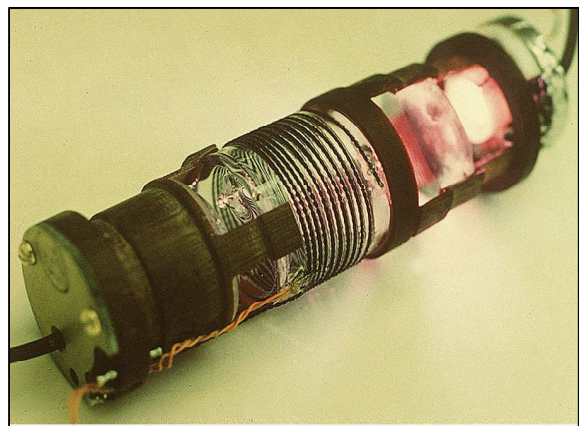
5.1. INSTRUMENTATION AND SAMPLING PROCEDURE

The principle of the magnetic prospection survey is based on the measurement of the total magnetic field or its gradient in a certain direction. The presence of the magnetic anomalies can be related to the presence of bodies that differ from their surrounding, in terms of their magnetic properties. For geophysical prospecting in archaeology the sensitivity, speed and spatial resolution are required (Becker 1999). However, since Palpa/Nasca geoglyphs has become the UNESCO World Heritage Site, the protection of the monument seems to be an equally important factor. While other near-surface geophysical methods such as the electrical resistivity profiling, ground penetrating radar or electromagnetic surveying may be assumed to be slow and/or invasive techniques in this area, due to the intense site preservation policy, magnetometry in contrary suits best the purpose of protection, being an excellent tool for the fast location of underground structures without destruction. While proton precession magnetometers are limited in speed and fluxgate gradiometers in sensitivity (see Figure 5.9), especially applied at most of the low susceptibility contrast sites (Becker 1999), caesium magnetometers become significant, regarding the speed of high resolution data acquisition and the ability to survey areas that are inaccessible to other methods.

Since fluxgate gradiometers measure the vertical component of the geomagnetic field, which near the geomagnetic equator is very low, thus the application of this instrument to geoglyphs of Palpa might have been rather ineffective. Hence, the principle of operation of only proton precession and optically pumped magnetometers will be briefly described.

The proton magnetometer exploits the nuclei of hydrogen atoms, which as a result of spinning are magnetized and behave as small bar magnets. The design of the proton detector is based on the polythene bottle containing a proton-rich liquid (Hall 1962). The bottle is surrounded by the coil, through which a DC current is passed, so that it acts as an electromagnet aligning the protons parallel with its axis. When the current is switched off, the protons turn to align with the ambient magnetic field, generating a small AC voltage in the coil, which now becomes a detector. The frequency of this current, which is measured, is exactly proportional to the strength of the magnetic field (Aitken 1974; Clark 1990).

Figure 5.1. *Caesium magnetometer sensor: caesium is pumped from a caesium-vapour lamp (far right) through the circular polarizer and a plastic condensing lens into an absorption cell (center). Coil around cell sets up a fluctuating magnetic field. Some of the energy of the beam is absorbed to pump atoms in cell to higher energy levels; the rest passes through the absorption cell and is measured by the photocell at far left (description after Bloom 1960; changed by the author)*



The function of caesium optically pumped magnetometer is analogous to the proton detector, but more complex. The sensor is a glass cell containing caesium vapour. The polarized and filtered light from the caesium vapour lamp is passed through the glass cell and to the photocell. The light causes the electrons in the vapour to undergo the energy-level transitions (Breiner 1965). When the atoms are irradiated with the light beam, electrons in one of the lower energy states are excited by photons and rise to the higher state. Because some photons are absorbed, the beam of light is dimmed and the photocell detects it. The electrons in the higher state almost immediately fall back to one of the two lower states with the chance that it may drop back to the state that cannot absorb light. Eventually, nearly all of the electrons end up there and the vapour, which is then completely pumped, is relatively transparent to light. If the radio-frequency fluctuating field, parallel to the light path, is applied to the glass cell by means of a coil around it, it causes the electrons to shuttle from one of the lower energy states to the other, undoing the optical pumping. As a result, the vapour again absorbs light. The exact energy required to do this, thus radio frequency, depends on the strength of the magnetic field. The radio frequency and optical

effects combine to give a particularly sharp resonance, and it is this resonance the optically pumped magnetometer exploits. If the field strength is known, the resonance serves as a measure of the radio frequency, and conversely, if the frequency is known, it can be used to determine the Earth's magnetic field (Bloom 1960; Lenz 1990, Clark 1990).

In the proton magnetometer a resolution of up to 0,1 nT is achievable, however, the two-stage polarization-measurement mode makes it slow and less adapted to the rapid gathering of high density information required in archaeological prospecting. It is unlike the optically pumped magnetometers, which with the advantage of generating a continuous signal, are several times faster than their proton counterparts. Additionally, the sensitivity of 0,01 nT, which derives from the high precession frequencies, make small signals much easier to measure than with the proton principle (Aitken 1974; Clark 1990).

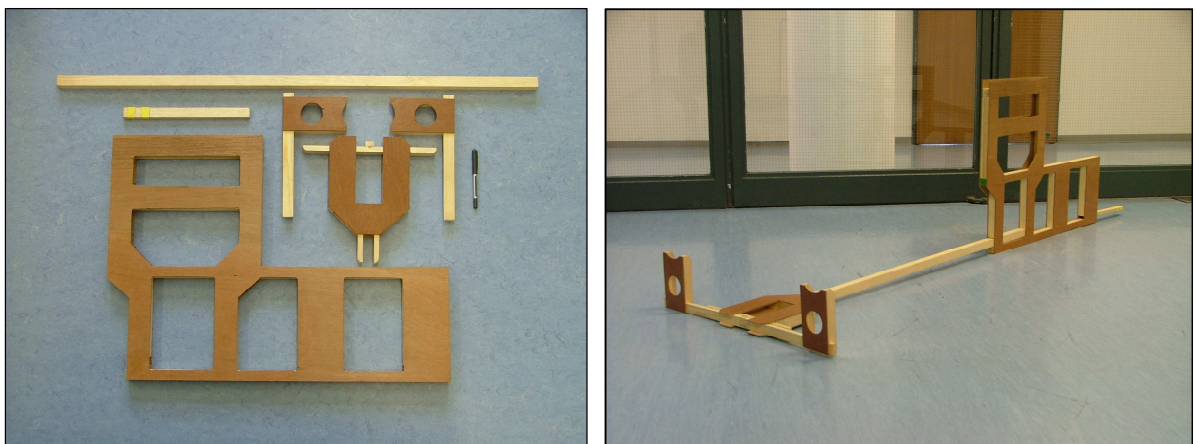


Figure 5.2. The complete Scintrex® SMARTMAG SM4G gradiometer kit consisting of magnetometer sensors with cables, sensor electronics, readout unit (SMARTMAG console), battery belt and additional accessories (source: Scintrex, Ltd.)

The Scintrex® SMARTMAG SM4G (Figure 5.2) is an optically pumped caesium vapour magnetometer for scalar measurement of the Earth's magnetic field. Due to its high sensitivity of 0,01 nT, excellent gradient tolerance, high cycling rates, fast response and low susceptibility to the electromagnetic interference, it has been chosen and successfully used by the geophysicists of the Bavarian State Department of Monuments and Sites (BLfD)

since the instrument for the first time has become available on the market in 1996 (Becker 1999). The success in subsequent use of the apparatus by the BLfD geophysical prospection team, among others in Yemen, Italy, Egypt, Syria, Iraq, South Siberia and Bavaria (see ref. Fassbinder and Irlinger 1999) encouraged to the further application of SMARTMAG on the geoglyphs of Palpa and Nasca in Southern Peru.

Beforehand, the hard- and software of the instrument has been modified and adapted to archaeological applications. The frame of the device (see Figures 5.3 and 5.4) was redesigned in the laboratory of the Bavarian State Department of Monuments and Sites and rebuilt in the workshop of the Geophysics Institute, LMU Munich. The whole apparatus was rearranged and reset in order to cope with the innovative methods of data acquisition in the new environments. For the field survey, sensor holders have been placed at one end of the 2 metre long wooden frame, at the other end of which the electronic package was carried. The batteries were slung around the operator's waist while the SMARTMAG console was hanged at the height of worker's abdomen, enabling observation of readings during the measurement (see Figures 5.5 and 5.6).



Figures 5.3 and 5.4. The new SMARTMAG SM4G magnetometer frame construction providing effortless set-up in the field and unproblematic transportation to the measurement area.

In one man carried equipment construction the so called duo-sensor configuration was chosen in order to reach a maximum speed of prospection combined with the highest possible sensitivity (Becker 1997). Two sensors were arranged horizontally, measuring the total intensity of the geomagnetic field and its gradient at two parallel tracks. They were moved along the 40 meter profile of the grid (40 x 40 meters) in a zigzag mode with a constant sensor height of 0,3 meter above the ground (Figures 5.5, 5.6, 5.7 and 5.8). In the WALKMAG (walking magnetometer) mode, data were acquired and recorded at the rate of

10 readings per second in the 0,5 meter separated traverses and 0,25 meter subsequently resampled intervals, as one walked at a steady pace along the survey line. Every five meters a station marker was triggered by pressing a single button in order to automatically assign the coordinates to the recorded data. The sampling speed of the magnetometer allows to measure a profile in less than 30 seconds, what gave the possibility to finish one square in approximately 30 minutes and complete an hectare (200,000 samples) in 4 to 6 hours with a spatial resolution of 10 –15 cm at normal to fast walking speed (Fassbinder and Irlinger 1999, Becker 1999). Because of the low geographical latitude a tilt correction of the probes of about 45° was necessary (see Figure 5.5).



Figure 5.5. Field measurement in Palpa, southern Peru; March 2006; magnetic sensors' correction 45°.



Figure 5.6. Field measurement in Palpa in March 2006; walking along the survey lines.

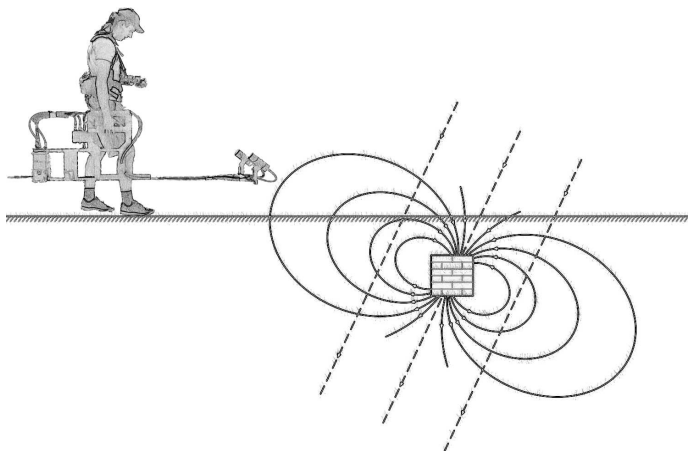


Figure 5.7. Simplified sketch of the measurement procedure; buried archaeological object generates the anomalous field producing the magnetic anomaly which can be measured by the sensitive magnetometer; field's inclination ca. 60°.

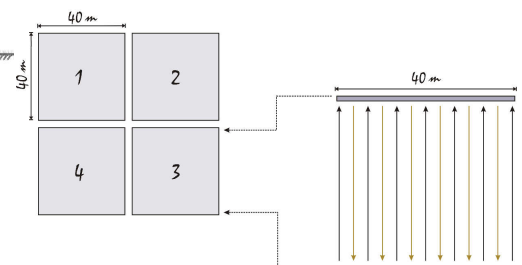


Figure 5.8. Measurement grid and survey walking pattern.

5.2. DATA ACQUISITION AND PROCESSING

Fast moving sensor systems need special procedures for data acquisition and processing. The base for high sensitive magnetic prospecting is the complete reduction of the natural and technical temporal geomagnetic variations (micro-pulsations, diurnal variations, powerlines, etc.) by measuring the difference between two sensors (Becker 1999) (Figure 5.8 and 5.9). According to Breiner (1965) the caesium magnetometer can be utilized successfully in such a differential mode, through the use of two sensors, one fixed and one mobile, connected together by a cable. In this so called *variometer* mode, a mobile sensor is moved across the area and the difference between it and a fixed reference sensor is recorded. The micro-pulsations sensed by two sensors located within a given distance of each other are almost identical, therefore the only change that is observed is due to the anomalies below the ground traversed by the mobile sensor. Another variation of this differential scheme is the use of both sensors as mobile instruments connected together on the wooden frame. This configuration is usually termed a *gradiometer*, as it actually measures the difference of the two intensities over the distance between them. Even better cancellation of micropulsations is achieved with this arrangement and the long cable link between the sensors, which may cause many problems under the rough surface conditions, is eliminated. The most important aspect however is that the gradiometer additionally filters out some of the background magnetic anomalies that originate in the deeper underlying geological strata (Breiner 1965; Becker 1999).

So far, magnetometry has rarely been used in South America for archaeological prospecting. As the magnetic inclination at Palpa is roughly 3° and the intensity of the total Earth's magnetic field hardly ever reaches 25.000 nT, the measuring equipment needed a further adaptation to the new conditions. For the reason of ideal compensation of the outer geomagnetic variations as well as the advantage of the system which can be operated as one man carried application, which eliminates the necessity of separation the sensor and data storage units (Becker 1999), the caesium magnetometer Scintrex® SMARTMAG SM4G-Special was adjusted in a *gradiometer mode* and as such for the first time applied to the geoglyphs of Palpa and Nasca. Due to the flat inclination, the magnetic sensors were arranged in a *horizontal configuration*, in order to enhance the visibility of magnetic data by

measuring the largest difference between two sensors aligned along the main course of the geomagnetic field.

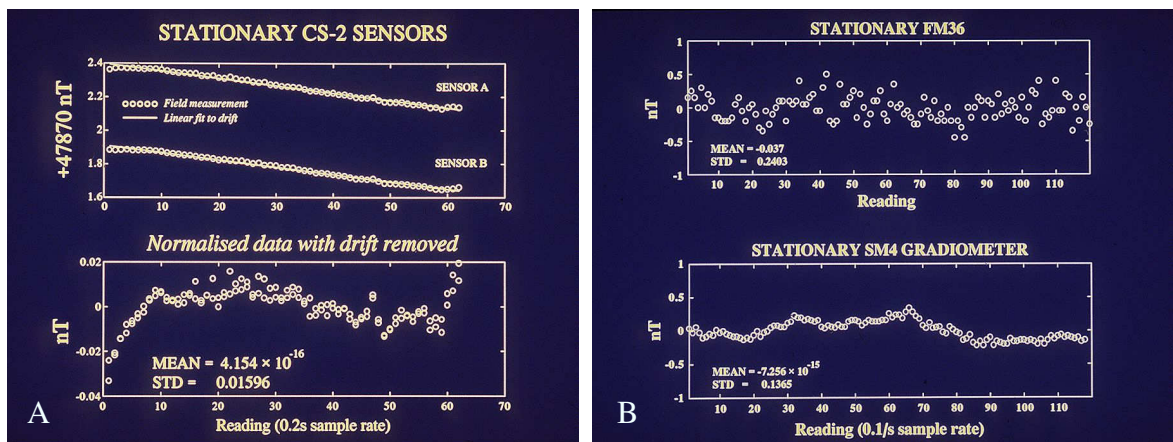


Figure 5.9. Temporal variations of the geomagnetic field; A - During a 60 second field measurement a linear decrease of about 0.3 nT is observed (top); while drift is removed (bottom), particular data present a 0.06 nT difference; B - in the gradiometer mode geomagnetic variations are reduced by the measurement of the difference between two magnetic sensors in the FM36 fluxgate gradiometer by Geoscan Research (top) and in the SM4 Gradiometer system by Scintrex (bottom) (Figure by Neil Linford, per. com).

After the readings of the magnetic field intensity have been taken and the necessary time corrections have been made, a further mathematical treatment of readings became an equally important task. For this study, all obligatory data computations have been completed in the interactive digital image processing techniques, by the use of highly developed graphic and processing programmes listed below:

- Geoplot 3.00, Geoscan Research, UK
- ArcheoSurveyor, DW Consulting, The Netherlands
- Self-made pre-processing software of BLfD and English Heritage
- Surfer 8, Golden Software, USA
- ArcGIS, ESRI Geoinformatik GmbH, Germany
- Procart, Condata GmbH, Germany
- AutoCAD, Autodesk Inc., USA
- AirPhoto, Irvin Scollar, Germany
- WuMap, CNRS, France
- Corel Draw/Photo Paint, Corel Corporation, Canada
- Adobe Photoshop CS, Adobe Systems, USA

For image processing the magnetometer readings (Figure 5.11) were typically imported to ArcheoSurveyor (Figure 5.10) or Geoplot and then converted into the 100 greyscale values ranging from 0 (black) to 99 (white). Any disturbances and disorders in the imported pictures were corrected by special digital image processing techniques, the result of which was the clearer and smoother representation of the magnetogram even for the raw data. The most frequently used procedures for the processing of the studied data set, based on the *ArcheoSurveyor (DW Consulting 2006)*, are summarized as follows:

- *Clipping* – this technique replaces all values in the current layer outside the specified minimum and maximum. The process is used to remove extreme data values, which force the display to show all values in the centre of the histogram in the same colour thus hiding fine details. Excluding these values allows the details to show through.

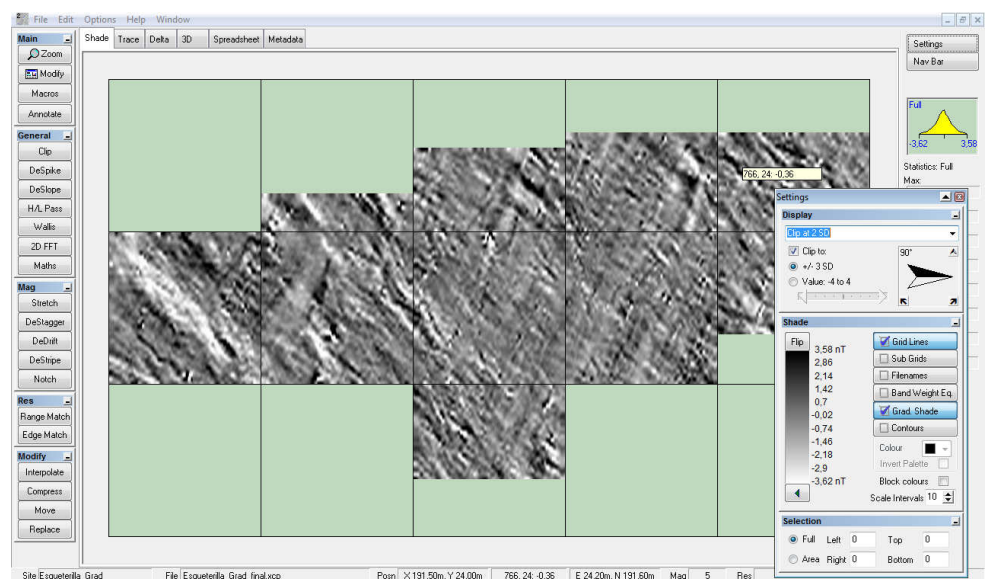


Figure 5.10. Screenshot of the ArcheoSurveyor version 2200 (DW Consulting) during the processing of the Peruvian test site Estequerilla (west of Palpa).

- *DeStripe* – it is used to equalise differences between the grids, which can be caused by directional effects inherent to magnetic instrument, instrument drift or orientation, delays between surveying adjacent grids or changes in the instrument set-up during the survey.
- *Interpolate* – increases the resolution of the selected area or survey by generating an extra data point between every existing pixel. It is usually

carried out as late as possible in the sequence of processes, as many of them depend on the original traverse data for their calculations.

- *DeSpike* – is typically used to remove spikes caused by small surface iron anomalies, which are generally the result of modern metal rubbish in the topmost layers.
- *DeDrift* – corrects for the drift in the readings taken by the instrument allowing for zigzag data collection method.

```

----- SCINTREX -----
/! Revision: 1.1
/! Line___: 0.00000 +
/! Date___: 06/03/23
/! Job___: 1306
/! Operator: tog
/! Serial__: 1101
/! Basefid_: 0
/! Rate___: 10.0
/! Bandw___: 2.0
/! Sens.sep: 0.5m
/! Mag_Data: X/Y/TotFid1/TotFid2/Hours/0=Uncor/Grac
/-----
0 0 25341.37 25340.45 8.367611 0 1.84
0 0.142857 25341.39 25340.46 8.367639 0 1.86
0 0.285714 25341.41 25340.46 8.367667 0 1.90
0 0.428571 25341.42 25340.46 8.367694 0 1.92
0 0.571429 25341.44 25340.47 8.367722 0 1.94
0 0.714286 25341.45 25340.49 8.367750 0 1.92
0 0.857143 25341.50 25340.58 8.367778 0 1.84
0 1 25341.54 25340.72 8.367806 0 1.64
0 1.14286 25341.60 25341.11 8.367833 0 0.98
0 1.28571 25341.60 25341.53 8.367861 0 0.14
0 1.42857 25341.32 25342.27 8.367889 0 -1.90
0 1.57143 25340.80 25342.69 8.367917 0 -3.78
0 1.71429 25339.54 25343.03 8.367944 0 -6.98
0 1.85714 25338.46 25343.04 8.367972 0 -9.16
0 2 25336.59 25342.77 8.368000 0 -12.36
0 2.14286 25335.29 25342.35 8.368028 0 -14.12
0 2.28571 25333.57 25341.27 8.368056 0 -15.40
0 2.42857 25332.75 25340.34 8.368083 0 -15.18
0 2.57143 25331.98 25338.93 8.368111 0 -13.90
0 2.71429 25331.73 25338.12 8.368139 0 -12.78
0 2.85714 25331.83 25337.30 8.368167 0 -10.94
0 3 25332.25 25337.09 8.368194 0 -9.68
0 3.14286 25333.24 25337.26 8.368222 0 -8.04
0 3.28571 25333.92 25337.57 8.368250 0 -7.30
0 3.42857 25334.80 25338.13 8.368278 0 -6.66
0 3.57143 25335.25 25338.50 8.368306 0 -6.50
0 3.71429 25335.80 25339.00 8.368333 0 -6.40
0 3.85714 25336.14 25339.27 8.368361 0 -6.26

```

Figure 5.11. Scintrex SMARTMAG SM4G magnetometer data set. The XYZ data format is compatible with the processing software written by DW Consulting and Geoscan Research. This format contains a header section with the information about the job/grid/line numbers, date of survey, operator name, sampling rate, bandwidth and sensor separation. Data is placed into columns: X, Y, Total Field Sensor 1, Total Field Sensor 2, Time, Gradiometer.

- *Wallis* – applies locally adaptive contrast enhancement to the surveys that display a pronounced slope across the area. This slope results in large portions of the survey being too “dark” and other areas too “light”, which make it very difficult to further process of the data without removing significant features.
- *Deslope* – corrects the errors seen in magnetometer data caused by large metal objects near a survey area. The process also corrects changes of the Earth’s magnetic field in time.

- *DeStagger* – compensates for data collection errors caused by the operator starting recording of each traverse to soon or too late. It shifts each traverse forwards (and/or backwards) by a specified number of intervals.
- *Stretch Traverse* – compensates for data collection errors caused by the operator walking to slow or fast. It stretches (and/or compresses) the end point of each traverse by a specified number of intervals, adjusting all the points in between by a proportional amount.
- *High/Low Pass Filter* –removes high or low frequency components in a survey. *Low Pass* calculates the mean of all the values within the specified window and replaces the centre value with the mean, while *High Pass* subtracts this mean from the centre value (ArcheoSurveyor program version 202X, DW Consulting 2006).

5.3. PRESENTATION AND INTERPRETATION OF RESULTS

5.3.1 PRESENTATION OF RESULTS

When a successful detection technique is applied to the survey of an appreciable area of an archaeological site, the presentation and analysis of the readings obtained is a serious task (Aitken 1974). After the filtering procedures, contrast enhancements and false colour transformations (Fassbinder and Becker 1999) have been completed, the next step which arises is an interpretation of the results in terms of possible archaeological features. For the satisfactory interpretation of readings, an adequate technique of the data display has to be applied. Various methods for data presentation have been used throughout the years, for example a succession of symbols each expressing a given strength of disturbance, contours, isometric drawings or random dots having a density proportional to the disturbance strength (Aitken 1974). Nowadays a digital image processing of the data allows a visualization of the measurement in a high resolution *shading* technique (Scollar et al. 1990; Fassbinder and Becker 1999), which is a primary display method and the most common procedure for the appearance of results for this work. It presents the data as a ‘map’ of the survey area using colours or greyscales to indicate the relative strength of the signal at each measurement point. Two shading modes are possible:

- *Block* – each measurement point colours a rectangular block whose size is determined by the measurement intervals,
- *Graduated shade* – calculates a continuously interpolated value for every pixel (DW Consulting 2006).

The alternate method for data presentation is a *trace* view. It presents the data as a trace or graph line for each traverse, which is displayed down the screen to provide a 3D-like visualisation of the survey area. The real *3D model*, as another presentation technique, converts the values in the current layer into relative heights, while the *relief* mode displays the survey as if it was 3D surface lit from an angle. This presentation can be effective for highlighting features in a survey which has a changing background signal level or slope. For all 3D or 3D-like display modes a sun position and the vertical scale can be applied, enhancing the visual effect, and therefore improving the interpretation procedure.

The special mode is a *delta* view, which is specifically designed to display the difference between any two layers as a simple shade plot using currently selected colour palette. By comparing two layers, the result of a process or set of processes can be seen, which gives the possibility to detect when the archaeology is being accidentally removed by possible over-processing of the data (DW Consulting 2006).

Although magnetic images are presented usually in the various *shading* techniques, which is also the common procedure for this work, the ultimate interpretation is always based on analysis of all possible display techniques studied separately.

5.3.2 INTERPRETATION OF RESULTS

In the interpretation of survey results, it is essential to know the strength and shape of the anomaly produced by the given type of the feature (Aitken 1974). As the magnetic conditions for the data collection in Peru are completely different from those in Europe, one has to be extremely careful in interpretation, in order not to make mistakes resulting from the shallow inclination of the geomagnetic field and consequently from the different shape of anomalies (compare Chapter 4.4). Therefore, the methods for interpreting the results of the magnetic survey are very important. Unfortunately, the complexity of many archaeological sites leads to an equal complexity in the magnetic results. Hence, much of the interpretation is rather a qualitative process based more on experience than on theory.

Even so, certain common factors, summarized by Linington (1970) and presented below, can be recognised:

1. Gaining an idea of the types of archaeological features and deposits, which determine the range and type of occurring magnetic anomaly. The information includes:
 - Whether significant magnetic contrasts is likely to be present,
 - How magnetic anomalies represent significant archaeological features,
 - The type and size of anomaly produced by each feature, which includes whether the anomaly is positive or negative,
 - The amount of overlap that occurs between anomalies and the possible range of complexity of the results.
2. Checking for the possible presence of any sources of magnetic interference.
3. Estimation of the anomaly shift which, as mentioned before, occurs to the south of the feature in northern hemisphere. This means that the features lie to the north of the anomalies. Two possible procedures are suggested:
 - For single anomalies the shift can be approximated from the assumed depth of the feature,
 - For complex sites the compensation might be done by shifting the magnetic pattern as a whole, using an average value for the depth of the deposit.
4. Identification of two parts of the single magnetic anomaly (main maximum and smaller subsidiary minimum). During the interpretation, the latter should never be mistaken for the anomaly from another feature.
5. Assessment of the width of the anomalies, which in the absence of severe overlapping effects, depends both on the width and depth of the features. The deeper the feature, the wider the anomaly, however, a wide anomaly might be also produced by a relatively shallow feature extended horizontally. In contrast, the narrow or sharply varying anomalies are only produced by shallow features. This enables the surface and near surface interferences, especially from fragments of iron, to be distinguished from those arising from deeper archaeological features (Linington 1970).

As a conclusion, it must be stressed that magnetic surveying, with all its possibilities and complexities, is mainly a matter for specialists, and therefore an adequate background of both the scientific and archaeological aspects is necessary (Linington 1970). As Becker (1999) states, the final result is usually based on the combination of several prospection and survey methods like: aerial photography, field walking, topographic surveying, digital terrain modelling and finally geophysical prospecting. Additionally, if possible, archaeological test excavations may be concentrated on specific areas for answering questions, which should give best possible information about the site.

5.4. COMMON LABORATORY PROCEDURES IN THIS WORK

For this study, the entire processing and interpretation work has been completed in the geophysical laboratory at the Bavarian State Department of Monuments and Sites (BLfD Munich). The processing has been done using previously described commercial software (see Chapter 5.2). All findings were digitized using Procart tablet for data collection from the hardcopy printouts. Images have been studied and analysed under the supervision of experienced geophysicists and interpreted in cooperation with the project archaeologists from the German Archaeological Institute (DAI Bonn). For the scrupulous interpretation, magnetograms of both total field and gradiometer modes have been printed on Din A0 paper format and examined from various perspectives and viewpoint angles with different lighting positions and sources. Additionally, for each site, 3D visualisations have been generated in Surfer 8 (Golden Software) and analysed similarly to 2D hardcopy printouts. As a support, different colour palettes, lighting positions, projection angles and vertical scales have been applied. This was of great assistance in finding the linear patterns in the magnetic images, although Din A4 figures, presented in the following chapters, do not precisely illustrate it, due to the limitations of the small format. For that reason, the present volume has been supplemented by the high resolution magnetograms in digital form to be found on the attached CD-ROM disc.

Chapter 6

Results of geophysical prospecting on site PP01-36 “Llipata”

The site PP01-36 occupies the south-western part of the Pampa the Llipata, south of Palpa. Although it is situated far from the modern settlements, a football field that was earlier used by children from neighbouring villages has been located exactly atop of the plateau. This modern feature has severely damaged parts of several geoglyphs. The site is composed of the main trapezoid, the spiral, and a series of flanking lines which are situated both to the north and south of the cleared area (Figure 6.2). At the south-western end of the complex, several lines, which seemingly existed prior to the trapezoid, can be recognized. They had presumably reached the very north-eastern end of the site, before they were removed together with the underlying zigzag line by the subsequent construction of the trapezoid. The remains of the zigzag line frequently reach the edge of the plateau, covering the furthest available parts of the site. It is due to the natural topography and shape of the area which enforces the arrangement and layout of the whole complex. Also the axis of the trapezoid follows the natural, northeast – southwest direction of the site.

The large trapezoid from site PP01-36 was the first geoglyph that was measured in total using geophysical methods in March 2004 (Figure 6.1, see also Figure 3.4). Apart from a number of test measurements in 2003, it was the first complete investigation of the whole geoglyph complex by means of magnetic prospecting (Fassbinder and Reindel 2005). As the soil conditions on those Peruvian monuments are understood to be unfavourable for geophysical prospecting (compare Chapter 4.5), this first measurement seemed not to bring much into the general understanding of the whole complex at the time. The results,

however, were unexpected which encouraged the team to the further development of the measurement techniques and to enlargement of the survey territory.

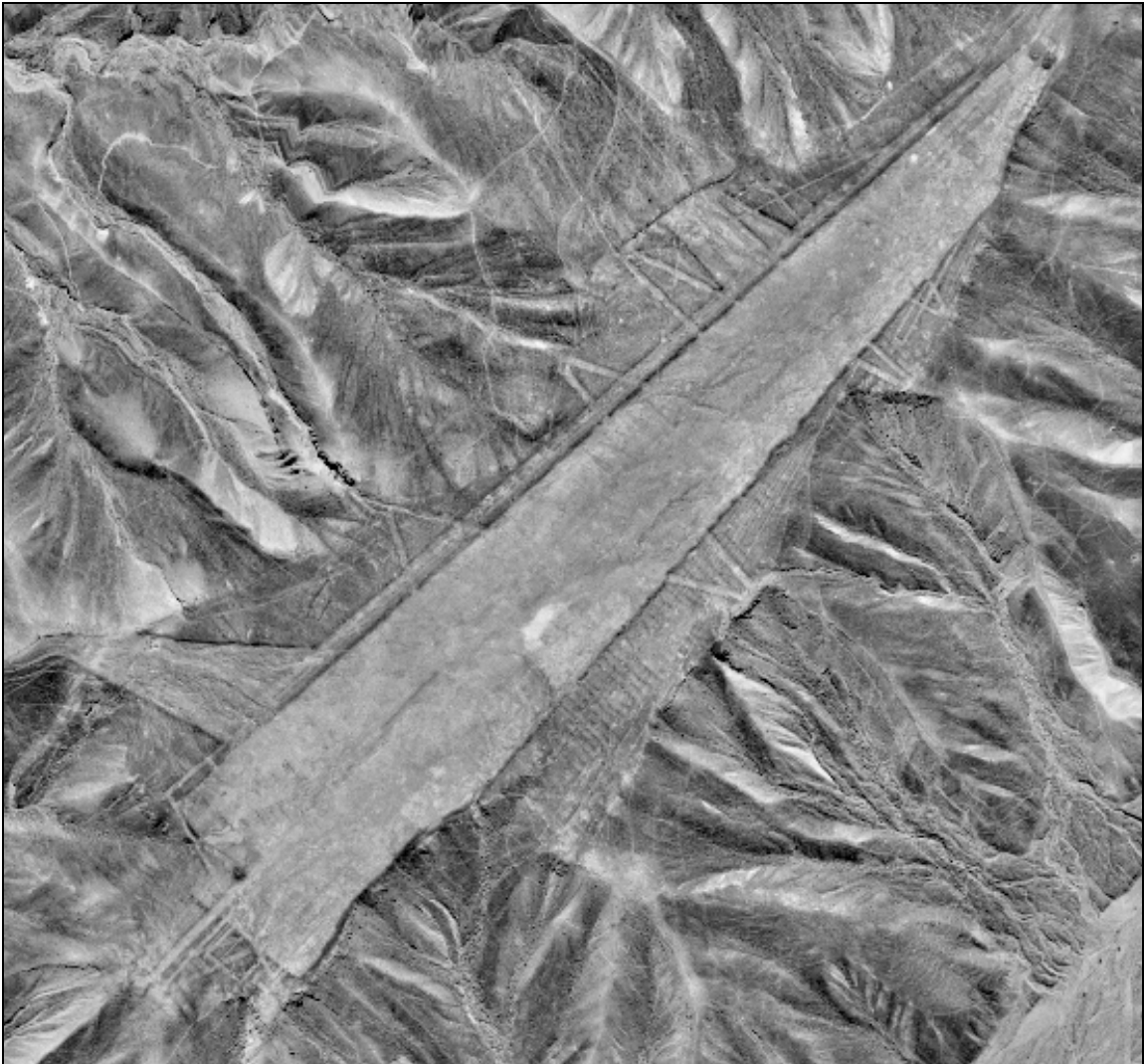


Figure 6.1. Orthophoto of the geoglyph site PP01-36 from the Pampa de Llipata, south of Palpa;
K. Lambers, Institute of Geodesy and Photogrammetry, ETH Zürich, Switzerland

The magnetic investigation on site PP01-36 amounts to 640 x 200 m (Figures 6.3 and 6.4), which makes 58 survey squares of 40 x 40 m grid. The whole measurement was completed during the second field campaign, but the final laboratory data processing and interpretation work has been finished much later, in 2008, after completion of all sites. Analysing the magnetic image of the total field measurement (Figure 6.3), a large number of archaeological anomalies that might be ascribed to traces of pits, small fireplaces and postholes could be recognized. Although at the first glance the magnetogram is dominated

by the sediment geology, more specific analyses reveal the remains of archaeological structures as well (Fassbinder and Reindel 2005).

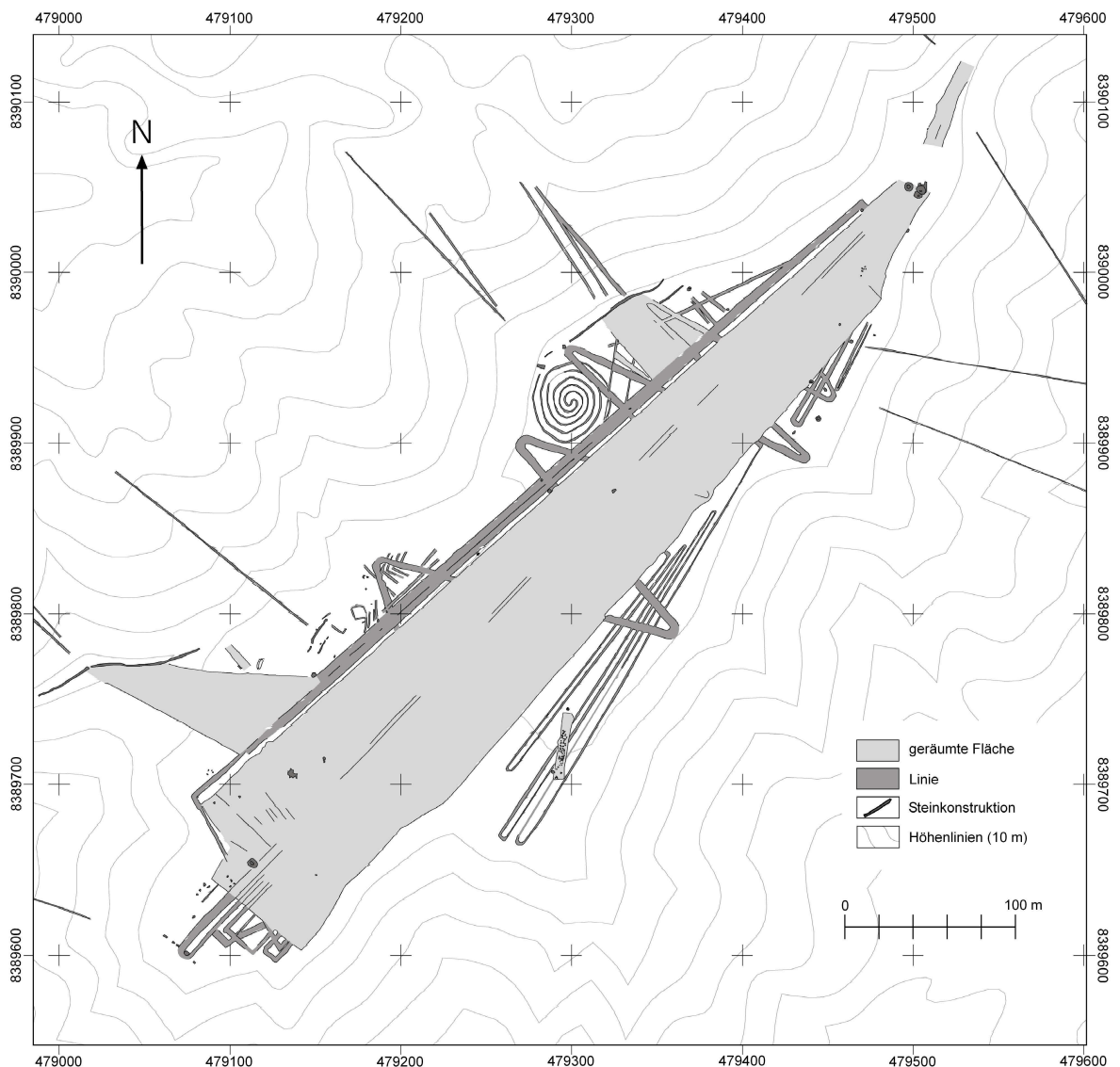


Figure 6.2. Detailed map of the geoglyph site PP01-36 from the Pampa de Llipata, south of Palpa; by K. Lambers, Institute of Geodesy and Photogrammetry, ETH Zürich, Switzerland

The most remarkable features, however, are the exceptionally strong star-shaped anomalies (up to ± 700 nT), which presumably originate from lightning strikes (Figure 6.5). These extraordinary features, the source of which is a lightning-induced isothermal remanent magnetization (LIRM) (compare Chapter 4.3) can be found in a large quantity on all investigated Peruvian sites. This fact is a noteworthy phenomenon given that only on very infrequent occasions LIRM has been the source of the magnetic signal on other archaeological sites, elsewhere in the world, measured by the BLfD geophysicist so far. LIRM usually occurs within a few meters of a lightning strike, where the magnetic field

created by the lightning discharge current imparts a secondary magnetization, overprinting the natural remanent magnetization (NRM) of the materials in the immediate vicinity. A lightning overprint is recognizable by its extreme intensity compared to the NRM that it replaces. There is usually no variation in magnetic mineral concentration, grain size, or composition between the LIRM samples and undisturbed soil as well as no fusion or high temperature discoloration of the soil may be observed (Maki 2005). For that reason, no diversity have been found by the numerous measurements of the magnetic susceptibility with a handheld Kappa Bridge SM30 meter (ZH Instruments, Czech Republic). Some of these star-shaped anomalies show only two strong 10 meter long dipole variations while the others extend over a length of 60 meters and have up to five dipole branches originating from one specific point (Fassbinder and Gorka 2007). Irrespective of their exact shape and length, they introduce a difficulty rather than assistance since they obliterate parts of the archaeological record and thus eliminate the possibility of interpretation of some portions of the magnetograms.

Nevertheless, these frequently occurring anomalies might be used as the indicators for climate change in the past. Although today's lightning occurrence rate in South America is understood to be high (see global distribution of lightnings based on the NASA observations: http://thunder.msfc.nasa.gov/images/HRFC_AnnualFlashRate_cap.jpg), the coastal region of Peru, where the geoglyphs are located, is nowadays characterized by the low annual flash rates. Therefore, in the past, different climatic conditions must have prevailed. This is also confirmed by archaeological findings as well as geomorphological and palaeoenvironmental investigations mainly based on the studies of loess deposits in the Palpa region (for more information see Mächtle et al. 2009; Eitel et al. 2004; Mächtle et al. 2006; Mächtle 2007; Eitel et al. 2009).

Although LIRM structures are the dominant features in the total field magnetic image, the remains of archaeological structures may be recognised as well. This, however, as the features are frequently faint, needs a more detailed look into the image, analysing magnetograms in different dynamic scales as well as applying diverse colour palettes and view modes. Some of the archaeological features found by magnetometry have been already known as they are clearly visible both from the air and from the ground perspective as well as they were excavated prior to the geophysical surveying. Recognized structures are traces of buildings, often dating to later phases such as Late Intermediate Period (see Table 2.1),

and two types of stone platforms: elongated ones on the edge of the plateaus and rectangular ones located at the ends of the cleared trapezoidal areas. Stone platforms are of the great interest as they were created together with geoglyphs and supposedly served together. Several of them, well preserved ones, were completely or partially excavated in order to determine their construction technique, age, function and relationship with the drawings. While low, elongated platforms apparently were built at the beginning or during the construction process of adjoining geoglyphs, only a few of rectangular ones were created at the same time as the geoglyphs. Furthermore, several of them show clear indications of later alterations which means that the structures were used in a long time period. Activity related to the platforms was the placing of maize cobs, ceramic vessels, seashells, and other materials on top of them. They may also have been used to stand on, but there is little evidence to support this idea (Lambers 2006). Holes up to 60 cm deep situated near the platforms suggest masts or poles several meters tall that served as orientation points during the construction process of the trapezoids. Other, shallower holes might have supported canopy-like roofs (Reindel et al. 2003; Curry 2007). The levelled and compacted ground around the structures indicates the frequent presence of people close to them. Compared to lineal geoglyphs, many of which are compacted along their whole course, the trapezoids are compacted, most likely by human activity, only around the platforms. Both the compaction and the traces of wooden posts can be distinguished in the total field magnetic image (Figure 6.3) as well as in the horizontal gradiometer one (Figure 6.4). It must be stressed, however, that all the listed archaeological structures can be recognized due to the prior knowledge of their approximate location. Otherwise, it would be extremely difficult to find them after the analyses of the magnetograms alone, because of the presence of many similar anomalies in the magnetic image which originate from the geology rather than archaeology. To differentiate them based on the anomaly shape and intensity alone is an unachievable task.

Fortunately, this is not true for the linear features, which being the main target of the magnetic surveying, form obvious and clearly identifiable patterns. That is why, from the whole range of the archaeological structures, only linear ones have been interpreted and presented in the following magnetograms. The rest have been largely ignored given that magnetometry had no contribution to their discovery. It is noteworthy, however, that they were detected and are present in the magnetic images as well.

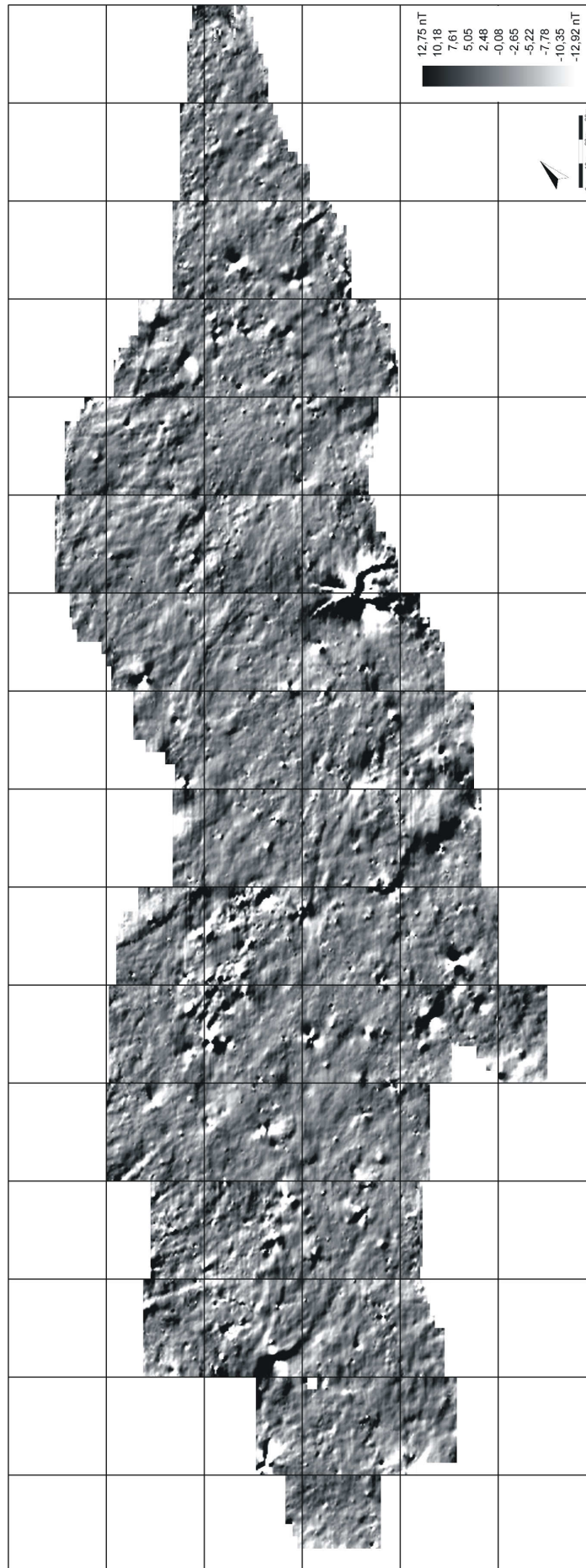


Figure 6.3. Magnetogram of the geoglyph complex on site PP01-36 “Llipata” located on Pampa de Llipata, south of Palpa; measurement in the Total Field Mode, SMARTMAG SM4G-Special in duo-sensor configuration; dynamics +/- 13 nT in 100 greyscale values from black to white, sampling density 50 x 12,5 cm, interpolated to 25 x 25 cm, resolution increased by ‘Graduated Shade’ function; Earth’s magnetic field ca. 25000 nT; grid size 40 x 40 m;

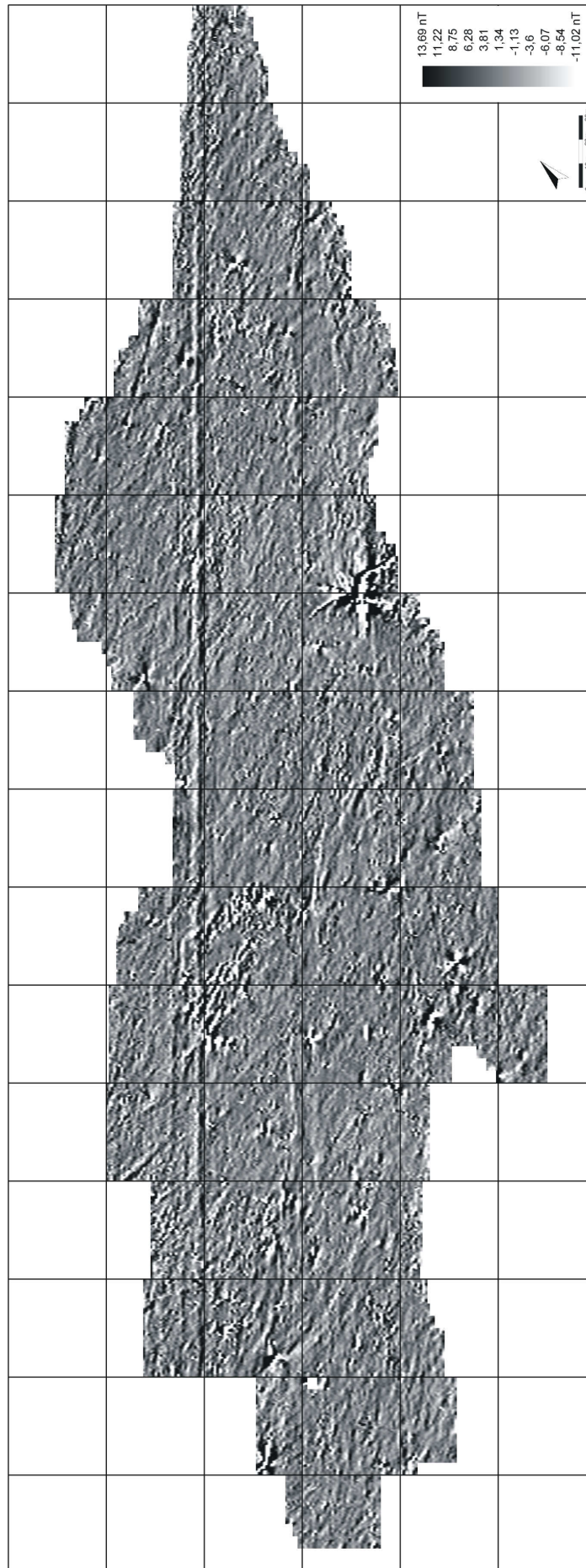


Figure 6.4. Magnetogram of the geoglyph complex on site PP01-36 “Llipata” located on Pampa de Llipata, south of Palpa; measurement in the Horizontal Gradiometer Mode, SMARTMAG SM4G-Special in duo-sensor configuration; dynamics ± 13 nT in 100 greyscale values from black to white, sampling density 100 x 12,5 cm, interpolated to 25 x 25 cm, resolution increased by ‘Graduated Shade’ function; Earth’s magnetic field ca. 25000 nT; grid size 40 x 40 m;

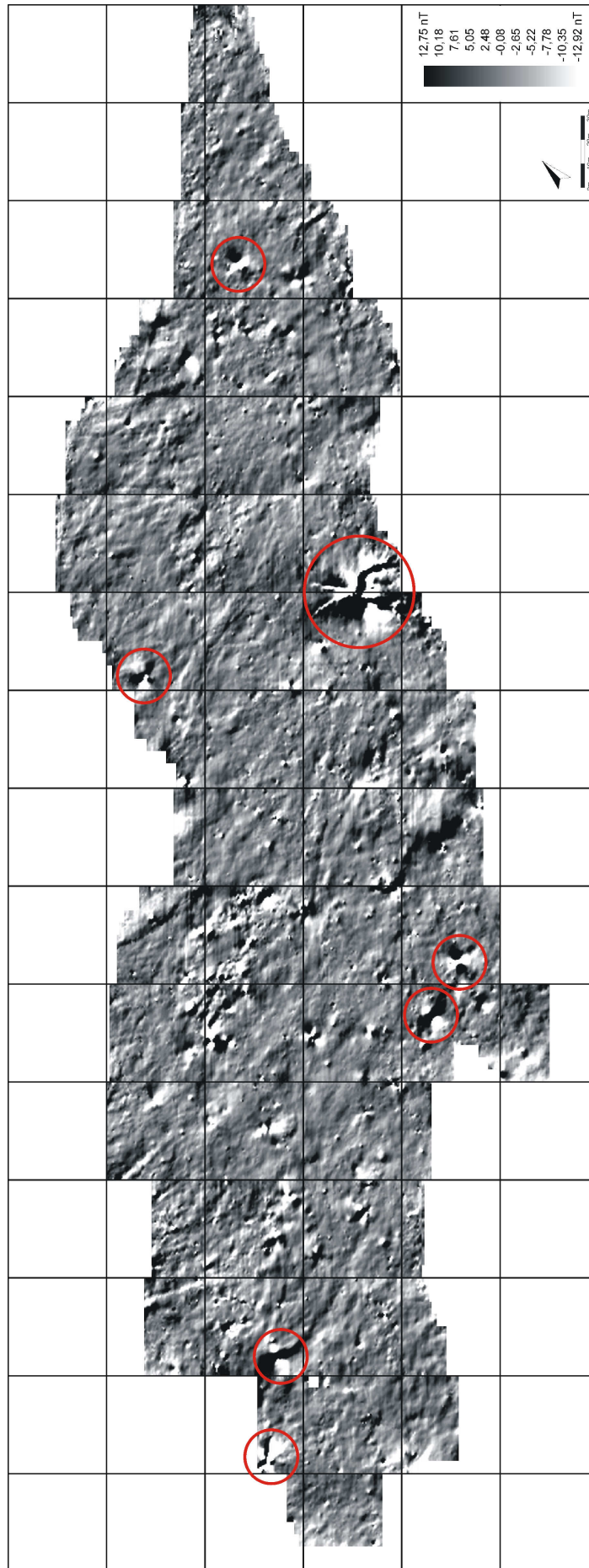


Figure 6.5. Location of the LIRM structures (red circles) superimposed on the total field magnetogram of the geoglyph complex on site PP01-36 “Llipata”, south of Palpa; Measurement with SMARTMAG SMAG-Special in duo-sensor configuration; dynamics +/- 13 nT in 100 greyscale values from black to white; sampling density 50 x 12,5 cm, interpolated to 25 x 25 cm, resolution increased by ‘Graduated Shade’ function; Earth’s magnetic field ca. 25000 nT; grid size 40 x 40 m;



Figure 6.6. Interpretation of the geograph complex on site PP01-36 “Llipata” plotted on the Horizontal Gradiometer Mode magnetogram; SMARTMAG SMAG-Special in duo-sensor configuration; dynamics +/- 13 nT in 100 greyscale values from black to white (with 50% of transparency applied), sampling density 100 x 12,5 cm, interpolated to 25 x 25 cm, resolution increased by ‘Graduated Shade’ function; Earth’s magnetic field ca. 25000 nT; grid size 40 x 40 m;

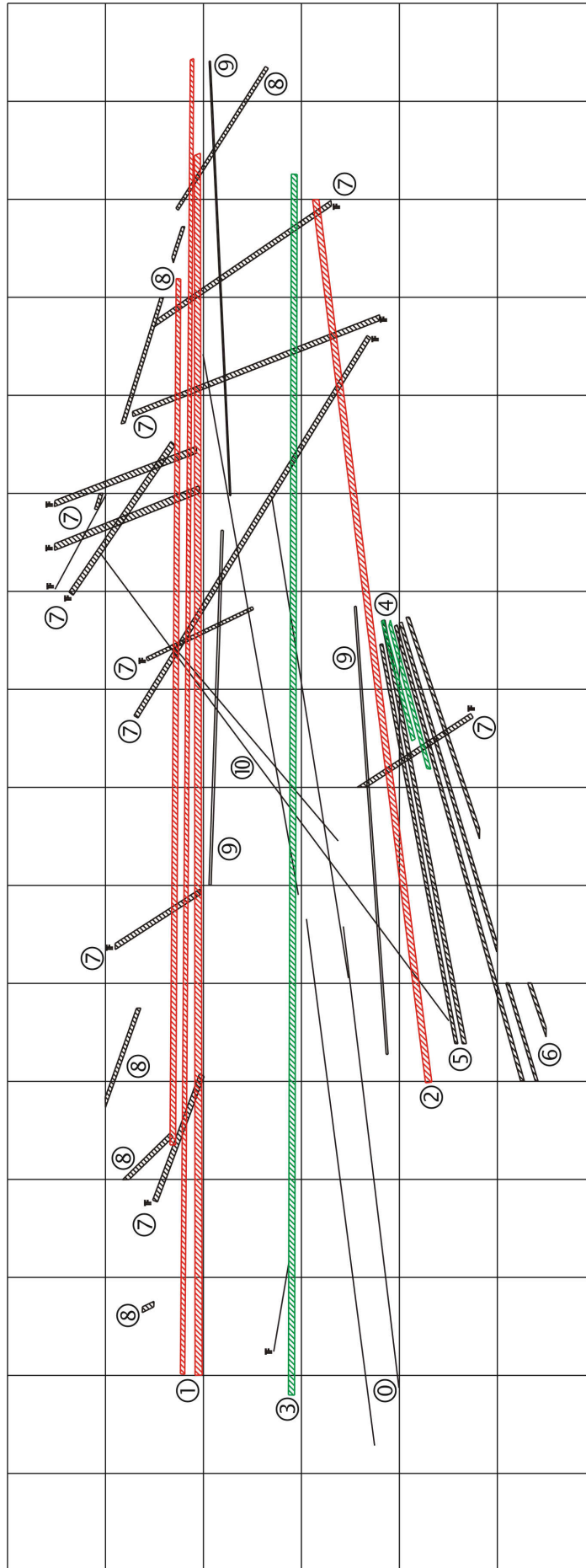


Figure 6.7. Interpretation of the geoglyph complex on site PP01-36 “Llipata” located on Pampa de Lipata, south of Palpa; red, green and black lines represent ancient linear structures found by geophysical prospecting combined with aerial photography; grid size 40 x 40 m; numbers ① - ⑩ correspond to the documented set of lines (see description in text)

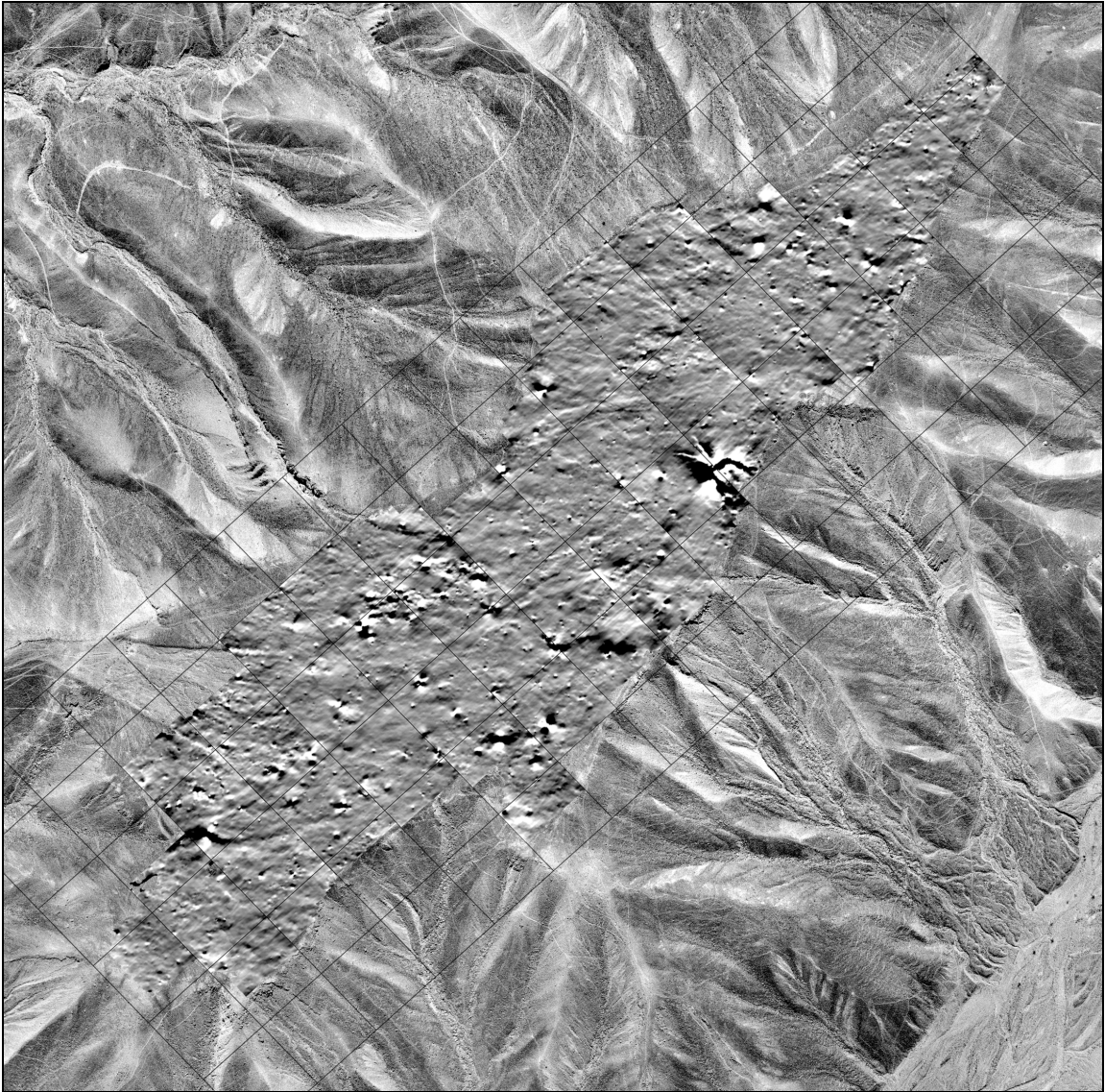


Figure 6.8. Magnetogram of the site PP01-36 “Llipata” superimposed on the orthophoto of the same area; Caesium SmartMag SM4G – Special applied in the duo-sensor configuration. Sampling rate 12,5 x 50 cm interpolated to 25 x 25 cm, grid size 40 x 40 meter, dynamics +/-20 nT, Earth’s magnetic field ca. 25.000 nT; orthoimage by K. Lambers, Institute of Geodesy and Photogrammetry, ETH Zürich, Switzerland.

In order to enhance the visibility of magnetic data, two sensors were arrayed in a horizontal gradiometer configuration (compare Chapter 5.2). To optimise the results it was necessary to set up a layout of the grid along the axis of the plateau and to position the probes in the same manner as it was used before in the total field mode. This enabled the recalculation of all former measurements as a differential mode. The application of the magnetometer in such an arrangement, in combination with the results of the total field magnetic data, enabled the crucial data enhancement to visualize so far undetected archaeological features. This allowed to trace older lines that had been obliterated during the construction of the larger trapezoids in the same place.

Figure 6.6 represents the interpretation of linear structures of both magnetic images in relation to aerial photographs of the geoglyph complex on site PP01-36. The red lines marked with the symbols ① and ② correspond to the major linear structures in this location. Those are the boundaries of the trapezoid and the nearest parallel flanking lines on the north-western side of the cleared area. Those lines are clearly visible in aerial images and magnetometry only confirmed their exact location. It is noteworthy however that as the line ② is an obvious south-eastern border of the trapezoid, in case of figure ①, magnetometry revealed three parallel stripes of anomalies, the very internal of which could be ascribed to the trapezoid margin, while the other two stand for the mentioned flanking lines. One of the most remarkable results on site, however, is the green line ③. It is a 500 m long structure, parallel to the set of lines ① within a distance of 40 m in the trapezoid's interior direction, right in the middle of the cleared area. Although the line is only partially visible for photogrammetric means, which leaves its verification in the sphere of assumption, it can be easily traced and confirmed by magnetometry. The location and the course of the line itself suggests that it might have been the first line on the plateau and/or served as an orientation strip during the construction of the trapezoid. However, judging from the similar structures on other investigated sites, the line presumably determined the previous edge of the cleared area, which was subsequently enlarged to the contemporary form.

On the south-eastern side of the trapezoid several further lines can be recognized. While the lines ⑤ and ⑥ can already be identified analysing orthoimages, two green lines marked with number ④ are the structures found only by the interpretation of the gradiometer magnetogram. Both of them, together with mentioned ⑤ and ⑥, constitute the south-eastern cluster of flanking lines. Those lines together with previously described ①, ② and ③ form the major linear design of the site.

Apart from it, a number of secondary lines may be distinguished. In the Figure 6.6 they are marked with the black hatched lines. Into this subclass fall lines ⑦ and ⑧, where former are identified by the total field measurement alone, while the later appear only in the gradiometer image. They are the elements of one of the first drawings on site, existing before the huge trapezoid was constructed. The most distinctive aspect is their direction, which is, depending on the line, approximately at an angle of 30° – 70° to the course of the north-western trapezoid margin. This together with the exact comparison with aerial images suggest that the most of those lines form the previously described zigzag line (see Figures

6.1, 6.2), which now, after magnetic analysis, could be in several places delineated on its whole extent, covering so far undetected fractions under the cleared area. The small parts of lines ⑦ and ⑧, however, do not match the zigzag stripe and therefore form the separate remains of some other previous lines, which presumably existed prior to trapezoid as well.

The last part of the interpretation image (Figure 6.6) make lines ⑨, ⑩ and ⑪. Those are supplementary lines of further category which are difficult to find in the magnetic images as they are generated by weak anomalies and naturally overprinted by the strong ones. Supposedly, they were narrow and/or not frequently walked on lines, which emerge only as faint variations of the geomagnetic field. However, as they are still noticeable, they supplement the whole image of the site. The location of lines ⑨ by the trapezoid margin implies the assumption that, despite inaccurate parallelism, they might have been traces of previous phases of the trapezoid construction, similarly to line ③. Unfortunately, it is not so clear regarding lines ⑩. Their direction is dissimilar to the main course of the other lines, which places the interpretation in the area of uncertainty. Small parts of them, however, can be found in the orthoimages outside the cleared area at the north-western side of the trapezoid (see Figures 6.1, 6.2). If so, that causes the lines ⑩ to be prolonged structures extended far until the very south-eastern side, but still enclosed in the trapezoidal area and therefore not visible for aerial photography. It is true also for lines ⑪ which lay entirely within the borders of trapezoid. They were detected exclusively by geophysical means and their direction, matching the course of the flanking lines ④, ⑤ and ⑥, may suggest some association with them. As far as the spiralled structure is concerned (Figures 6.1, 6.2), it is only partially visible in magnetic images. Such situation has been found also on other investigated sites and will be presented in due course of this study.

Chapter 7

Results of geophysical prospecting on site PV67A-15/16 “Yunama”

The geoglyph complex PV67A-15/16 is located to the west of Palpa, on a slightly inclined plateau over the river plain, halfway up to the southern hillside of the Cresta de Sacramento (Fassbinder et al. 2007) (Figure 7.1, see also Figure 3.4).

According to Lambers (2006) geoglyph sites on hillsides usually lack the complexity of sites on plateaus, since drawings are usually more separated from each other. Alternatively, they are more difficult to date in terms of relative and absolute chronology, since erosion has usually destroyed their stratigraphic sequence. Moreover, datable ceramics associated with geoglyphs on hillsides is not so frequently found as on plateaus. However, the placement of different geoglyph types on slopes indicates that the site was strongly developed in time. The anthropomorphic figures, which are the earliest features, are usually located on the steepest parts of the slopes. Most other types of the geoglyphs come from all periods, from Initial Nasca to Late Nasca (Table 2.1) and cannot be dated only on the basis of shape. Lineal geoglyphs originate from the common point on the edge of the plateau or they branch from the main line running downhill. Trapezoids, which are significantly smaller than those on plateaus, are located on the lower parts of slopes, where the inclination of the terrain is lower (Lambers 2006). Similarly to their plateau counterparts, they are flanked by meandering lines and/or spirals.

The most remarkable illustration of geoglyph complexes on sloped terrain makes the famous *Reloj Solar* (Sun Dial) (Figure 1.1) placed on Cresta de Sacramento. However, the site PV67A-15/16 (Yunama), which is located on the southern flank of the same ridge, also serves as an excellent example, although it is much more destroyed.



Figure 7.1. Orthophoto of the geoglyph site PV67A-15/16 from the Cresta de Sacramento, west of Palpa; K. Lambers, Institute of Geodesy and Photogrammetry, ETH Zürich, Switzerland

Apart from a series of smaller geoglyphs, the site PV67A-15/16 is dominated by a large trapezoid (geoglyph 52) (Figure 7.2), which is approximately 400 m long. Close to its narrow end, it crosses a diagonally oriented, earlier meandering line 55, which together with parallel (56), originally formed the northern part of the complex. Subsequently, by removing

the stones of the desert pavement between two lines, the initial drawing was converted into a huge cleared rectangle (57) (Fassbinder et al. 2007; Lambers 2006). Further alteration of the complex was the lateral enlargement of trapezoid 52 on its northwestern side (Lambers 2006).

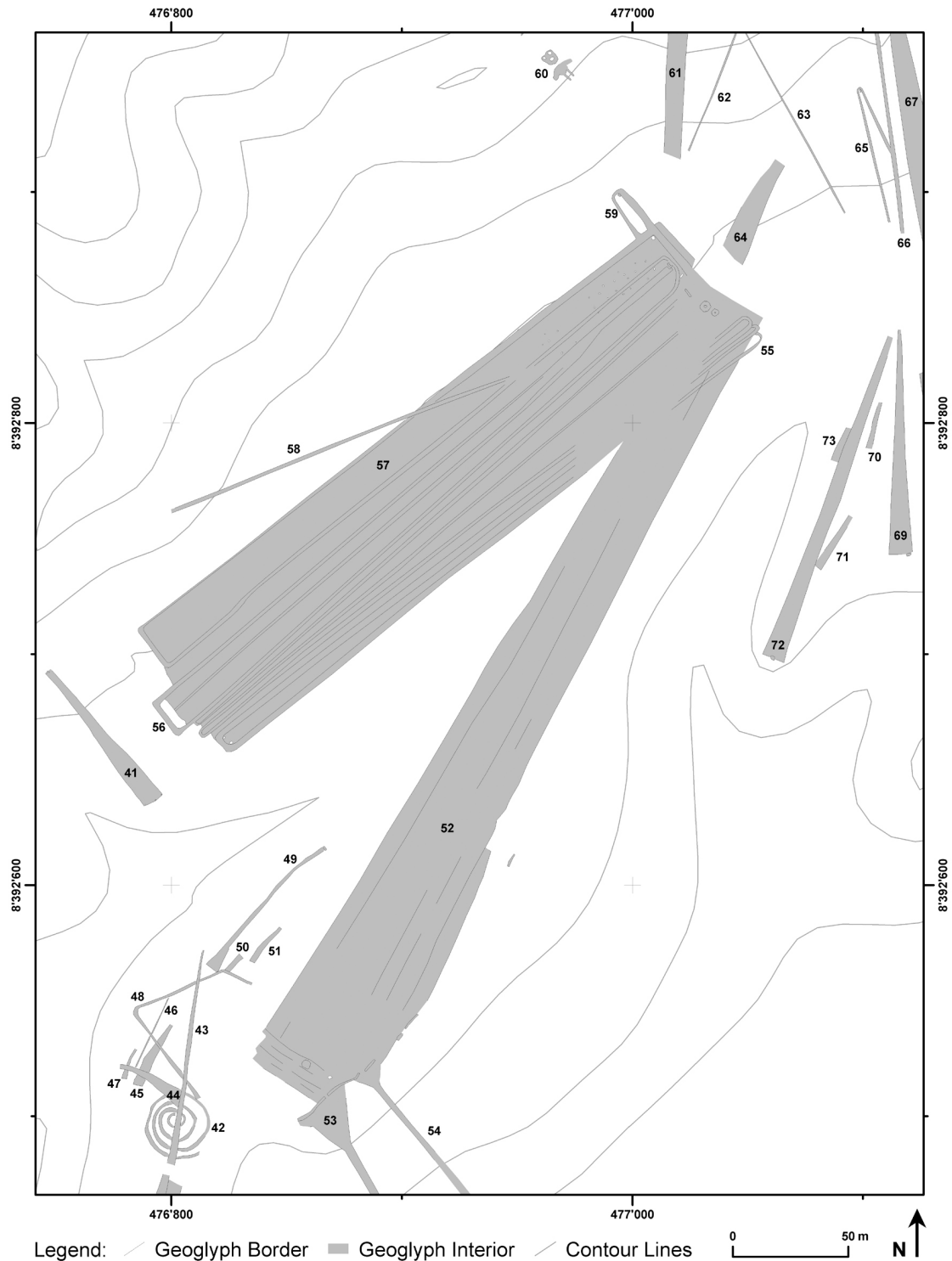


Figure 7.2. Detailed map of the geoglyph site PV67A-15/16 from the Cresta de Sacramento; the geoglyph assemblage with a stratigraphical sequence of different phases of construction and reworking drawn after an aerial photograph; K. Lambers, Institute of Geodesy and Photogrammetry, ETH Zürich, Switzerland

All drawings in this area, similarly to the other complexes, were first mapped with photogrammetric means. This basic documentation was then revised and complemented by on-site field observations carried out by archaeologists from the German Archaeological Institute. This part of the fieldwork encompassed detailed description of each geoglyph together with the recording of associated finds, the registration of the stratigraphic sequence of the geoglyphs, and trench excavations (Reindel et al. 2003). Eventually, a magnetometric prospection was undertaken (Fassbinder et al. 2007).

The surveying, carried out entirely in September 2004, was the second, after Llipata, large-area magnetic measurement of the whole geoglyph complex on the Peruvian desert. The investigation area approximates 440 x 220 m, in which 45 survey squares were placed. The site is strongly disturbed by modern footpaths and the frequent presence of goat herds pastured in the neighbouring *quebrada*. Therefore, many features in magnetic images are overprinted by this modern record and thus difficult to interpret. The detailed analyses of both resulting magnetograms (Figure 7.3 and 7.4) show that the trapezoid 52 has a different geological background than the rectangle 57. The granite rocks, abundant on the southern part of the site have the highest magnetic susceptibilities, which in magnetogram typically show up as a magnetic dipoles, making interpretation more difficult (Fassbinder et al. 2007; Fassbinder and Gorka 2009). The area of the rectangular geoglyph 57, free of granite rocks, is much more limited to small magnetic anomalies and so the magnetic image much better exposes concerning geoglyph construction elements. The magnetometer data show dynamics of +/- 20 nT and thus significantly differ from the Llipata (PP01-36) values (Fassbinder and Gorka 2007). Only on the topographically more to the edge exposed trapezoid 52, typical strong LIRM anomaly occurs. Unlike the other sites, the total field measurement alone gives surprisingly high-quality results, reducing the gradiometer mode image to the fine supplement outcome. It may be due to the localisation of the whole complex on the hillside and thus to resulting differences in geological background. Yet, it has to be stressed that the gradiometer image, similarly to all other sites, constitutes the major product on which the most important part of the interpretation work is based. Furthermore, this type of survey usually better reflects the constructional arrangements made of stone, known already from Llipata site.

Correspondingly, on site PV67A-15/16, during the archaeological fieldwork, two stone structures have been localised on the narrow end of the trapezoid 52, where several

geoglyphs (52, 55/56, 57) meet. Moreover, a single larger structure, close to the wide base of the drawing, was also found (Lambers 2006). Despite the fact that two former ones are not placed exactly on its central axis, but shifted a little bit in north-west direction, this typical combination of structures indicates that they were built as part of the trapezoid. Two looted stone heaps on the narrow end are nearly rectangular platforms used to deposit offerings of ceramic vessels, field crops, *Spondylus* shells, and fragments of crawfish. In between the platforms, the remains of a wooden post were found. Judging from the depth of buried remains it probably reached high above the ground. On the other end of the trapezoid, the bigger construction was excavated, which revealed that in the early stage it contained a room before it was converted into the platform as well. The remains of several smaller wooden posts associated with the first building stage were also found. Ceramics recovered from the platforms date to all phases of the Nasca era, indicating the use of the site between 1 BC and 600 AD. The location and stratigraphy of the stone structures show that although they are integrated part of the whole complex, they were built after the original construction of the trapezoid. Such sequence has been observed on other sites as well (Lambers 2006; Fassbinder et al. 2007).

Besides stone structures and traces of mentioned wooden posts, both magnetic images of the total field measurement (Figure 7.3) as well as the gradiometer one (Figure 7.4) revealed some regular anomalies indicating the presence of other constructional elements on site. Some of the structures may be ascribed to the remains of buildings, usually from later archaeological periods, the anomalies of others suggest the occurrence of pits. Some of them have been previously found by archaeological excavations and magnetometry only confirmed their presence on site. In the magnetic image they are difficult to trace and might be easily misinterpreted, however, since they usually possess equal intensities, they demonstrate similar constructional practices. It is confirmed with the fact that they are filled in the same way with the material of higher magnetic susceptibility such as burnt objects or pottery sherds (Fassbinder et al. 2007; Fassbinder and Gorka 2009).

The intensity itself is a frequently used technique during the interpretation process. It assists in finding regularities in setting of anomalies by the identification of equal values and allows to distinguish desirable archaeological structures from the confounding modern constructions as well as from the geological background and strong lightning magnetization. It was one of the fundamental tools used on PV67A-15/16 and other Peruvian sites.

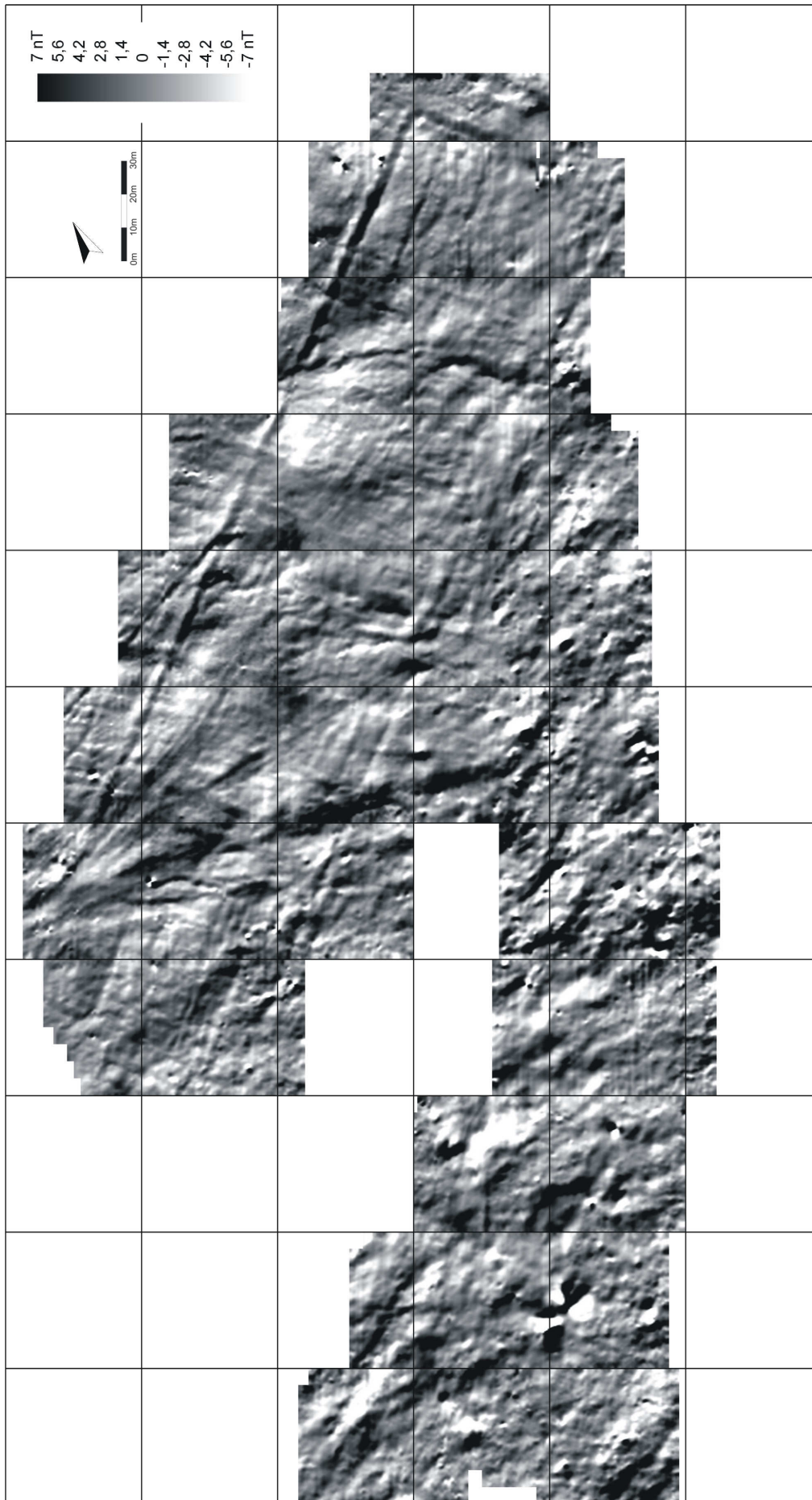


Figure 7.3. Magnetogram of the geoglyph complex on site PV67A-15/16 “Yunama” located on Cresta de Sacramento, west of Palpa; measurement in the Total Field Mode, SMARTMAG SM4G-Special in duo-sensor configuration; dynamics +/- 7 nT in 100 greyscale values from black to white, sampling density 50 x 12,5 cm, interpolated to 25 x 25 cm, resolution increased by ‘Gratuaded Shade’ function; Earth’s magnetic field ca. 24000 nT; grid size 40 x 40 m;

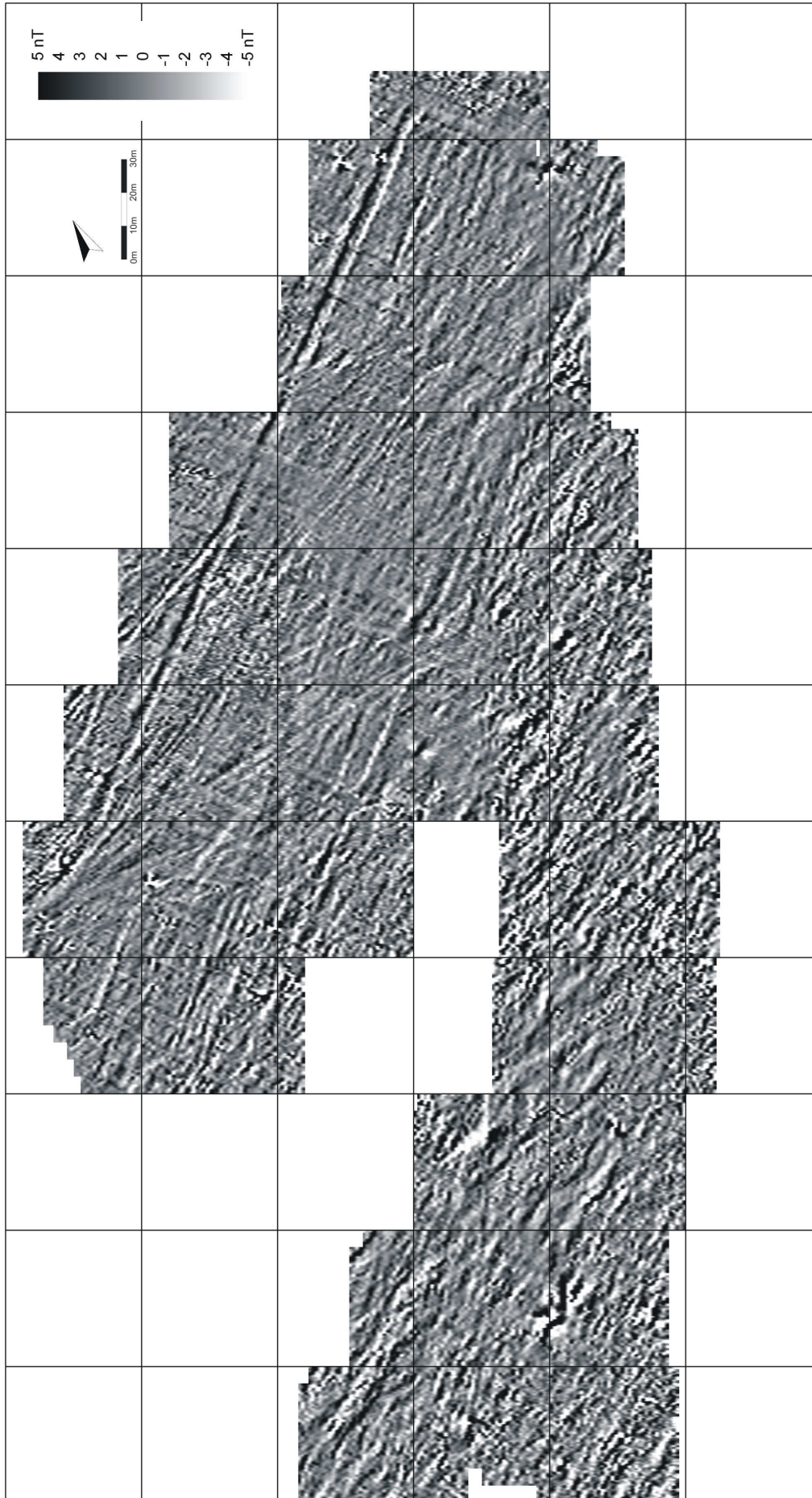


Figure 7.4. Magnetogram of the geoglyph complex on site PV67A-15/16 “Yunama” located on Cresta de Sacramento, west of Palpa; measurement in the Gradiometer Mode, SMARTMAG SM4G-Special in duo-sensor configuration; dynamics +/- 5 nT in 100 greyscale values from black to white; sampling density 100 x 12,5 cm; interpolated to 25 x 25 cm, resolution increased by ‘Graduated Shade’ function; Earth’s magnetic field ca. 24000 nT; grid size 40 x 40 m;

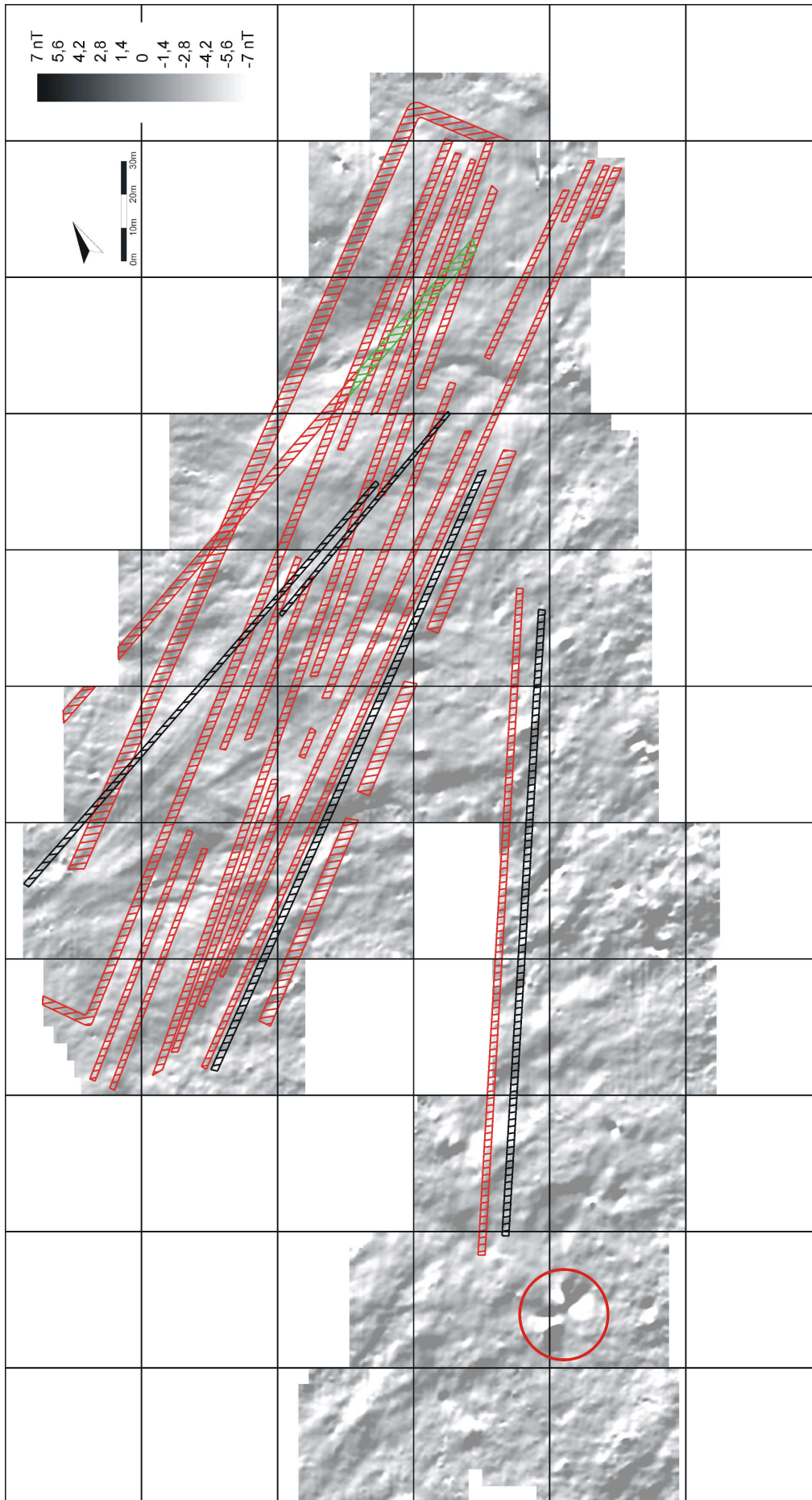


Figure 7.5. Interpretation of the geoglyph complex on site PV67A-15/16 “Yunama” plotted on the Total Field Mode magnetogram; SMARTMAG SM4G-Special in duo-sensor configuration; dynamics +/- 7 nT in 100 greyscale values from black to white (with 50% of transparency applied); sampling density 50 x 12,5 cm, interpolated to 25 x 25 cm, resolution increased by ‘Graduated Shade’ function; Earth’s magnetic field ca. 24000 nT; grid size 40 x 40 m; red circle – location of the LIRM structure.

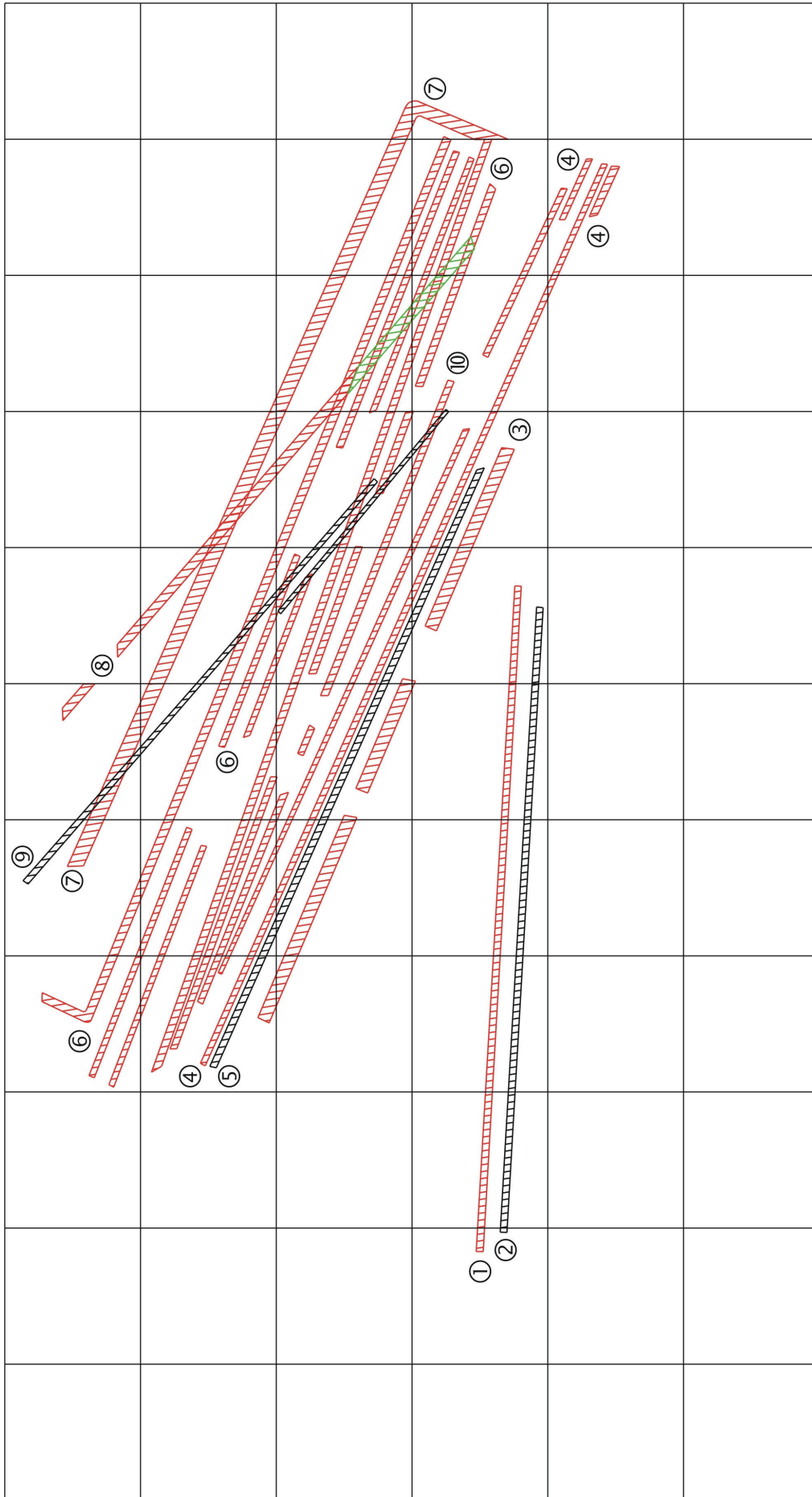


Figure 7.6. Interpretation of the geoglyph complex on site PV67A-15/16 “Yunama” located on Cresta de Sacramento, west of Palpa; red, green and black lines represent ancient linear structures found by geophysical prospecting combined with aerial photography; ; grid size 40 x 40 m; numbers ① - ⑩ correspond to the documented set of lines (see description in text)



Figure 7.7. Magnetogram of the site PV67A-15/16 “Yunama” superimposed on the orthophoto of the same area; Caesium SmartMag SM4G – Special applied in the duo-sensor configuration. Sampling rate 12,5 x 50 cm interpolated to 25 x 25 cm, grid size 40 x 40 meter, dynamics +/- 7 nT, Earth’s magnetic field ca. 25.000 nT; orthoimage by K. Lambers, Institute of Geodesy and Photogrammetry, ETH Zurich, Switzerland.

Except some mentioned stone assemblies, the interpretation work on site PV67A-15/16, likewise other complexes, was concentrated mainly on linear structures. They are

the most important features and predominate types of prehispanic geoglyphs found on the large flat plateaus (compare Chapter 2). The final interpretation result represent Figures 7.5 and 7.6, however, in case of site PV67A-15/16, for the first time the supplementary 3D-like visualisation (Figure 7.8) was made.

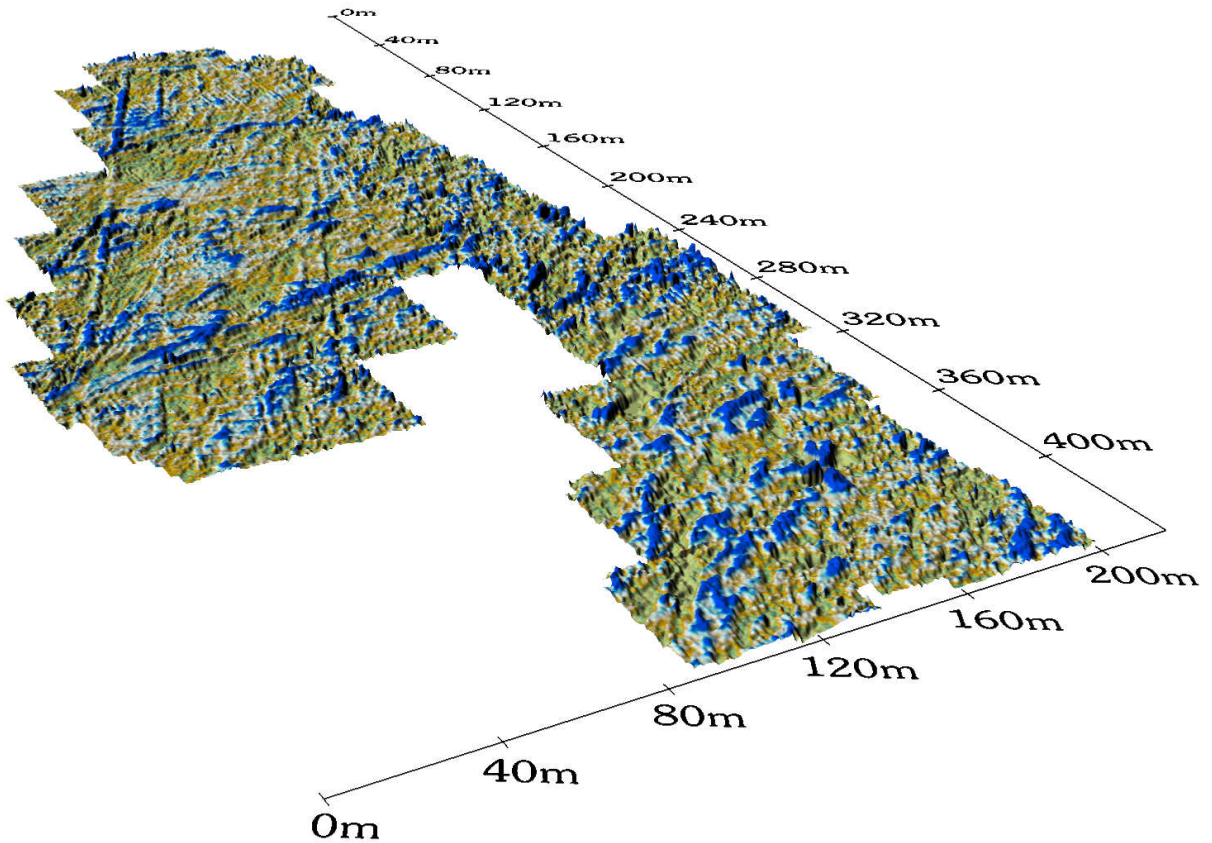


Figure 7.8. Magnetogram of the Total Field measurement on site PV67A-15/16 in a 3D-like visualisation seen from SW at the view angle 24°; Caesium SmartMag SM4G – Special applied in the duo-sensor configuration. Sampling rate 12,5 x 50 cm interpolated to 25 x 25 cm, grid size 40 x 40 meter, dynamics +/- 7 nT in colour spectrum values from green to blue; Earth’s magnetic field ca. 25.000 nT; top of the image pointing NE.

The red and black lines marked with the symbols ① and ② (Figure 7.6) correspond to the only remains of the trapezoid 52 that were found in both magnetic images. This scarceness is due to the mentioned high magnetic susceptibilities of granite rocks. In this case, the aerial photography clearly prevailed over the magnetic prospecting, seeing that more features could have been recognised by photogrammetric means. However, the line ② makes an outstanding result alone, since it confirms the presence of the inner structure, which could have served as a trapezoid margin, before it was enlarged to the present form.

The lines ③ to ⑩ compose the rectangular area 57. While the line ⑦ is an obvious northern boundary of the trapezoid, clearly limited by heaped stones, the southern

fraction is fragmentally obscure and not so understandable. Whereas the aerial photography proves the existence of the meandering line 55 on the south-eastern border, the geophysics verifies those results with analogue lines ③, ④ and ⑤. However, as lines ④ and ⑤ could be indeed the residual fragments of the regarded meandering feature, the lineal anomaly ③ might be either the part of the same structure or an additional south-eastern trapezoid margin. Analysing the magnetogram superimposed on the aerial image (Figure 7.7), the latter seems to be logical as the feature ③ occurs slightly to the south of the line 55.

The superimposed images make up an excellent tool for exact location of magnetic anomalies in terrain and for evaluation of differences in aerial and geophysical means. The method relies on overlying the magnetogram on orthoimage with a varying level of transparency, which gives a fine possibility to identify new findings and compare them with the previous results. In such a way the line ③ suggests the occurrence of the south-eastern border, which in comparison to carved meandering line is a heaped feature created by deposition of material removed from the mentioned line or from the whole rectangular area. If so, the line ③ reveals no bright layer of sand and silt, which could contrast with the surrounding surface, and therefore is not as strong visible for photogrammetric techniques as the lines ④ and ⑤. Although the line ⑤ undoubtedly belongs to the same meandering feature as line ④, it is formed only by a faint anomaly, which not evidently match any visible lineal structure in an aerial image. The line ⑤, marked black in Figure 7.6, could be therefore classified either as a newly found branch of the meandering feature 55 or only as a reverse anomaly of the line ④ (see Chapter 4.4 and 5.3). The latter seems to be reasonable as both structures occur close to each other.

The other meandering structure on site makes the line 56 (Figure 7.2), which in interpretation image (Figure 7.6) is presented by a series of lines marked with number ⑥. This feature is a similar drawing to the described lines ④ and ⑤, however, it has a slightly different course, approximately 3 - 4° closer to the north – south direction. Although it is difficult to determine if both features constitute the one continuous structure or form two different patterns, it is obvious that they were created at the same time and existed together, before they were transformed into the huge rectangular area 57. Some parts of the line ⑥ are not visible in magnetic images, as the whole complex is strongly destroyed by goat's pathways that cross the site in several places. For that reason the continuity of the line is only assumed. Generally, the line ⑥ matches its photogrammetric equivalent 56 and

consists of five parallel lines, which indeed form one meandering structure, judging from several linking curves, observed on orthoimages. Those curves, oriented 90° to the course of the lines, have not been detected by magnetometry, what in effect makes a noteworthy result, described in more detail by the way of partially discerned spirals on site PV67A-47 “Sacramento” (Chapter 8).

From the hillside above the rectangle 57, a straight line ⑧ runs in north-eastern direction towards the set of lines ⑥. It is cut by the northern section of them, which would suggest that the line ⑧ is older. However, as the stratigraphic relation with rectangle 57 was not clear on the basis of evidence from surface observations and aerial images alone, magnetometry helped to resolve this question by revealing a continuation of line ⑧ beneath the north-eastern part of the rectangular geoglyph 57 (green line in Figure 7.6). The line points directly to one of the mentioned stone platforms at the narrow end of trapezoid 52 and ends up in a pit (Fassbinder et al. 2007). This is one of the most remarkable results on site, demonstrating the clear relation of stone structures with the drawings. The similar relation reveals line ⑩, which as the transition drawing between meandering features ④ and ⑥, also aims the same stone platform. More significant, however, is the detection of line ⑨, the course of which is parallel and lays 30 – 35 m to the south of the line ⑧. The presence of this most likely multiple but fragmentary line, found in a gradiometer image, utterly changes the conception of discussed line ⑧. It may no longer be regarded as a single line pointing the stone platform, but as a trapezoid margin, which together with line ⑨, delimits an early stage rectangle running down the hill in SW – NE direction. This geoglyph crosses the northern part of the whole complex and ends up far beyond hitherto assumed cleared area borders. Additionally, with the rectangle 57 and the trapezoid 52 as well as with the meandering lines ④ and ⑥, it has one common point laying precisely on line ⑧. The exact location of this point matches previously described stone platform, which in this case earns an additional meaning and becomes the most significant point of the whole complex.

On site PV67A-15/16 a wooden scraper, presumably used for flattening and cleaning the linear geoglyphs, was found. Since the ¹⁴C dating revealed the age of the tool for around 1300 AD, the time period in which the geoglyphs were in use, may be assumed to be longer than it was previously believed. It must be noted, however, that at this time, all constructional activities have been already abandoned and only actions of cleaning and preservation maintained (Fassbinder et al. 2007).

Chapter 8

Results of geophysical prospecting on site PV67A-47 “Sacramento”

The site PV67A-47 occupies the central part of the main plateau of Cresta de Sacramento above the famous *Reloj Solar* geoglyphs (Figure 1.1) on the southern slope of the ridge. Although the eastern end of the complex has been destroyed by a Late Intermediate Period site (Table 2.1) already in prehispanic times, its location close to the tourist point over *Reloj Solar* has led to regular presence of people on the main geoglyphs and consequently to the further destruction. Additionally, although the site is located far from the main roads, many parts of it have been marked by modern car tracks. Fortunately, the preserved amount of drawings is enough for the detailed study of the development of this significant geoglyph complex (Lambers 2006).

The one of the earliest geoglyphs constructed on site was the zigzag line (183) (Figure 8.3), which linking the neighbouring site on the same plateau, crosses the free space between them and immerses under the later constructions on site. The zigzag line, which dominated the site at the beginning, was afterwards accompanied by several isolated straight lines (184 and 205) and the second line of the same shape (203). Both were subsequently covered by the large trapezoid (189), on which the ceramics date to the early phases of the Nasca period (Lambers 2006). Two spirals (206, 208) on the northern edge of the site were constructed at the same time, just like several lineal geoglyphs (190, 193, 202) flanking the main trapezoid. The S-shaped spiral (206), remodelled during later constructional activities to 207, was created at the same time as the aeral geoglyph (196). By Middle Nasca times, several lineal geoglyphs were added on the southern side of the main trapezoid (195, 199-201) and on its western end (187). The spirals on its northern side were partially cut or

covered by several lines (191, 210) as well as one of the smallest registered trapezoids (209). Additionally, the narrow end of the central trapezoid (189), was converted into a large rectangle (213). In Late Nasca times, the largest trapezoid on Cresta de Sacramento (188) has been constructed. It cuts through most of the existing lines and the trapezoid 189 at an angle. According to Lambers (2006), it was oriented in the way that it made the best use of the remaining free space on both sides of the central complex of geoglyphs. Additionally, close to its narrow end, the trapezoid partially covered unfinished areal geoglyph with sherds of later archaeological phases on it. The presence of Late Intermediate Period findings on this part of the site, is probably due to the construction of buildings from this phase, which is the evidence for later activities on site, not related to the drawings. For that reason, later alterations of the site will not be described further. For more information about the complex arrangement and constructional sequences on site PV67A-47 see Lambers (2006).

The magnetic prospecting, accomplished throughout the September 2005, was the largest, in terms of an area coverage, geophysical investigation carried out on the Peruvian geoglyphs. The measurement, reaching 720 x 240 m, contains 79 complete and shortened survey squares, which makes the investigation on site PV67A-47 the foremost achievement in large-area magnetic surveying in Peru. Moreover, the density of drawings, the variety of geoglyph repertoire as well as its complex stratigraphical sequence, places the site atop of the most important assemblages of the region. Therefore, also the geophysical investigation was believed to bring the most spectacular results of all sites. Likewise other complexes, it was possible to detect pits and older lines beneath the trapezoidal areas. The diversity of forms, however, allowed for the first time to identify new shapes, which so far has not been detected by magnetic methods on the previously measured locations. The site PV67A-47 is particularly rich in spiral elements, which concentrated on the northern side of the main trapezoid (Figures 8.1 to 8.3), form an extraordinary pattern, supplementing the whole assemblage. Although pits were found also in the centre of the spiral, the spiral itself has turned out to be visible only partially in the total field magnetic image (Figure 8.4). The visibility was best in the west – east oriented parts, which fading away towards north and south, disappeared entirely in the north – south course. The similar result was also observed on site PV67A-15/16, regarding undetected curves of meandering lines (see Chapter 7).

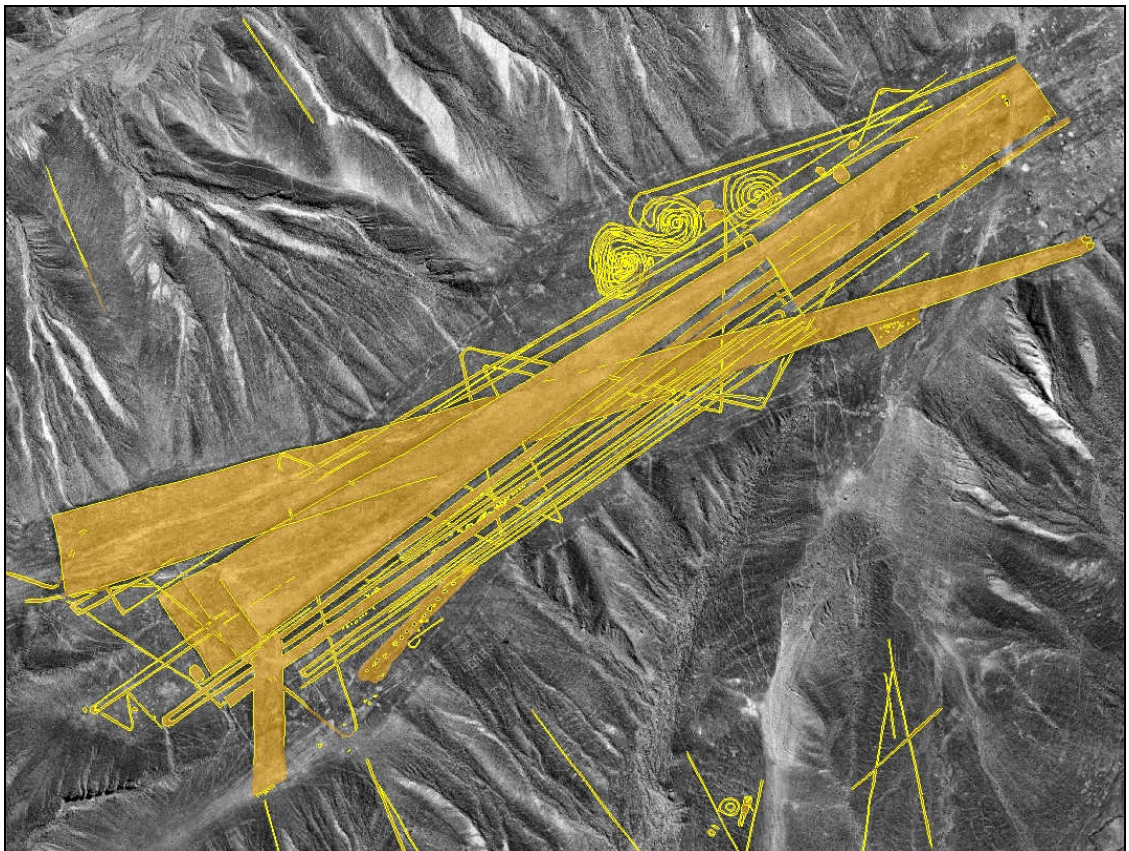
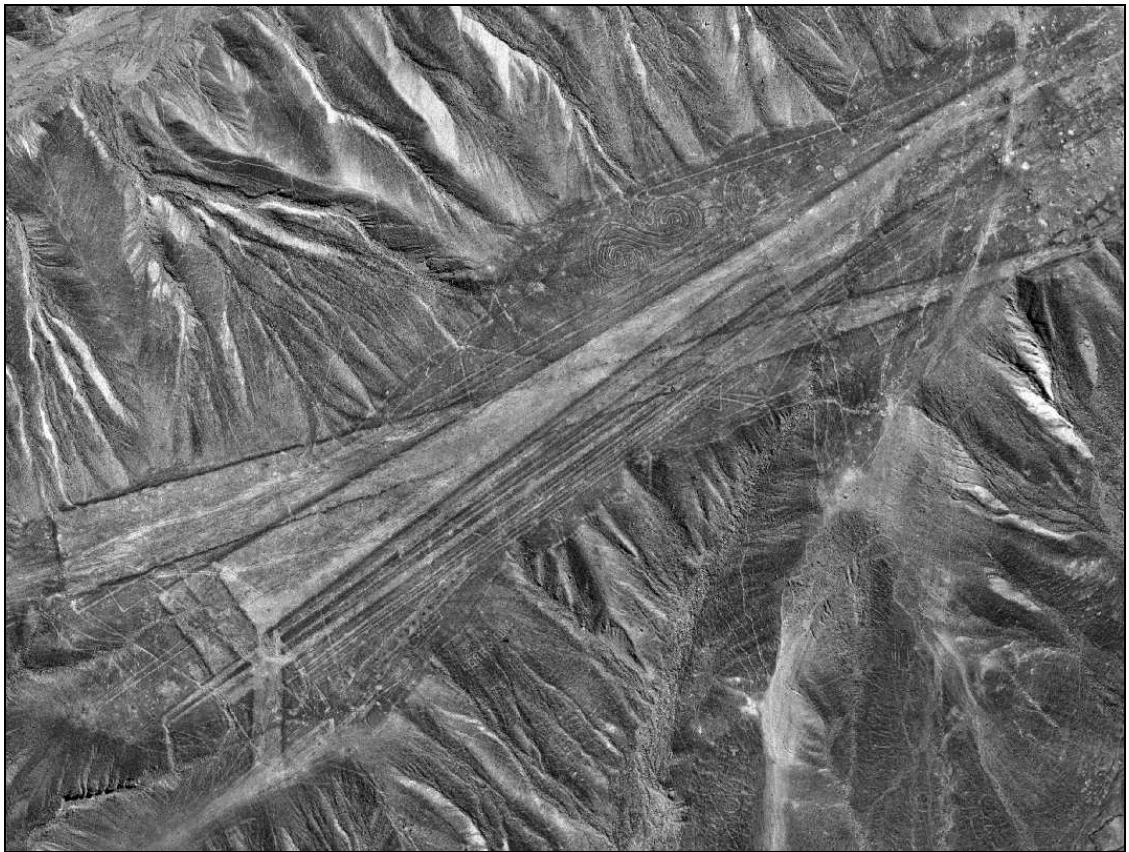


Figure 8.1. Orthophoto of the geoglyph site PV67A-47; Cresta de Sacramento, north of Palpa (upper);
Figure 8.2. Interpretation of geoglyphs on site PV67A-47 (lower); K. Lambers; Institute of Geodesy and
Photogrammetry, ETH Zürich, Switzerland

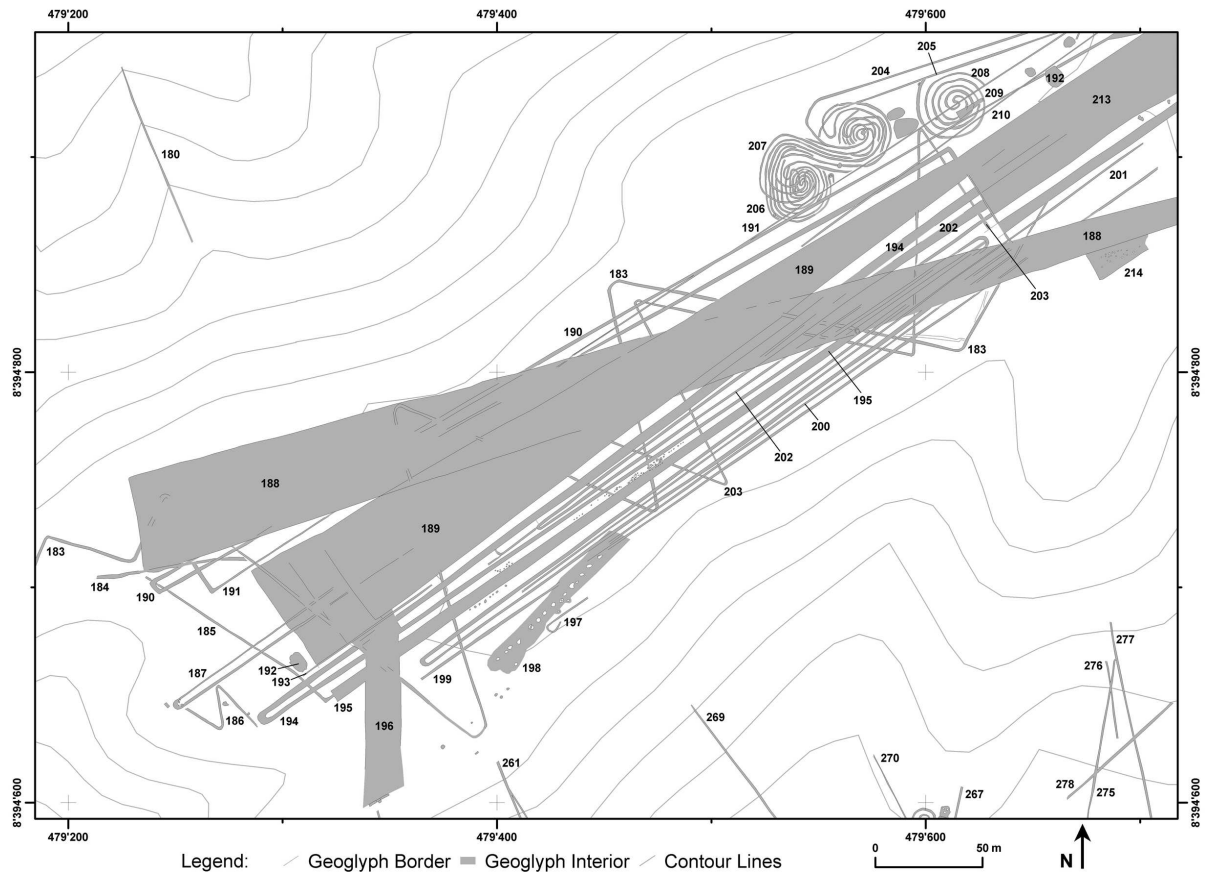


Figure 8.3. Detailed map of the geoglyph site PV67A-47 from the Cresta de Sacramento; the geoglyph assemblage with a stratigraphical sequence of different phases of construction and reworking drawn after aerial photograph (Figure 8.1); K. Lambers, Institute of Geodesy and Photogrammetry, ETH Zürich

In both cases the visibility was due to the asymmetry of magnetic anomalies, which is most marked in a magnetic north – south direction while it disappears for the magnetic east – west profiles across the anomaly (Linington 1970) (see Chapter 4.4). Although profiles in magnetic north – south course are of more practical value, for operative reasons, the grid was usually oriented after the long axis of the plateau, which not always matched the geographical north – south direction. Therefore, the visibility, especially in gradiometer images, might have been affected by the traverse orientation, which was additionally influenced by the shallow inclination of the geomagnetic field. The small angle of dip might have had an enormous effect on the shape of magnetic anomalies over some parts of spirals and other skewed structures, making them invisible for magnetic site exploration techniques. Given that the curves on site PV67A-15/16 match precisely the course of undetected spiral parts on PV67A-47, and that both sites were measured in similar northeast – southwest direction, the suggestion that the visibility was dependant on the layout and the geographical orientation of the magnetometer survey grid, has confirmation in both magnetic

measurements. Nevertheless, it must be stressed that the visibility is a complex function of the anomaly shape, geomagnetic inclination and the grid orientation.

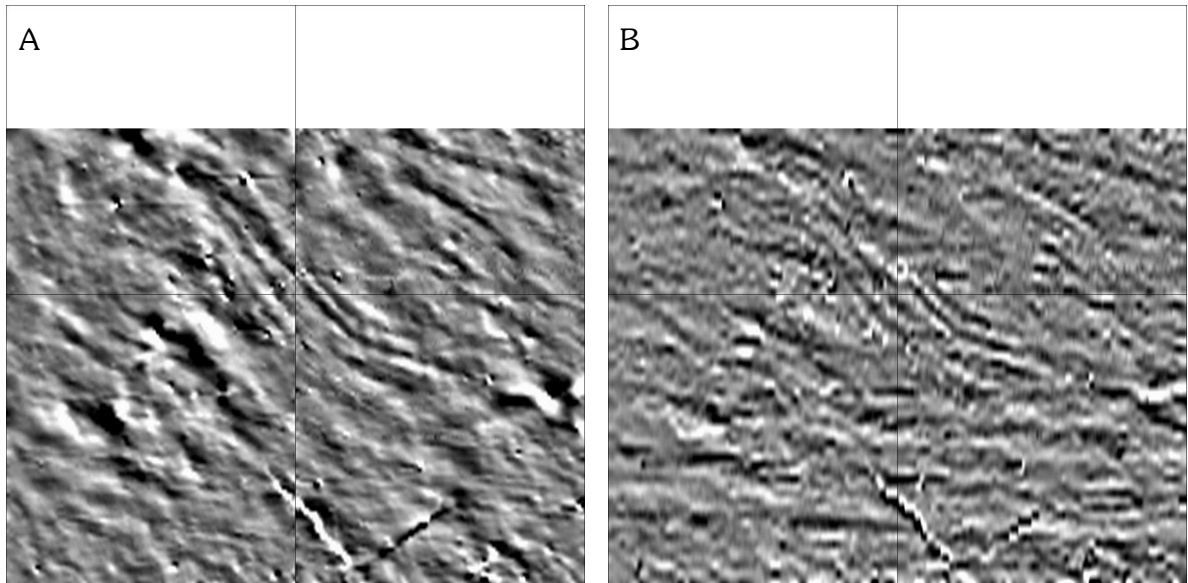


Figure 8.4. Magnetogram of the spiral structures on site PV67A-47 “Sacramento”; A – Total Field measurement with Caesium SmartMag SM4G – Special applied in the duo-sensor configuration; sampling density 12,5 x 50 cm interpolated to 25 x 25 cm, dynamics +/-10 nT; B – recalculated Gradiometer image of the same structure; sampling increment 12,5 x 100 cm interpolated to 25 x 25 cm; dynamics +/-18 nT; grid size 40 x 40 meter; Earth’s magnetic field ca. 25.000 nT

The partially discerned spirals from Sacramento not only forced the discussion on the cause of their fragmentary visibility but also for the first time originated the idea of the new application of the total field magnetometer in a horizontal gradiometer configuration. For this purpose it was not necessary to re-measure the entire area, but to use a previous twin sensor arrangement for a gradient recalculation. Although the following outcome, regarding spirals, proved to be only to some extent satisfactory (Figure 8.4), the result for the rest of the site was astounding. The geoglyphs which were not visible for a single total field sensors have been converted into the clear anomalies in the gradiometer mode.

The only disadvantage of gradiometer data reprocessing was the twofold reduction of resolution in the traverse direction. The distance between two neighbouring lines fell from 0,5 m to 1 m, as one-line-march did not provide values of two sensors, but the gradient between them. Nevertheless, after resampling and interpolation or in some cases following application of Graduated Shade technique (see Chapter 5.3), gradiometer images were obtained, which offer much better results than their total field counterparts. It must be stressed, however, that plenty of structures were discovered only in the total field mode.

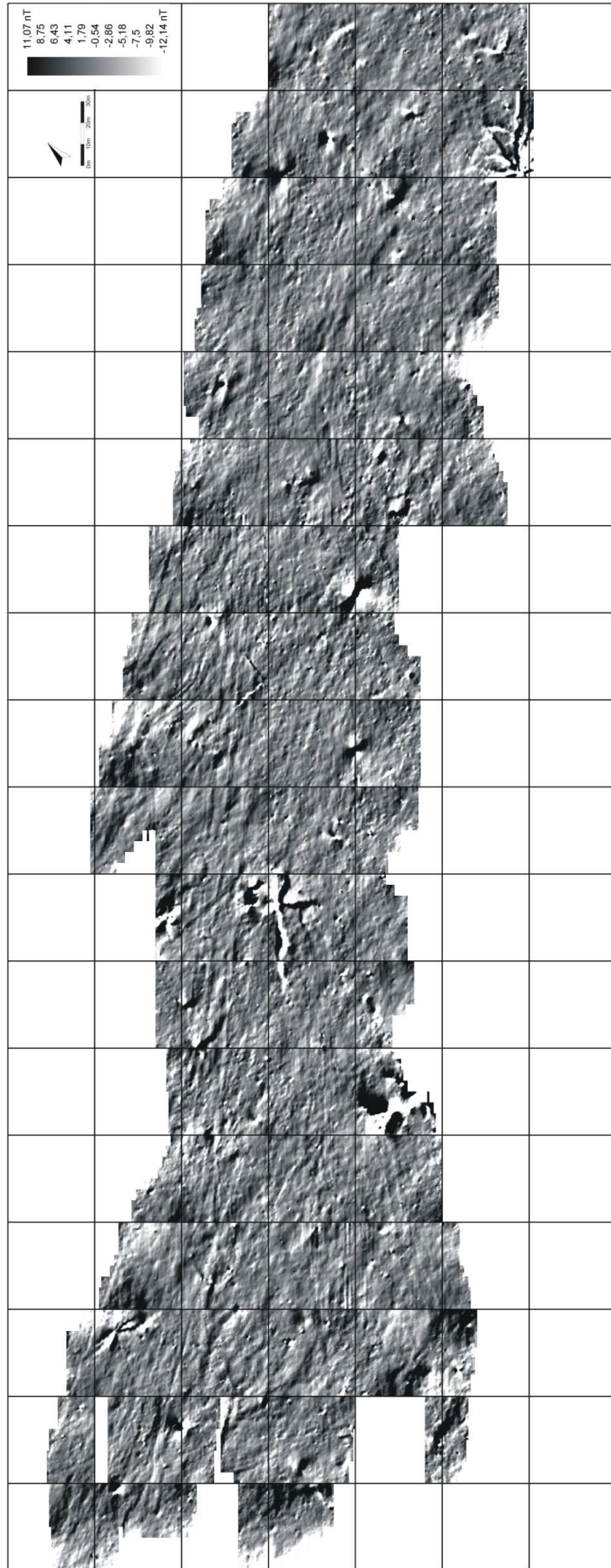


Figure 8.5. Magnetogram of the geoglyph complex on site PV67A-47 “Sacramento” located on Cresta de Sacramento, north of Palpa; measurement in the Total Field Mode, SMARTMAG SM4G-Special in twin sensor configuration; dynamics approx. +/- 12 nT in 100 greyscale values from black to white, sampling density 50 x 12,5 cm, interpolated to 25 x 25 cm, resolution increased by ‘Graduated Shade’ function; Earth’s magnetic field ca. 25000 nT; grid size 40 x 40 m;

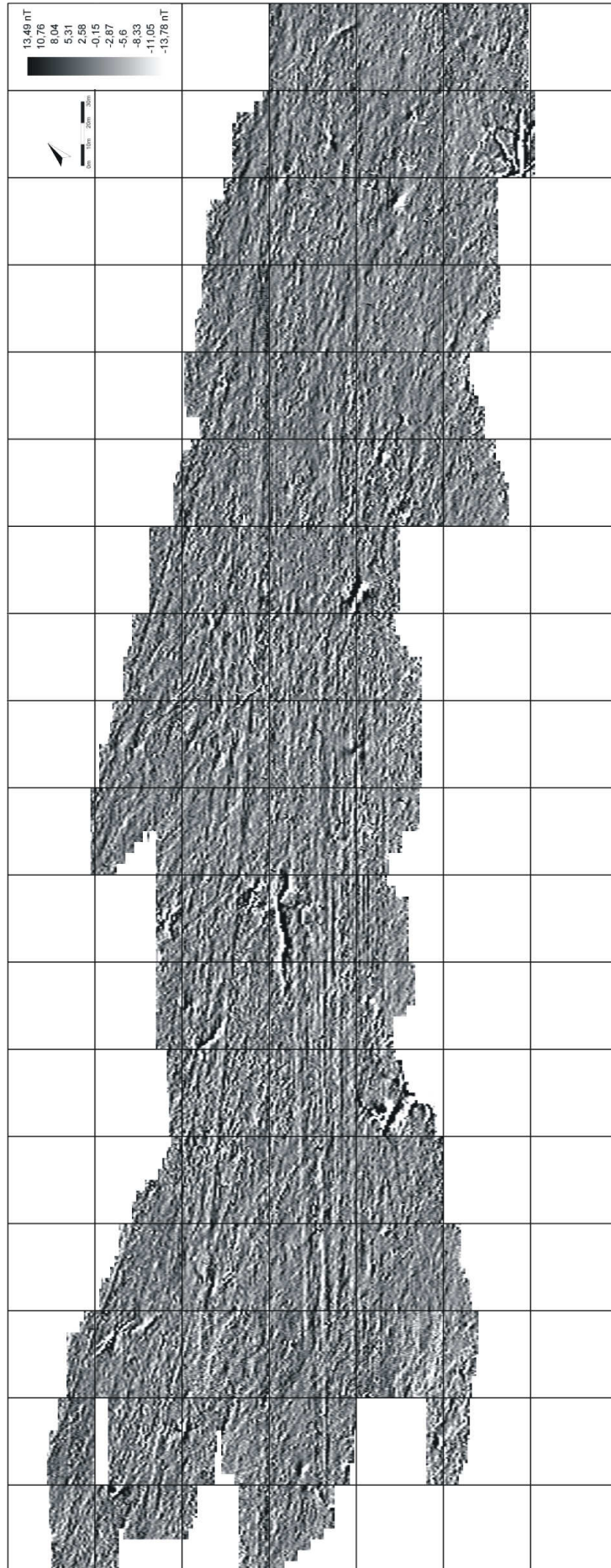


Figure 8.6. Magnetogram of the geoglyph complex on site PV67A-47 “Sacramento” located on Cresta de Sacramento, north of Palpa; measurement in the Gradiometer Mode, SMARTMAG SM4G-Special in twin sensor configuration; dynamics approx. +/- 13 nT in 100 greyscale values from black to white, sampling density 100 x 12,5 cm, interpolated to 25 x 25 cm, resolution increased by ‘Graduated Shade’ function; Earth’s magnetic field ca. 25000 nT; grid size 40 x 40 m;

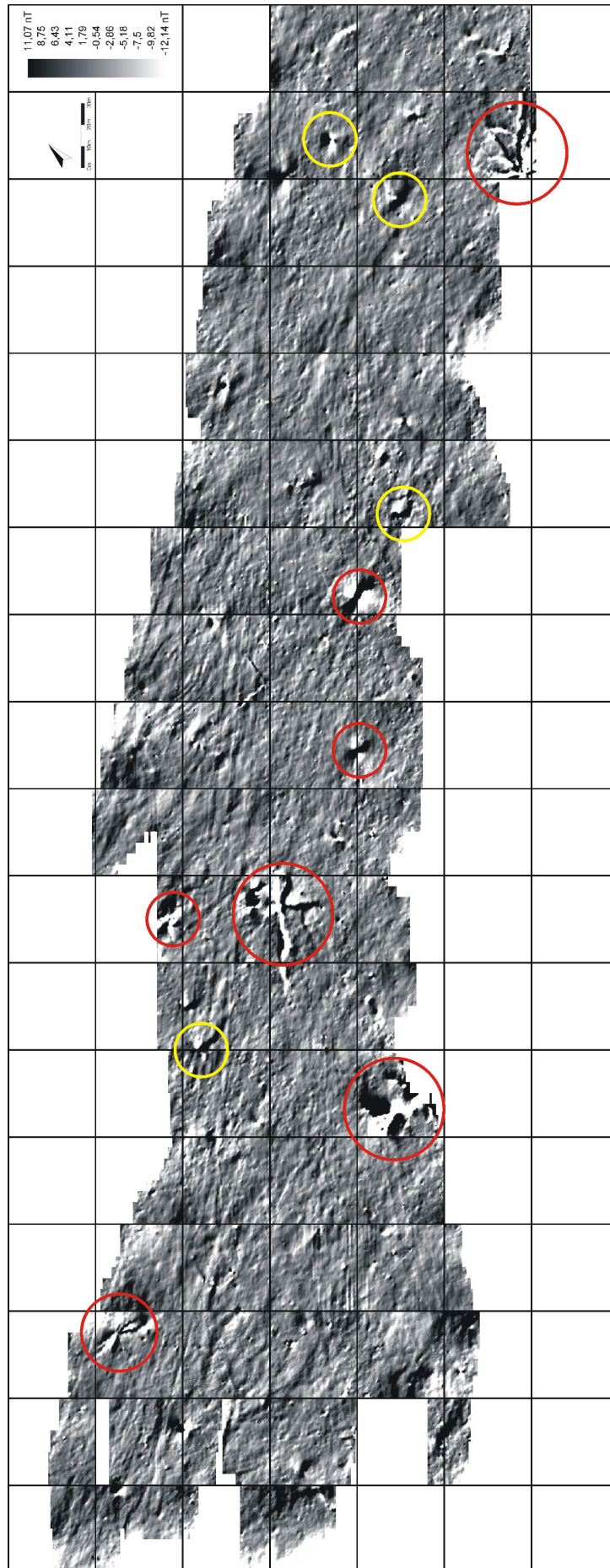


Figure 8.7. Location of the LIRM structures (red circles) and possible LIRM structures (yellow circles) superimposed on the total field magnetogram of the geoglyph complex on site PV67A-47 “Sacramento”, north of Palpa; SMARTMAG SMAG-Special in duo-sensor configuration; dynamics +/- 12 nT in 100 greyscale values from black to white; sampling density 50 x 12,5 cm, interpolated to 25 x 25 cm, resolution increased by ‘Graduated Shade’ function; Earth’s magnetic field ca. 25000 nT; grid size 40 x 40 m;

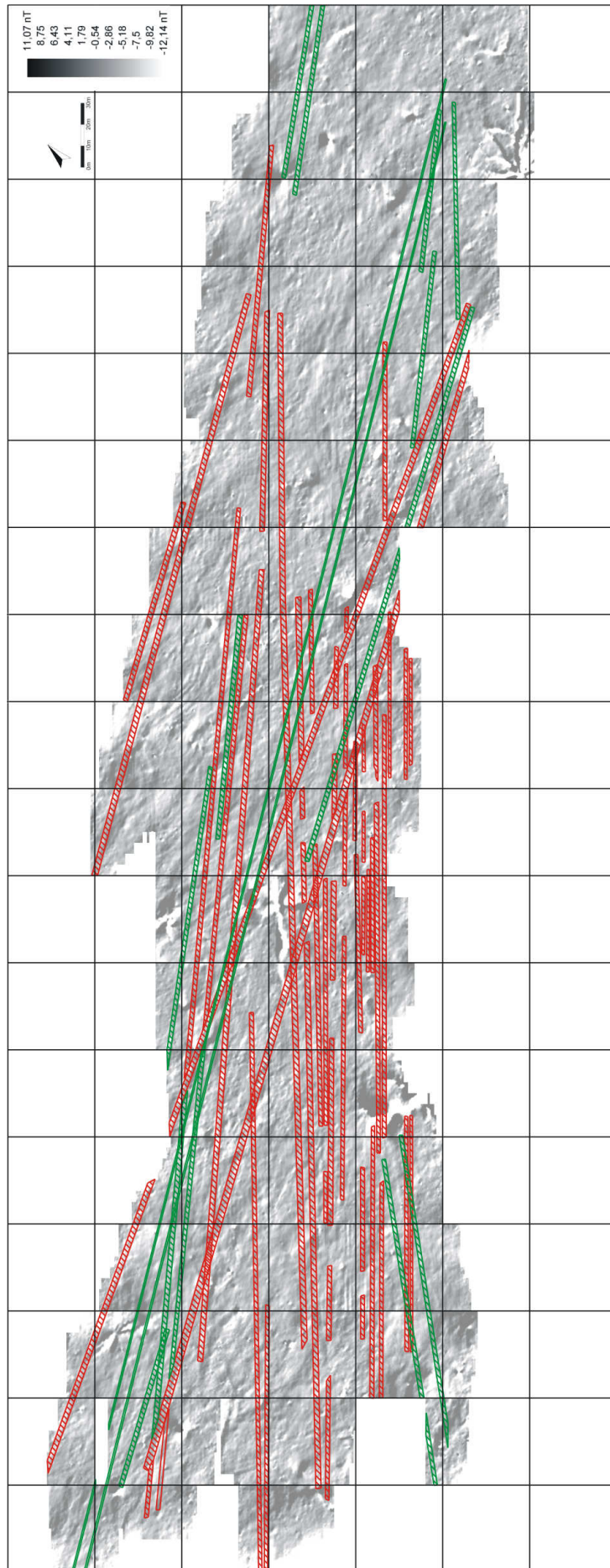


Figure 8.8. Interpretation of linear structures (red and green) on site PV67A-47 “Sacramento” plotted on the Total Field Mode magnetogram; SMARTMAG SMAG-Special in duo-sensor configuration; dynamics approx. +/- 12 nT in 100 greyscale values from black to white (with transparency factor 50%), sampling density 50 x 12,5 cm, interpolated to 25 x 25 cm, resolution increased by ‘Graduated Shade’ function; Earth’s magnetic field ca. 25000 nT; grid size 40 x 40 m;

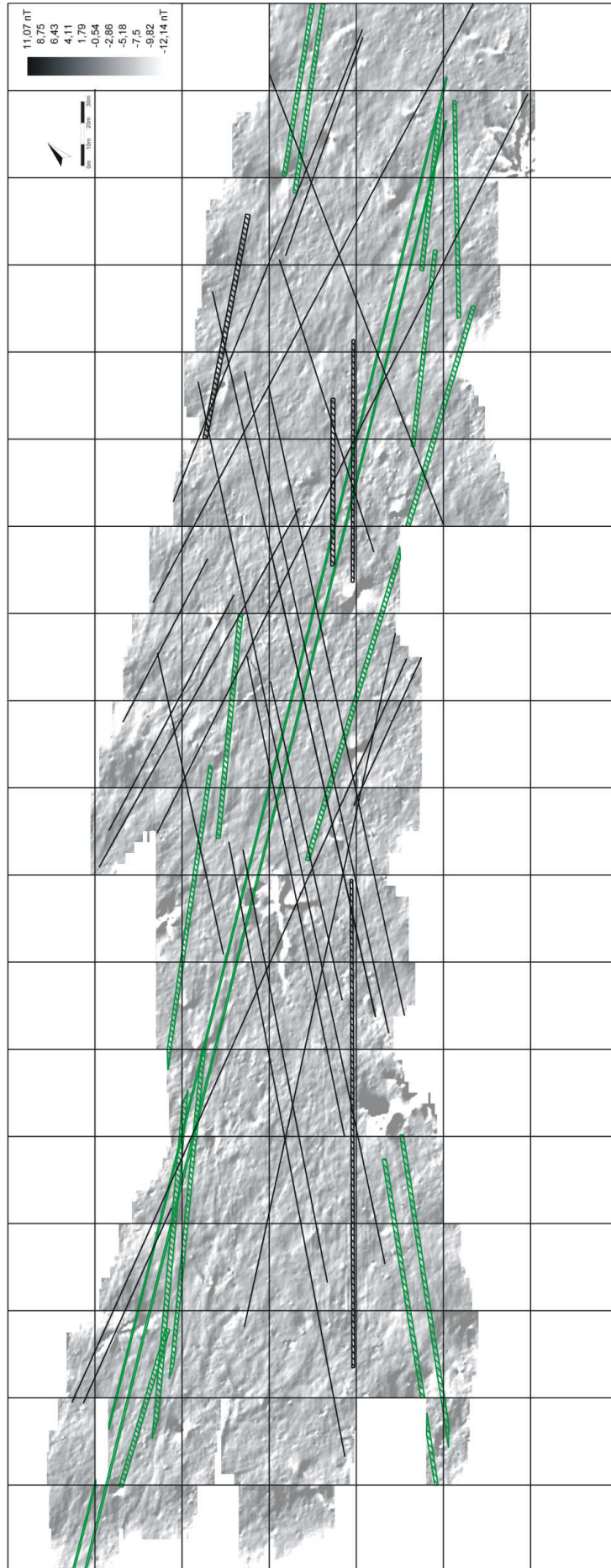


Figure 8.9. Interpretation of additional linear structures (black) on site PV67A-47 “Sacramento” plotted on the Total Field Mode magnetogram; SMARTMAG SM4G-Special in duo-sensor configuration; dynamics approx. +/- 12 nT in 100 greyscale values from black to white (with transparency factor 50%), sampling density 50 x 12,5 cm, interpolated to 25 x 25 cm, resolution increased by ‘Graduated Shade’ function; Earth’s magnetic field ca. 25000 nT; grid size 40 x 40 m;

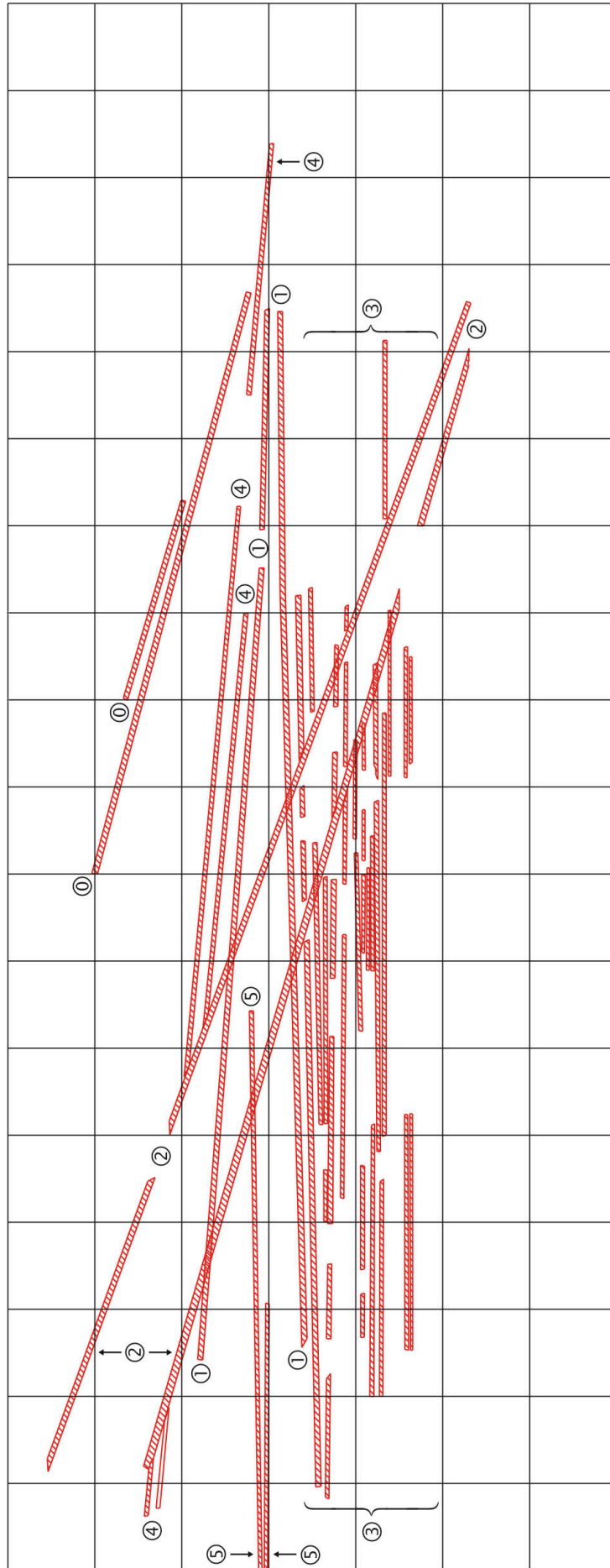


Figure 8.10. Interpretation of the geoglyph complex on site PV67A-47 “Sacramento” located on Cresta de Sacramento, north of Palpa; red lines represent ancient linear structures found by geophysical prospecting combined with aerial photography; grid size 40 x 40 m; numbers ① - ⑤ correspond to the documented set of lines (see description in text)

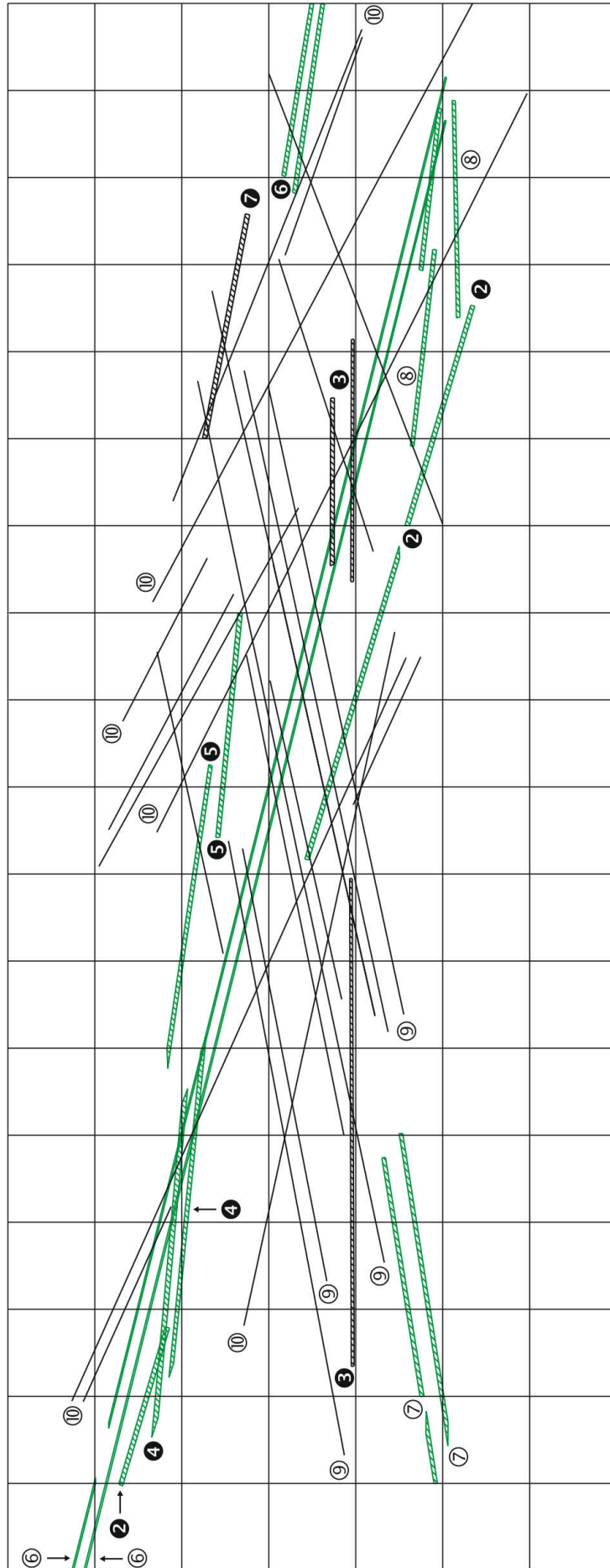


Figure 8.11. Interpretation of the geoglyph complex on site PV67A-47 “Sacramento” located on Cresta de Sacramento, north of Palpa; green and black lines represent ancient linear structures found exclusively by geophysical prospecting; grid size 40 x 40 m; numbers ② - ⑩ and ② - ⑦ correspond to the documented set of lines (see description in text)

On site PV67A-47, similarly to the previously measured locations, a low stone platform is situated on the edge of the flat terrain and overlooks the Palpa valley. It is located on the southern end of a roughly rectangular cleared area (196), and is oriented southwest – northeast, following the general direction of the Sacramento ridge. It has an elongated shape and is composed of six chambers of roughly equal size organized in the irregular row (Lambers 2006). Unfortunately, in the magnetometer images it is hard to identify due to its constructional characteristics. The chambers are outlined by a single row of boulders standing vertically in the soil, and are additionally filled with gravel composed of stones of different size. According to Lambers (2006), the structures were constructed in a simple manner using only materials available on the spot, thus both the outline and the filling consist of the same material that forms the surrounding desert pavement. Therefore, the magnetic contrast may be too low in order to differentiate the structures from the adjoining stone layer. It is opposite to the heaped trapezoid borders, which shaped by identical material, are formed by relatively high piles of stones, giving in such a way a strong record in a shape of the positive magnetic anomaly. This, in fact, makes a noteworthy phenomenon, given that the stones used to construct the platforms were most likely gathered simultaneously, when a new geoglyph was constructed and its borders were formed. As far as the position of the structures is concerned, Lambers (2006) declares that they are usually found on the edges of high plateaus, so both the valley and the geoglyph sites can be viewed from these points. Without the platforms the trapezoids cannot be seen from the valley floor.

At first glance total field magnetic images (Figures 8.5 and 8.6) are dominated by strong, known from the other sites, LIRM structures. As in previous cases, they form dipole star-shaped patterns irregularly distributed on site. On the Sacramento ridge, however, this phenomenon is particularly pronounced. The LIRM anomalies here occur in a quantity, that has never been observed so far, and their dimensions frequently exceed the size of similar structures measured on the other sites (Figure 8.13). It is most likely due to the strong exposition of the whole ridge which makes an easy target for the strikes. However, it may also support the idea that lightning strikes could have been attracted by archaeological structures such like pylons or posts, which on this site might have been frequently erected.

Besides LIRM anomalies, the linear structures as well, markedly demonstrate more complicated patterns, as the site was strongly remodelled over time. Due to this complexity,

the interpretation work has been divided and presented as two separate figures (8.10 and 8.11). The former is concentrated on structures recorded by magnetometry, but visible also for aerial imaging, while the latter presents features detected exclusively by geophysical prospecting of the site. The additional outcome constitutes a 3D-like visualisation (Figure 8.12), on which a supplementary interpretation work was based.

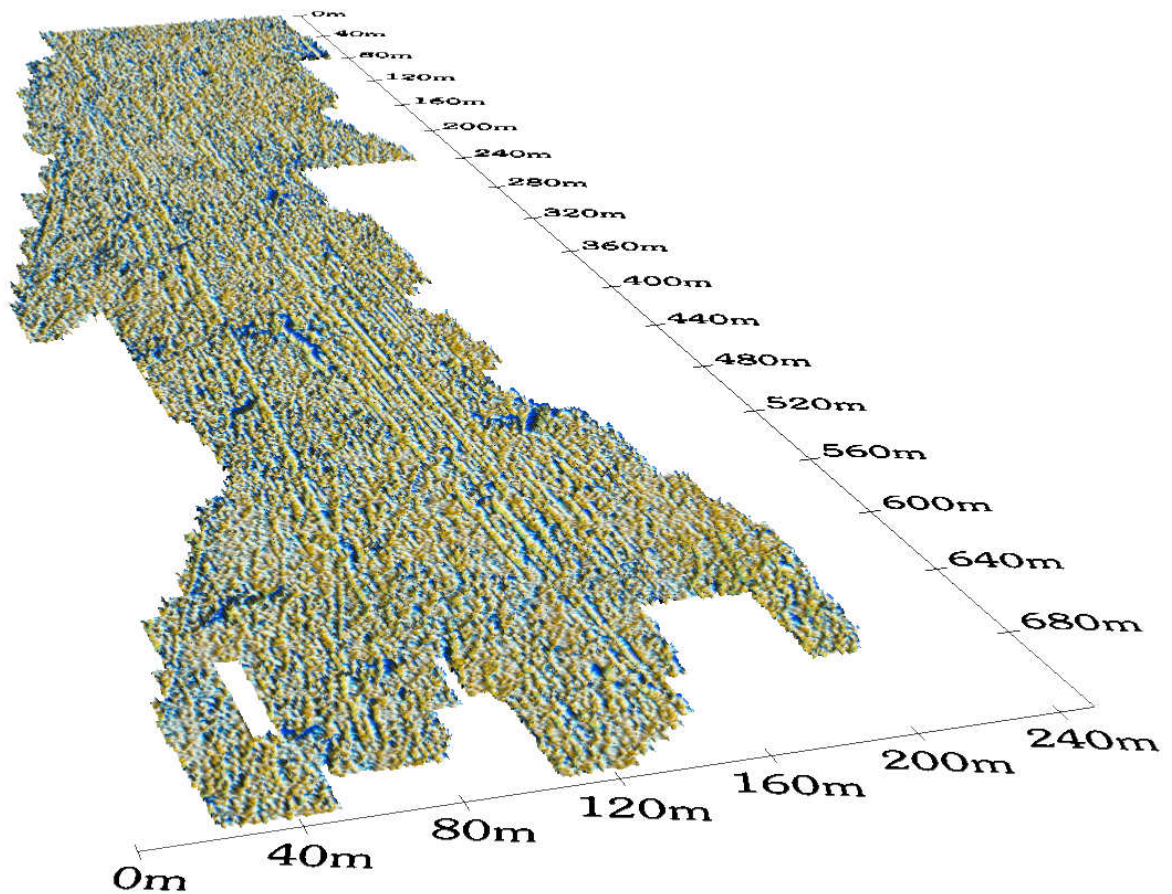
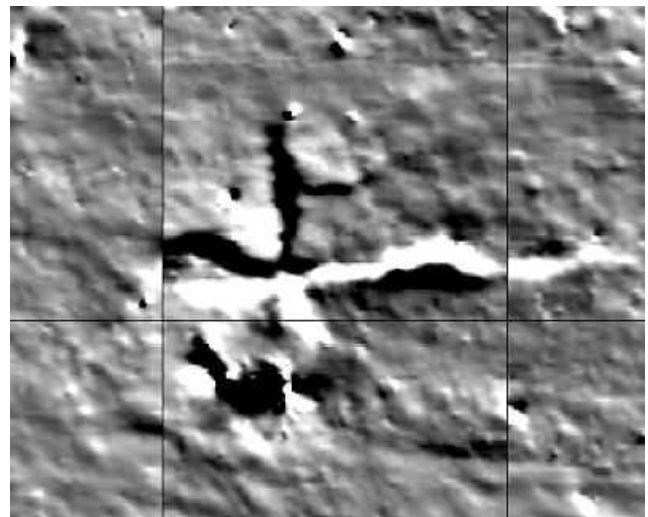


Figure 8.12. Magnetogram of the Total Field measurement on site PV67A-47 in a 3D-like visualisation seen from W at the view angle 20°; Caesium SmartMag SM4G – Special applied in the gradiometer mode. Sampling rate 12,5 x 100 cm interpolated to 25 x 25 cm, grid size 40 x 40 meter, dynamics +/- 13 nT in colour spectrum values from green to blue; Earth's magnetic field ca. 25.000 nT; top of the image pointing E.

Among the dense cluster of lines on site PV67A-47, number ① and ② (Figure 8.10) compose the most elementary structures recognized in magnetic images. Apart from the LIRM features, they create the strongest magnetic anomalies on site and are effortlessly distinguishable even in the total field measurement (Figure 8.5). Both structures constitute the margins of two main trapezoids, which crosscutting each other in an oblique direction, form one of the most recognizable geoglyph complexes in the Palpa region. Lines marked with the symbol ①, which delimit trapezoid 189 (Figure 8.3), do not follow the straight

course, but are slightly bent inwards, which is particularly pronounced close to the narrow end of the trapezoid. Moreover, the north-western margin loses its continuity, which might be due to the transition to the large rectangular area (213). The lines ②, demarcating trapezoid 188, on the other hand, run straight, being at the same time one of the longest straight features of the whole complex. Although they cross several older lines (①, ③ and ④), the anomalies caused by them are apparent and comprehensible. In addition to them, a supplementary line ❷ (Figure 8.11) has been found. It is located between the trapezoid borders ②, running parallel to the southern margin. Judging from the similar structures found on the other sites, the line ❷ can be classified as a former cleared area boundary. It existed until the enlargement phase, after which it was wiped out, making it invisible for the conventional aerial photography techniques. The magnetometry, however, yet again proved its existence in the past and defined its exact location in the field.

Figure 8.13. Star-shaped magnetic anomaly from site PV67A-47 “Sacramento” caused by the lightning induced remanent magnetisation; Caesium SmartMag SM4G – Special applied in duo-sensor configuration; Sampling rate 12,5 x 50 cm interpolated to 25 x 25 cm, grid size 40 x 40 meter, dynamics +/- 250 nT in 99 greyscale values from black to white; Earth’s magnetic field ca. 24.000 nT



The most complicated cluster on site compose lines ③, which form a group of lineal geoglyphs, flanking the main trapezoid from its south-eastern side. They are exceptionally difficult to interpret, as they occur close to each other. The anomalies of neighbouring lines are therefore in an immediate proximity, which in effect causes an overlap of reverse anomalies (see Chapter 4.4) in the magnetic image. This all forms an assembly of parallel stripes, the coexistence of which, even with the help of aerial photographs, is hard to understand. For that reason, even obvious anomalies, like those caused by the lines ❸ (Figure 8.11), have been classified only as a possible features and therefore marked black. However, as it was found by the photogrammetry, the whole assemblage ③, likewise similar features on the other complexes, is in fact a meandering

structure, which possibly is continued under the trapezoid 189. Unfortunately, this could not have been confirmed neither by aerial imaging nor the magnetic prospecting, since the later construction of two huge trapezoids 188 and 189 utterly obscured the previously created features. It is therefore not obvious if the lines ④, which form on the north-western side of the trapezoid 189 the analogous flanking arrangement, are together with lines ③ the one continuous meandering structure. The existence of two diverging lines ⑤, which were detected on the south-western part of the trapezoid 189, might be the evidence answering this question. As the remnants of discovered mentioned lines, located exactly in between features ③ and ④, seem to be the perfect link between them, the continues structures beneath the trapezoidal cleared areas is a probable eventuality. Moreover, as the magnetic surveying further verifies, the lines ③ are not only joined to their northern counterparts ④, but also to the additional flanking structures on this side of the trapezoid, which are the lines ⑤ and ⑥. What's more, the single line ⑦, which lays close to and matches the course of the mentioned ⑤ and ⑥, could also fall into this group. However, as it is outlined by the faint and unclear anomaly, such assumption is questionable.

On the contrary, two parallel lines ④, being the prolongation of previously described lines ④, with reference to magnetic prospecting, constitute one of the best results on site. Although their existence was generally assumed, the actual magnetic confirmation was needed. It was also important in terms of method's potentiality, since it yet again provided evidence for capabilities of geophysical techniques in archaeology. In that way, lines ④, obliterated by the construction of trapezoid 189, could have been identified, delineated and coupled with ④ (Figure 8.8 and 8.11).

The longest linear structures on site PV67A-47 are the lines ⑥ (ca. 700 m) (Figure 8.11). These two perfectly parallel features run from south-east to north-west, crossing almost the entire plateau, inclusive of the large part of the trapezoid 188. Their direction, however, slightly differs from the course of the main axis of the trapezoid, swerving several degrees to the north in the trapezoid's narrow end area (Figure 8.8). Consequently, it is hard to determine, if mentioned lines has anything in common with the trapezoid, particularly given that they are built by the weak magnetic anomalies, distinguishable only in the certain angles and projection plains of 3D view. Although their direction is similar to the most northerly located lines ⑥ (Figure 8.10), the lack of evidence denies any relation to them. In addition, lines ⑥ seem to represent the special form of linear structures, emerging

from or fading away in the curves of spirals 206 and 207 (Figure 8.3). Furthermore, it is hard to verify the stratigraphic correlation of lines ⑥ with any other drawing on site.

The last pair of apparent structures found by magnetic prospecting make green lines ⑦ and ⑧ (Figure 8.8 and 8.11). The former are built by two parallel anomalies located in the south-western part of the plateau, in the vicinity of previously described stone platforms, while the latter are placed in the opposite end, close to the apex of trapezoid 188. Lines ⑦ run in the unique direction (close to north – south), not frequently observed on site PV67A-47, whereas the lines ⑧, precisely reflect the course of cleared area margins ①, forming a similar trapezoidal contour. Although both ⑦ and ⑧ have approximately 150 – 200 m in length, compared to the whole assemblage reaching 720 m, they are rather short for an appropriate assessment of their function. Presumably, the later constructions on site destroyed parts of them, what at present excludes the right judgements and makes the final conclusion not viable. This is a frequent problem on all investigated sites, to which magnetic prospecting, although usually supportive, not always makes the complete solution. As it proves, some lines, regrettably, have been erased forever and cannot be reconstructed by any sophisticated technique now.

However, occasionally a very weak structures, which in the network of stronger magnetic anomalies should not be visible, can be surprisingly found. Such situation occurs on site PV67A-47, where questionable lines ⑨, together with ⑩, form a relatively dense system of lines. Both of them are built by extremely feeble anomalies, which in the rich maze of hitherto described stronger ones, are particularly difficult to locate. Besides Sacramento, such netting of secondary lines was successfully found on the similar investigated plateau – Carapo (see Chapter 9). On both sites the lines form a cluster, which does not fit to any known plan of site arrangement and design. Consequently, project archaeologists find them highly unlikely and doubtful. However, as some of them certainly form part of the first drawings on site, the mentioned zigzag lines 183 and 203, the author decided to add them to the whole ensemble (Figure 8.9 and 8.11).

Chapter 9

Results of geophysical prospecting on site PV67B-55 “Carapo”

This site PV67B-55 occupies the western foothills of the ridge between Río Palpa and Río Viscas (Figure 9.1) and is the only plateau on the Carapo ridge, which could be compared to the large flat surfaces on Cresta de Sacramento and Pampa de San Ignacio. Although it is located closer to Río Viscas, the site is accessible only from Río Palpa through the narrow path on the slope, also covered by geoglyphs. From the south, the steep scarp separates it from the Viscas valley, providing relatively well protection for the geoglyphs, since no cars have access to the plateau. However, likewise Sacramento, constructions built during Late Intermediate Period (see Table 2.1), among them walled enclosures, graves, and a ditch, slightly damaged the central trapezoid of the site (Lambers 2006).

Similarly to the Yunama and Sacramento sites, the first geoglyphs constructed on Carapo were several narrow straight lines distributed on different parts of the plateau (among others 595, 599, 612, 613, 615, 620, 624) (Figure 9.3 and 9.4). According to Lambers (2006) the associated ceramics date these lines as well as the construction of the angular spiral (596) and the large meandering line (593) to the Early Nasca. Roughly at the same time, the first large trapezoid of the site (605) was started but never finished. The stratigraphic position of two large zigzag lines crossing the plateau shows that they also were constructed in the same phase, cutting several earlier geoglyphs. Although a large group of geoglyphs dates to that period, a continued use of the site in Middle Nasca times was also observed. Then the new geoglyphs were added to the complex, among them several shapeless ones (592, 597, 598, 602) and probably some lineal. The large trapezoid 591 that dominates the southern half of the site was also constructed during Middle Nasca times,

covering the series of earlier geoglyphs. In that way, in Middle Nasca times, the large part of the free space on the plateau was already covered by the drawings (Lambers 2006).

The magnetic surveying on Carapo, similarly to other investigated sites, followed the photogrammetric mapping, which provided support for selection the prospecting area. As the northern part of plateau is in detail identified by aerial archaeology, the geophysical research on site, carried out in April 2006, was concentrated exclusively on its southern fraction, covered by the rectangular cleared area. Even so, it still reached 560 x 160 m, in which 42 complete or shortened survey squares were placed.

Here again, both total field and gradiometer images (Figure 9.5 and 9.6) are dominated by anomalies originating from lightning strikes. However, they are not so frequent, wide-ranging and evident as on Sacramento. This contrast may be due to the differences in site exposition, given that Carapo is slightly covered from the east by the range of hills and from the south by low heaps towering above the scarp. Therefore, in contrary to Sacramento, Carapo seems to be better shielded from the lightning strikes. Moreover, different magnetic properties of geological background are responsible for limited LIRM anomalies as well. Since the geoglyphs of Carapo, unlike other complexes, are placed on the cretaceous bedrock with the thinner layer of quaternary alluvial deposits (see Chapter 3.3) the ground properties that transmit and maintain the lightning-induced magnetic record may simply differ from Sacramento sites.

Besides LIRM features, in magnetic images dominates huge, 100 m long anomaly originating from Late Intermediate Period ditch. Although from archaeological viewpoint the result may seem uninteresting as it derives from the later cultural phase than the investigated one, for geophysics, it makes a considerable outcome regarding the anomaly nature. Despite the fact that the function of the ditch is unknown, its measurement confirms the differences in shape of anomalies according to magnetic inclination. Whereas ditches measured in Europe almost always reflect as positive anomaly, since the refilling material is frequently more magnetic than adjacent deposits, in Peru the maxima and minima are reversed, giving the negative image of the similar structure (see Chapter 4.4). On Carapo, quite the opposite, the ditch revealed positive characteristics, but it was never refilled with any material. Therefore, the anomaly has its source in destroyed remanent magnetization of sediment and carry a positive signal because of the near-equator reversed polarity.

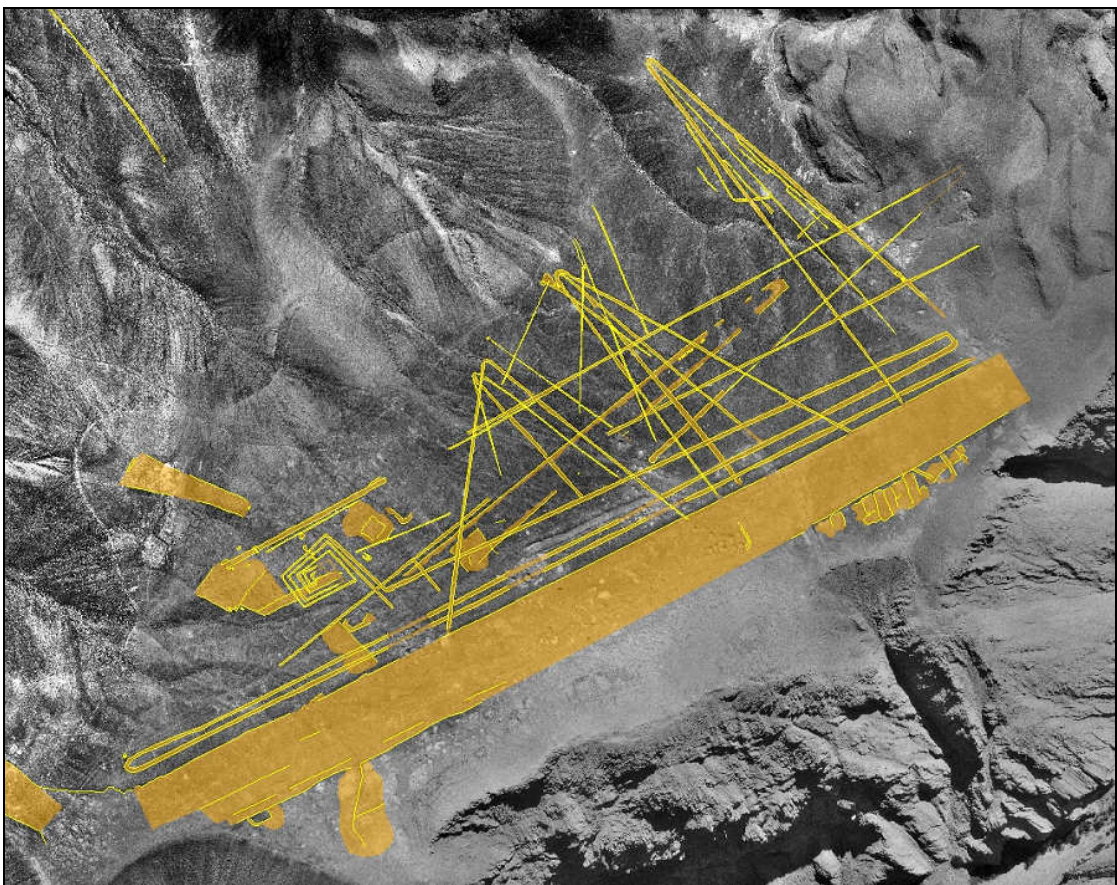


Figure 9.1. Orthophoto of the geoglyph site PV67B-55; Cerro Carapo, east of Palpa (upper);
Figure 9.2. Interpretation of drawings on site PV67B-55 (lower); after K. Lambers; ETH Zürich

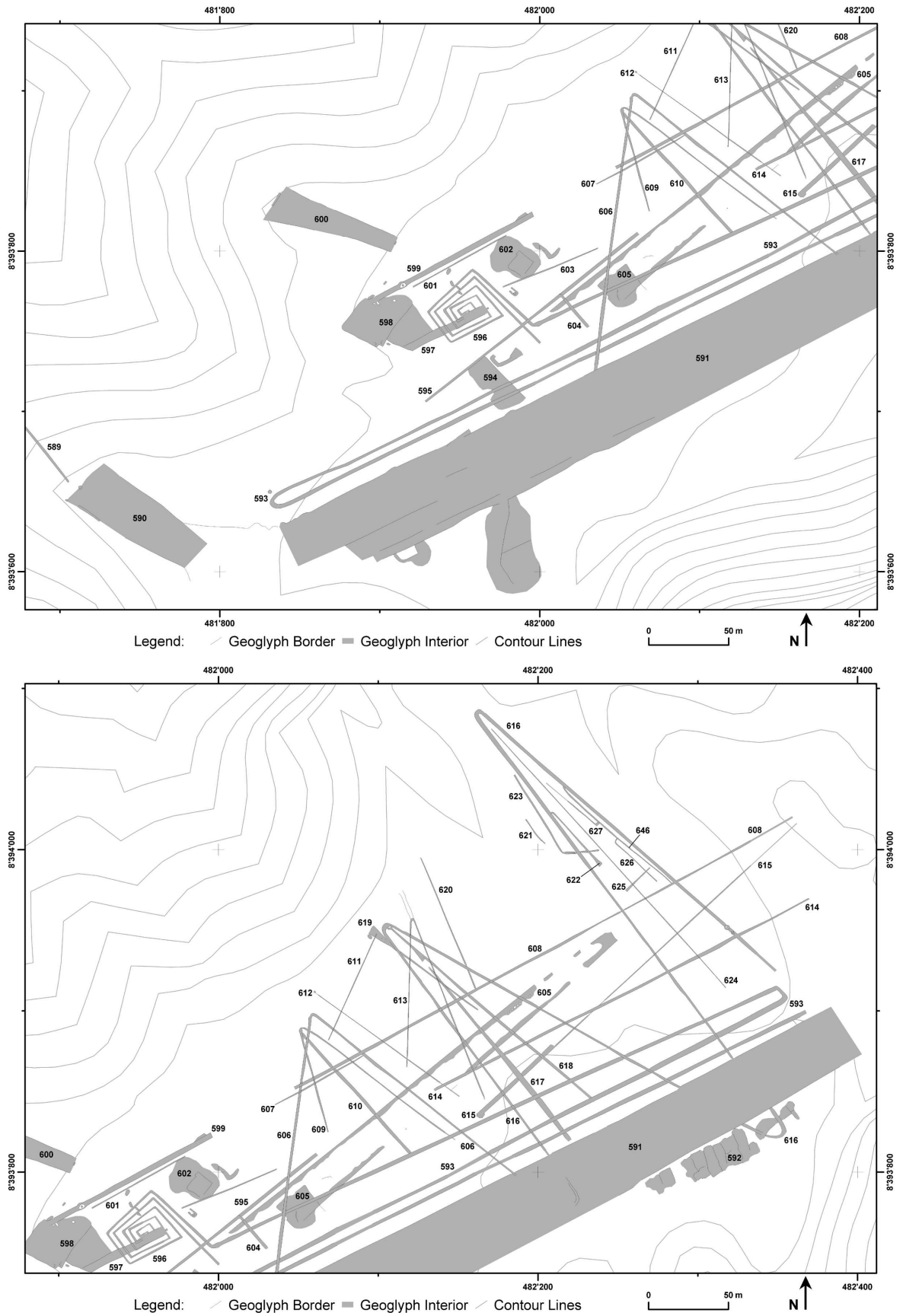


Figure 9.3 and 9.4. Detailed maps of the geoglyph site PV67B-55 from Cerro Carapo; geoglyph assemblage with stratigraphical sequence of different phases of construction and reworking drawn after aerial photograph (Figure 9.1) by K. Lambers, Institute of Geodesy and Photogrammetry, ETH Zürich

Although the survey grid on Carapo, similarly to previously measured sites, was for practical reasons still oriented after the long axis of the plateau, a layout of the traverse lines as close as possible to the east – west direction was made. Such arrangement has been developed after test measurements on small Estequerilla site, located in the Rio Palpa valley, at the footsteps of Sacramento ridge, close to Yunama geoglyphs. The surveying, carried out in March 2006, not only confirmed the assumption of a horizontal gradiometer potential, which was supposed during measurements on site PV67A-47, but also revealed certain grid arrangement necessities:

- Firstly, the total field surveying, which was performed in the north – south direction, exposed some negative aspects of this configuration. At low latitudes close to the geomagnetic equator, sensors arrayed with electronics parallel to the geomagnetic field, unfavourably changed the signal to noise ratio, producing interference, which formed a problematic striping in the total field magnetic image,
- Secondly, given that the angle of dip is exceptionally low, the gradient between two sensors is bigger when it is measured in a horizontal plain,
- Finally, for the precise gradient calculation both sensors had to be arrayed along the course of the geomagnetic field.

In order to apply tested arrangements, it was essential to set up a layout of the grid and to keep the probes tilted in the north – south direction, walking at the same time along the west – east arranged traverses (Figure 9.5). Such exact ordination was met only on San Ignacio site (see Chapter 10), while on Carapo it was as near as the plateau elongation let.

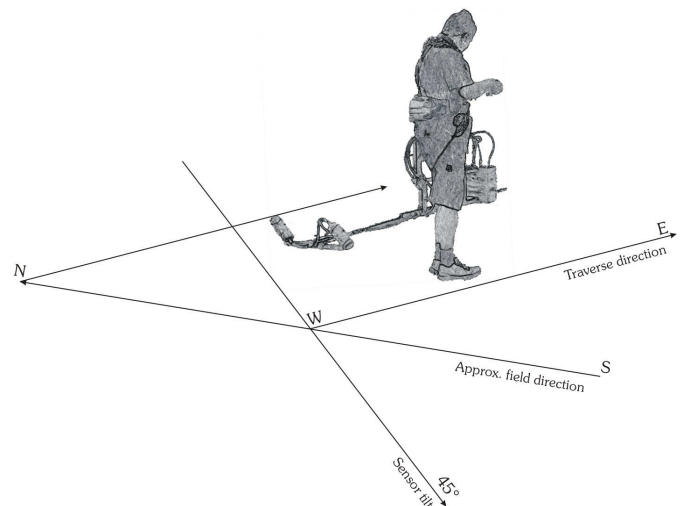


Figure 9.5. Traverse layout and magnetometer grid arrangement on Peruvian geoglyph complexes Carapo and San Ignacio.

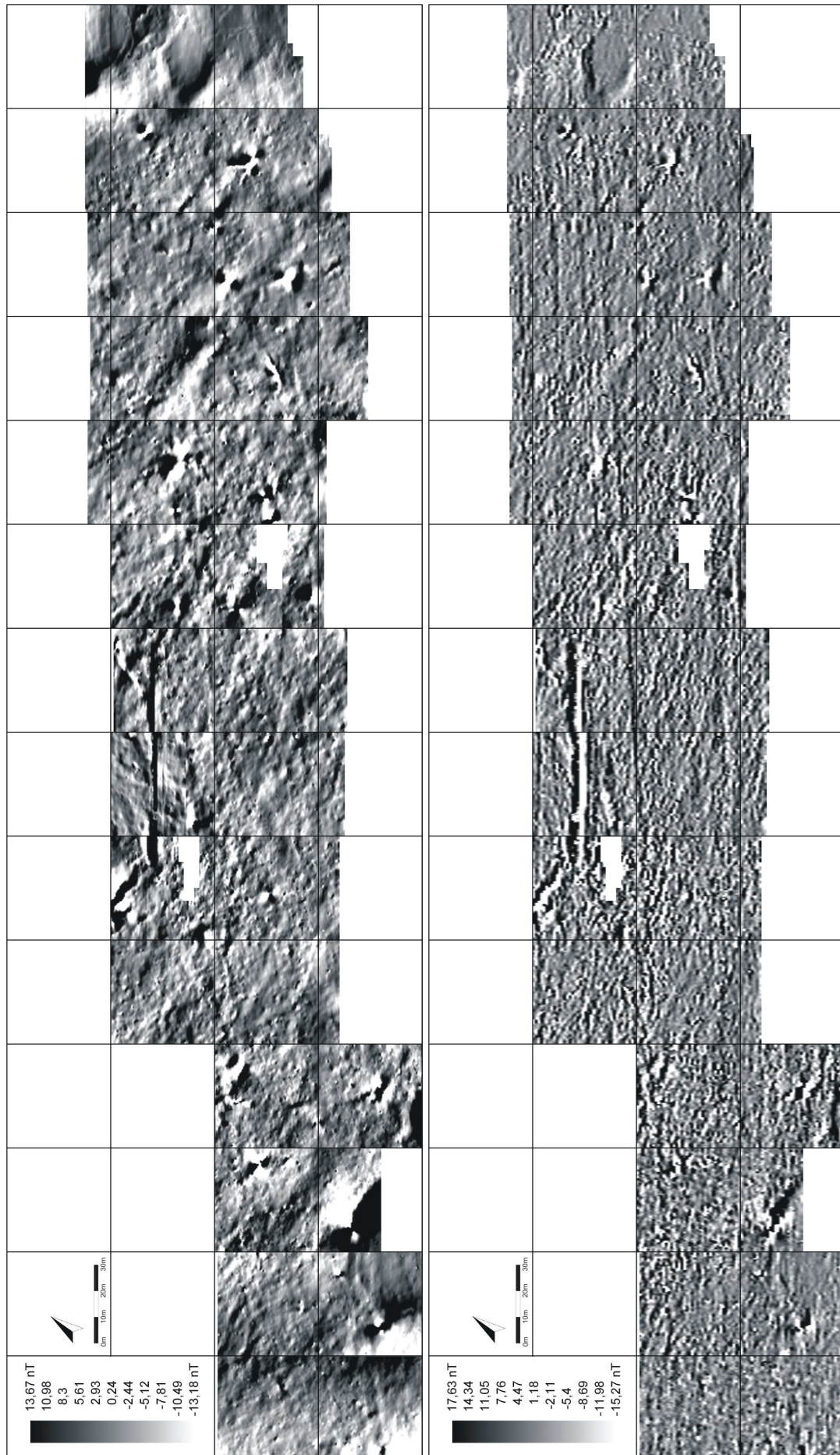


Figure 9.6 and 9.7. Magnetograms of the site PV67B-55 “Carapo” located on Cerro Carapo east of Palpa; measurement in the Total Field Mode (upper) and the Gradiometer Mode (lower) with dynamics approx. +/- 13 nT and +/- 17 nT respectively; SMARTMAG SM4G-Special in twin sensor configuration; sampling density 50 x 12,5 cm and 100 x 12,5 cm, interpolated to 25 x 25 cm, resolution increased by 'Graduated Shade' function; Earth's magnetic field ca. 25000 nT; grid size 40 x 40 m

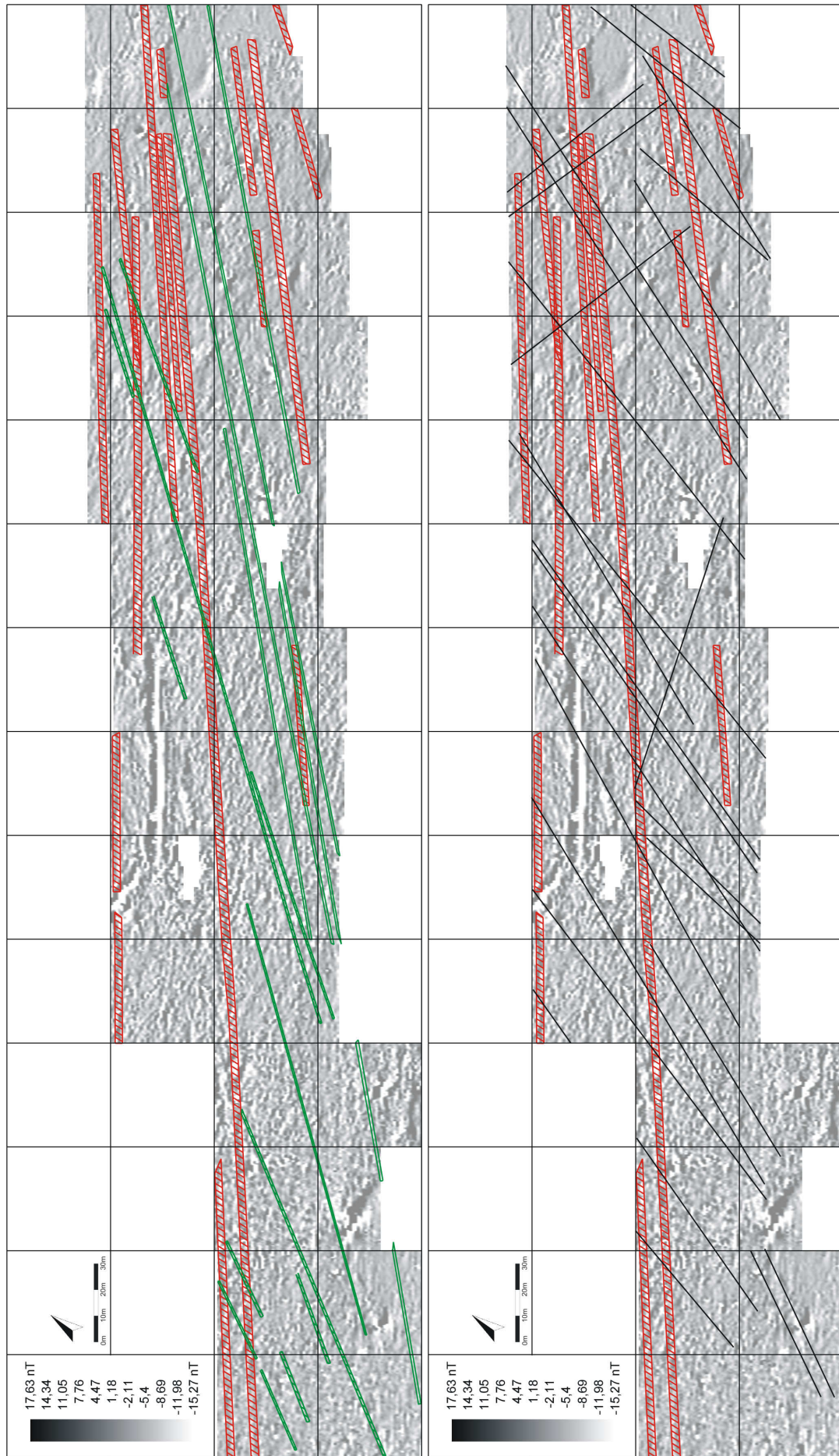


Figure 9.8 and 9.9. Interpretation of linear structures (red, green and black) on site PV67B-55 “Carapo” plotted on the Gradiometer Mode magnetogram; SMARTMAG SM4G-Special in duo-sensor configuration; dynamics approx. +/- 12 nT in 100 greyscale values from black to white (with transparency factor 50%), sampling density 100 x 12,5 cm, interpolated to 25 x 25 cm, resolution increased by ‘Graduated Shade’ function; Earth’s magnetic field ca. 25000 nT; grid size 40 x 40 m;

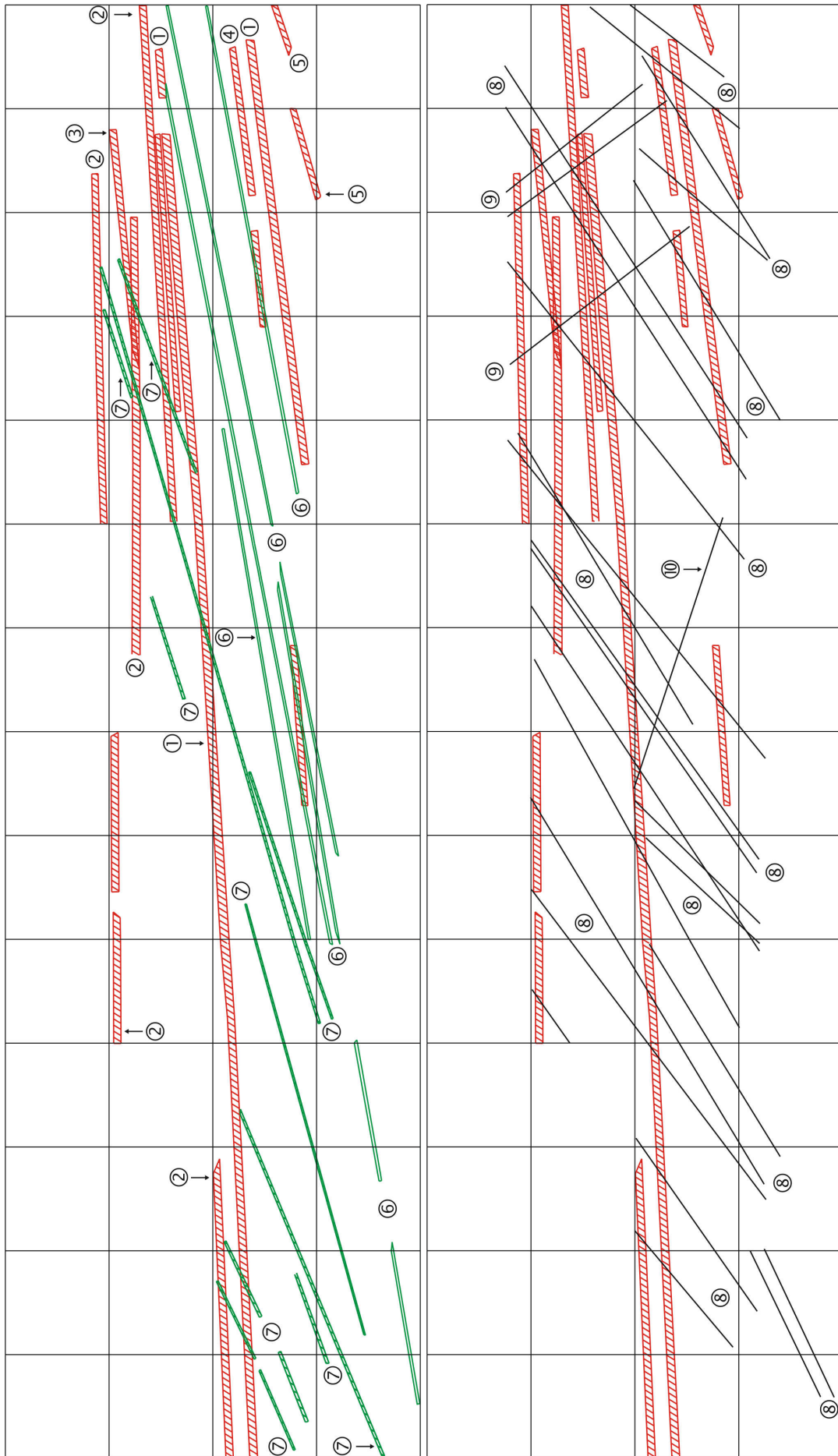


Figure 9.10 and 9.11. Interpretation of the geoglyph complex on site PV67B-55 “Carapo” located on Cerro Carapo, east of Palpa; red, green and black lines represent ancient linear structures found by geophysical prospecting combined with aerial photography; grid size 40 x 40 m; numbers ① - ⑩ correspond to the documented set of lines (see description in text).

Similarly to previously presented sites, on Carapo, the red lines marked with the symbols ① and ② correspond to the major linear structures in this location. The features ① are the margins of the rectangular cleared area and create the strongest magnetic anomalies on site. While the north-western border can be effortlessly distinguishable even in total field measurement (Figure 9.6), the south-eastern one is only partially visible, as it runs close to the heaps on which Late Intermediate Period site is located. The construction of the site has presumably damaged several drawings, inclusive of a part of the south-eastern margin, what was confirmed by the aerial images as well (Figure 9.1). The north-western border, on the other hand, runs through the total length of the measurement area, forming one of the best preserved features of the whole complex. Likewise the edges of Sacramento main trapezoid, it does not follow the straight course, but is slightly bent, acquiring the shape of a slight arc.

Following the already know pattern, structures ② compose the long meandering line, which deriving from an angular spiral, flanks the trapezoid from its north-western side. The spiral itself was not covered by magnetic surveying, since it is located to the north of the furthest measured traverses. That is why, the partial visibility, known from Sacramento, could not have been assessed here. Alternatively, the central part of line ② is not evident in magnetic images nor it is noticeable for aerial imaging. It is due to the damage caused by the construction of Late Intermediate Period ditch and modern cavities on site. Therefore, its continuity is only assumed as well as is its occurrence under the trapezoid. Here however, with the answer comes the magnetic prospecting, revealing a parallel cluster of structures ③. The direction of structures differs slightly from the course of the trapezoid margins as well as from the meandering line ②. This is particularly visible in most northerly located parts as well as in additional branches, for example line ③, which on the other hand matches the direction of ⑥. Therefore, since the line ② does not reveal the ideal parallelism either, the newly discovered features ⑥ can be interpreted as the continuation of line ②, especially given that the arrangement of both structures resembles the similar constructions on other sites, particularly on Sacramento.

An equally interesting feature constitute the partially obliterated line ④. Similarly to structures ⑥, it is located within the trapezoid area, being the parallel feature to its south-eastern margin. This, after comparison with the analogous lines from the other sites, allows the assumption that the line ④ could be the previous trapezoid boundary, before ① took its place at the time of trapezoid enlargement.

Not really understood is the occurrence of lines ⑤. As they are close and parallel to the assemblage ⑥ they may indicate some association with them, however, their proximity to the scarp as well as their shortness does not permit an adequate explanation. Conversely, the set of lines ⑦, constitute the cluster, to which the satisfactory clarification can be found. Opposite to ④ and ⑥, they are not located within the trapezoid borders, but cut them and the meandering line ② in an oblique direction. Most likely they were one of the initial drawings on site as they resemble the course of the first lines 595, 615 and the unfinished trapezoid 605 (Figures 9.3 and 9.4). Some of them might be the prolongation of mentioned lines, while the other may constitute newly discovered features, particularly in the area of trapezoid 591.

In addition to described primary features, the dense netting of secondary lines ⑧, ⑨ and ⑩ has been found (Figure 9.11). Most frequently they run north – south or northeast – southwest (lines ⑧), however, other directions approximating northwest – southeast (lines ⑨) or nearly west – east (lines ⑩) are also present. Correspondingly to site PV67A-47, they are formed by exceptionally weak anomalies, reflecting particularly narrow obliterated lines. As already mentioned in Chapter 8, they do not fit to any known plan of site arrangement and design, therefore from the archaeological point of view, as the resulting finding, they are rather poor. Magnetically however, they again reveal the potential of geophysical methods, concerning, among others, the sensitivity and resolution of used magnetometer system. Although for archaeology their occurrence as a part of the advanced drawing concept for ceremonial practices or geometric expression can be doubtful, still they may portray the broad movement activities, transportation and communication patterns. This, however, as it is not the area of geophysical expertise, will not be discussed further.

Chapter 10

Results of geophysical prospecting on site PP01-49 “San Ignacio”

The site PP01-49 occupies the entire Pampa de San Ignacio and archaeologically constitutes the largest geoglyph complex of the whole investigated area. Separated by Rio Palpa and Rio Viscas valley as well as the modern city of Palpa, it forms the counterpart to Cresta de Sacramento. From the north it is framed by the slope descending towards Palpa while from the south it reaches the first dry valley floors. Five trapezoids placed on the site form an approximately two kilometres long assemblage. The magnetometer prospecting area of 320 x 240 m covered only the central part of it, from where all drawings seem to diverge and the most interesting structures were believed to find. Therefore, the site PP01-49 is the only complex from the Palpa region that has not been measured entirely. Firstly, it was due to the size of the survey area, which did not allow to complete the measurement in one field campaign and secondly to the financial supplies of the project, which headed at the time towards the end. Thus, the site PP01-49, should be understood as supplementary area only and in that way it is treated in the present study.

As already mentioned, the whole site is composed of five main trapezoids, the longest of which is extended over an area of two kilometres (Figure 10.1). It is elongated northeast – southwest, which matches the main course of the whole plateau. The four other trapezoids, remarkably smaller, cut the central one in oblique directions, supplementing the whole complex in cleared area forms. Similarly to other sites, meandering and flanking lines, at the sides of some of the trapezoids, can be recognized. However, they do not form already known patterns, but seem to occur somehow irregularly in comparison to the other complexes. Straight lines are common forms and cut the plateau in all directions. Some of

them occur individually, while the other form parallel clusters. Smaller trapezoids as well as unfinished ones are quite frequent and one can find rare spiral forms between them. This all compose already known pattern of an exceptional size, which magnetically was measured in April 2007. The investigation was limited to 37 survey squares and covered the central part of the territory.



Figure 10.1. Orthophoto of the geoglyph site PP01-49 from the Pampa de San Ignacio, south of Palpa; K. Lambers, Institute of Geodesy and Photogrammetry, ETH Zürich, Switzerland

To take the full advantage of the newly developed magnetometer system, an exact layout of the grid with the traverse lines in the east – west direction, for the first time was made. Such arrangement was possible since the layout was no longer restricted by the orientation of the ridge. To the west of the survey area it covered the plain reaching the edge of the plateau and enclosed the measurements of the stone platforms on the very border of the terrain. To the east it arrived at the main crossing point of the trapezoids, including two unfinished ones and a double spiral (Figure 10.2). Straight lines supplement the ensemble crossing the terrain in all directions. Since the survey area constitutes only the small fraction of the larger site, all magnetic anomalies of the linear structures cannot be interpreted exclusively on the basis of this little portion. Conversely, in order to find correlation with the other drawings from the same plateau, they have to be compared to the

aerial image of the whole site and so further interpreted. The trapezoidal forms, which form a complicated overlaying pattern, are relatively good visible even in aerial photographs. Contrary to other complexes, the relic margins are well preserved, still forming the clear heaped boundaries. This not only helps archaeologists to track the stratigraphic sequence, but also serves the geophysicists as a strong anomaly signal in magnetic images.



Figure 10.2. *Orthophoto of the survey area on site PP01-49 from the Pampa de San Ignacio, south of Palpa; K. Lambers, Institute of Geodesy and Photogrammetry, ETH Zürich, Switzerland*

The one of the most remarkable findings on site are uncompleted trapezoids. On San Ignacio they are particularly well preserved, carrying the record of constructional development. On their surface the numerous heaps of stones may be observed, revealing the ongoing building process. This finding evidently documents the creation technique, which is believed to be fitting for major trapezoidal and rectangular forms. Following this assumption it can be stated that numerous cleared areas were converted from two parallel or approaching lines by repeated surface clearing between them. In the first stage the stones were picked up and placed in more or less regular piles, which subsequently were removed, exposing the underlying yellowish silt over the whole area. Some of the heaps, however, for some reason, had not been removed, allowing the study of constructional techniques now.

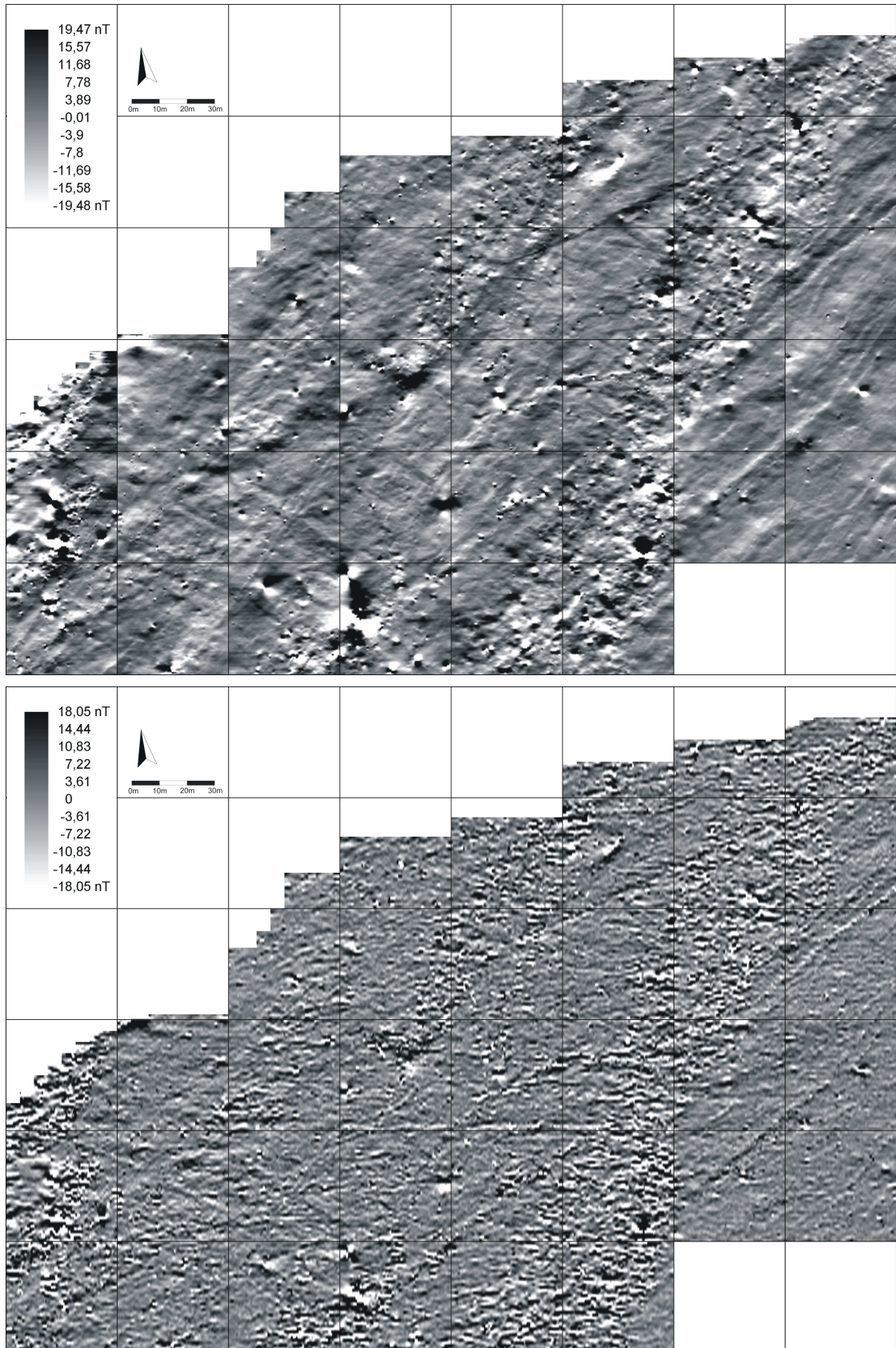


Figure 10.3 and 10.4. Magnetograms of the site PP01-49 “San Ignacio” located on Pampa de San Ignacio; south of Palpa; measurement in the Total Field Mode (upper) and the Gradiometer Mode (lower) with dynamics approx. ± 19 nT and ± 18 nT respectively; SMARTMAG SM4G-Special in twin sensor configuration; sampling density 50 x 12,5 cm and 100 x 12,5 cm, interpolated to 25 x 25 cm, resolution increased by ‘Graduated Shade’ function; Earth’s magnetic field ca. 25000 nT; grid size 40 x 40 m

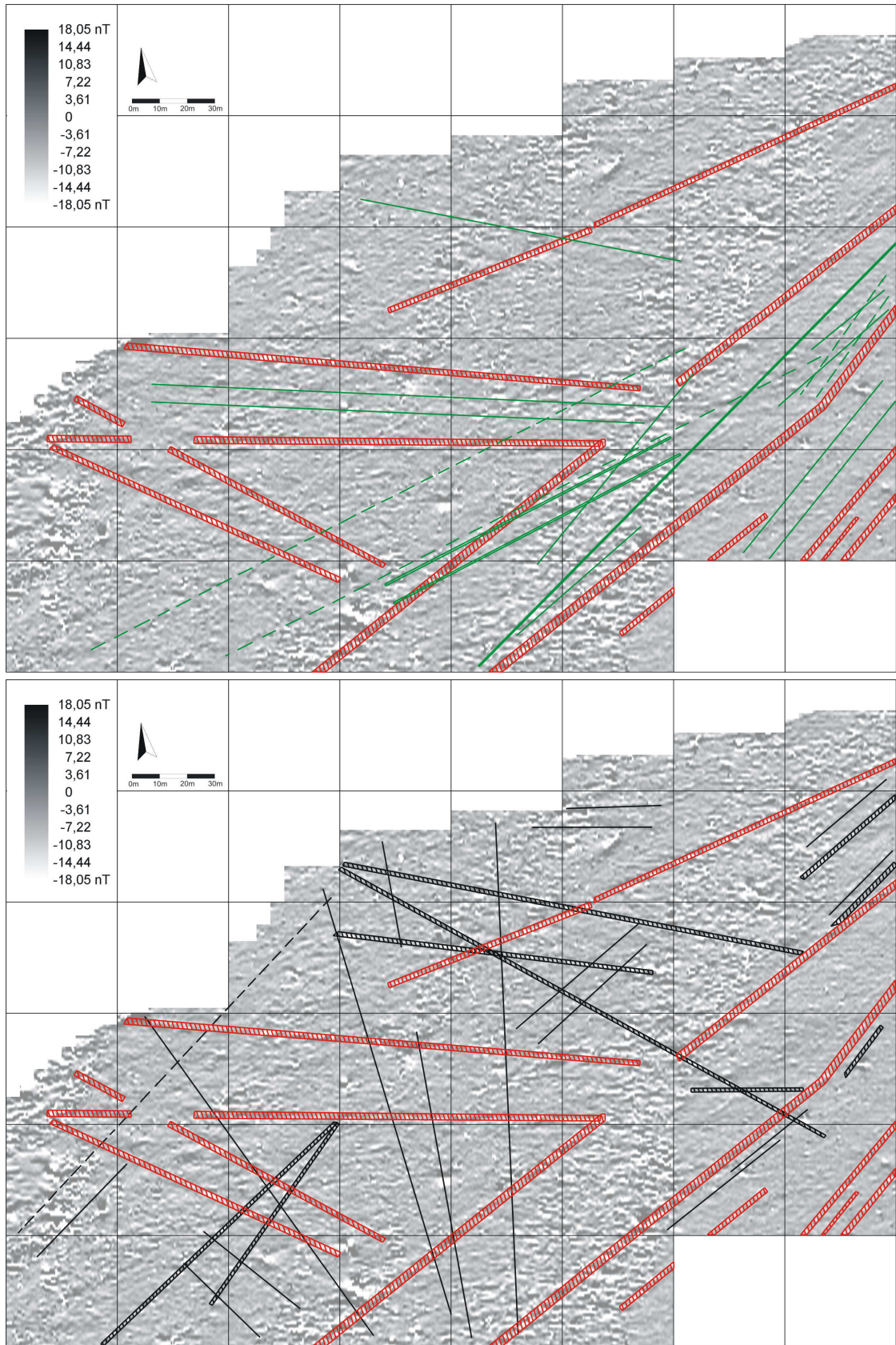


Figure 10.5 and 10.6. Interpretation of linear structures (red, green and black) on site PP01-49 “San Ignacio” plotted on the Gradiometer Mode magnetogram; SMARTMAG SM4G-Special in duo-sensor configuration; dynamics approx. +/- 18 nT in 99 greyscale values from black to white (with transparency factor 50%), sampling density 100 x 12,5 cm, interpolated to 25 x 25 cm, resolution increased by ‘Graduated Shade’ function; Earth’s magnetic field ca. 25000 nT; grid size 40 x 40 m;

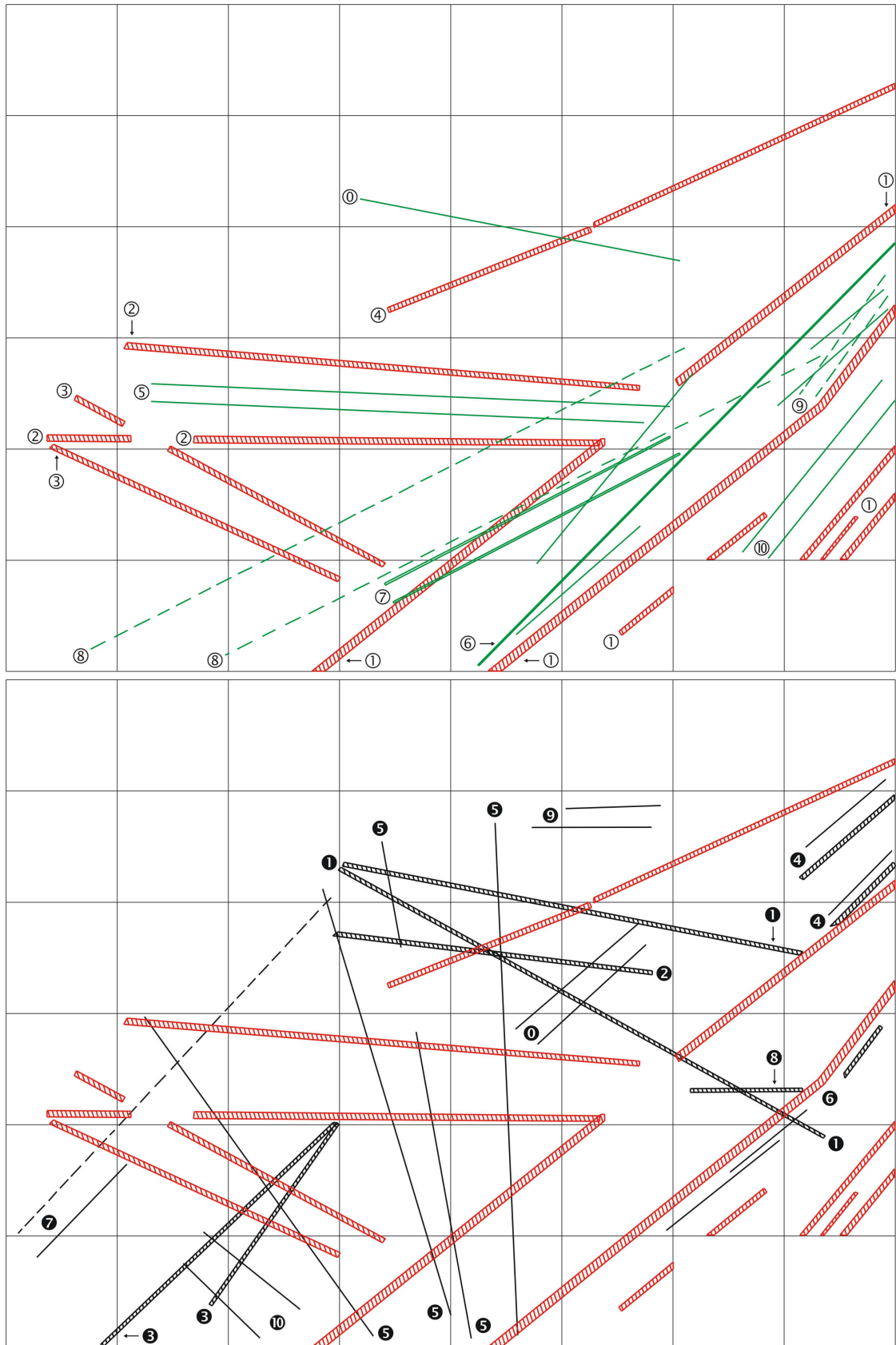


Figure 10.7 and 10.8. Interpretation of the geoglyph complex on site PP01-49 “San Ignacio” located on Pampa de San Ignacio, south of Palpa; red, green and black lines represent ancient linear structures found by geophysical prospecting combined with aerial photography; grid size 40 x 40 m; numbers ① - ⑩ and ① - ⑩ correspond to the documented set of lines (see description in text).

The outcome of magnetic prospecting on site PP01-49 is presented in figures 10.3 and 10.4, while the interpretation in figures 10.5 to 10.8. Likewise other complexes, on San Ignacio, most of the information has been obtained from the gradiometer magnetogram, whereas the total field image, served as a significant supplementation. Naturally, the aerial photographs acquired with photogrammetric means, provided a comparative illustration.

The red lines marked with the symbol ① represent the boundaries of two main trapezoids. Taking into consideration their actual size, the magnetically detected portion constitutes only a small part of the real length of these structures. Obliquely to them, from the west, two smaller trapezoids marked with symbols ② and ③, meet the main ones, jointly forming the major cleared feature on the measured territory. This, together with the straight line ④ compose the best visual pattern, formed at the same time by strongest magnetic anomalies. For aerial photography detectable are also lines ❶, ❷ and ❸, which outline two additional trapezoids on site, as well as some of the lines ❹, particularly those running in north – south direction. As far as lines ❶ and ❷ are concerned, it is hard to determine which one actually defines the additional trapezoid. Aerial imaging would suggest the layout of the main structure with its apex directed eastwards, while magnetic prospecting implies the occurrence of opposite oriented feature or even arrangement with two trapezoids.

The rest of the identified structures, which are presented in Figures 10.7 and 10.8, were detected exclusively by geophysical means. Similarly to the other sites, most of them are located within the trapezoid borders. Lines number ❺ are the typical structures of that type. Known already from other complexes, they run parallel along the trapezoid margins ②, in the middle of the cleared area. Compared to similar ⑥ and ⑦, which course is less regular, lines ❺ might be interpreted as a trapezoid margins shaped in gradual surface clearing. Such assumption is questionable for ⑥, ⑦, ❹ or even ❸ due to the mentioned irregularity. Those lines, despite location within cleared area borders, run in various directions, none of them exactly matching the course of the structures, in which they are incorporated. This, together with the inconvenience of the small section measurement, greatly impedes their exact interpretation. The same concern the rest of identified structures. No matter if they are freely running dashed lines ❽ and ❾ or reflecting the direction of the trapezoid alongside which they occur lines ⑩, ⑪ and ❻, or eventually short and hard in classification lines ❹, ⑩ and ❶. All of them lack the broader viewpoint of the large surveying territory. Therefore, irrespective of the quantity of structures present in one

magnetic image, the apparent conclusion appears, that the smaller the measurement area is, the less information one can get from it. Thus, for the accurate and truthful interpretation work, particularly in such a territorially extensive locations, possibly the widest perspective is required. Hence, it is essential that any geophysical prospecting performed on geoglyphs of Palpa/Nasca, covers as much of the survey territory as it is achievable, especially if the research is not supported by other investigation techniques. It is therefore important that the particular lines may be correlated with their counterparts from the outside of the measurement area as well as from the utterly other locations. Consequently, the geophysical measurements on several different complexes is a prerequisite for the proper understanding of the one individual site.

Chapter 11

Synopsis

For the successful realization of defined objectives, a number of tasks have had to be completed in due course of the considered research activities. Throughout the project, techniques from the various scientific disciplines, among them geophysical prospecting, have been applied for archaeology, which considerably helped to get the understanding of one of the most mysterious monuments on Earth. It is believed that not only archaeology profited from the technical support, but all employed disciplines used this interdisciplinary collaboration opportunity to earn new ideas and broaden own perspectives, also for future applications. Certainly, magnetometry has taken the advantage of the cooperation, gaining the inspiration for the innovative data acquisition techniques as well as for the processing and interpretation methods. The final outcome of the geophysical contribution to the project, has been briefly summarized and presented below:

1. The new magnetometer system for archaeological prospecting based on the commercial instrument Scintrex Smartmag SM4G-Special has been developed and applied to the geoglyphs in the vicinity of the modern city of Palpa, Southern Peru. The apparatus has been arranged in a twin-sensor configuration for double speed of prospection with a spatial resolution of 0,25 m/0,5 m. Two sensors have worked parallel, measuring the total intensity of the geomagnetic field. Additionally, the horizontal gradient between them has been calculated, which in combination with the total field data turned out to be the most suitable configuration for the detection of obliterated patterns in the region close to the geomagnetic equator.

2. Five main complexes surrounding Palpa have been measured completing 790 km of walking profile and 60 Ha of scanned territory. Through the combination of modern data acquisition, processing and interpretation techniques, the older stratigraphic layers of the geoglyph constructional phases have been detected. In the course of research activities, numerous drawings, obliterated by the later construction of trapezoids, have been found and their exact location has been given. The number of other archaeological structures, among them traces of buildings, stone platforms, posts, pits and ditches, have been identified.
3. By the location of obliterated patterns, magnetometry assisted in the verification of the relative chronology of geoglyphs. It has also played a significant role in the systematic documentation of the cultural heritage of the region. Although magnetometry proved to be an important tool for finding the buried past, some of the archaeological structures on geoglyphs have been regrettably erased forever and cannot be reconstructed by any sophisticated technique now.
4. The new digital image processing techniques have been developed and applied to the raw data set. Among standard procedures presented in Chapter 5.2, the development included horizontal gradient recalculation of the total field data. The improvement of the processing software for the support of Scintrex SMARTMAG data has been made and the innovative interpretation methods such as “gradual transparency image overlay”, “equal intensity value identification” and “3D visualisations” have been employed. For the precise interpretation of territorially extensive sites, it has been confirmed, that the widest possible perspective, in terms of large area coverage, is required. If possible, the support based on other investigation techniques is valued. Hence, the comparison of the resulting magnetograms with the aerial images obtained by the photogrammetric means has been made.
5. The novel techniques for the reduction of daily variations of the geomagnetic field based on the profile and grid mean value recalculation have been used. The sensitivity of the measuring device by the introduction of the horizontal gradiometer system has been enhanced and the fieldwork methods for further applications have been improved. The new layout of the survey grid with the probes lined in the north – south direction and the west – east arranged traverses has been tested and ever since applied to the sites measured worldwide.

6. The measurement conditions in Peru in comparison to Europe have been assessed and resulting dissimilarities in size and shape of magnetic anomalies have been recognized. The origin of anomalies in Peruvian archaeological settings has been distinguished.

The accomplishment of specified objectives and tasks was possible by the correct understanding of the relations between them and the systematic realisation of defined work.

Chapter 12

Last Word and Conclusions

The magnetic prospecting method relies on the fact that almost all common soils reveal the enhancement of magnetic minerals in the topsoil (Fassbinder 1994). The occurrence of small sized and small scale magnetic anomalies measured ca. 30 cm above the surface, can be ascribed both to magnetic enhancement and remanence forming processes (Le Borgne 1955). The former may occur due to the enrichment of magnetic minerals in the archaeological features, the latter appears as a result of remanence building or destruction. As the southern Peruvian coast is one of the driest regions in the world, with the precipitation of less than 5 mm per year, it was necessary to verify not only all processes responsible for the formation of magnetic minerals in topsoil but also the types of remanent magnetizations. For the archaeological interpretation of the magnetic field data it was therefore crucial to understand the pathways of magnetic minerals formation as well as the type and origin of different remanent magnetizations (Fassbinder and Gorke 2009).

Given that the areas, on which the trapezoidal geoglyphs are located, were never subjected to any irrigation fields, no geochemical processes responsible for the formation of new magnetic minerals in the topsoil were observed. Additionally, the geoglyphs were never used as a settlement site, hence, the pedogenic processes producing magnetic minerals in topsoil by the use of fire could be also excluded there. Therefore, the magnetic anomalies found by the magnetic prospecting are believed to be mainly remanence based. Following this assumption, the older lines that are visible in the magnetic images are detectable due to the destroyed remanence of the soil beneath the line by the heavy compaction of the desert vesicular horizon. This occurred simply by intensive and multiple walking on the lines in the

course of ritual activity taking place on geoglyph sites. On the other hand, the same ritual procedure might have led to the enhancement in magnetic susceptibility of deposits, the primary structure of which has been condensed. Enrichment of magnetic minerals by wind separation may have contributed to the detection of magnetic anomalies on lines as well. The anomalies found over pits are made by the backfilling with the higher magnetic materials. These could be the magnetic remains of fireplaces or the accumulation of offerings such as pottery sherds.

The total field magnetometry combined with the development of the horizontal gradiometer system proved to be the most suitable configuration for detection of structures near the geomagnetic equator. The development of the new magnetometer arrangement not only revealed previously obliterated lines as well as other hitherto unknown features beneath the surface, but also gave a better archaeological understanding of the sites. All discoveries have been achieved by non-destructive geophysical methods and may therefore serve as an important archaeological tool for the further research on this extraordinary UNESCO World Heritage site. Apart from the new data acquisition techniques, the common processing tools and innovative interpretation methods have been developed and applied. Combined interpretation included total field and horizontal gradiometer data analyses, supplemented by the study of 3D images and aerial photographs.

Apart from the described archaeological structures, the most remarkable features are the extreme magnetic anomalies of lightning strikes. The detection of these structures in the desert may also contribute to the understanding of a changing climate. Although at the first glance they may seem to be insignificant for archaeology, it should be mentioned that strikes could have been attracted by archaeological constructions such like pylons or posts, which were also excavated on geoglyph sites.

While an excavation and a magnetic prospection are both a matter of discovery, in case of studied Peruvian geoglyphs, the latter is recommended as a tool for mapping the archaeological sites. While the effect of an excavation is a total destruction of the monument, magnetic prospection leads to similar results without devastation. Obviously magnetometry does not provide the archaeological artefacts, and therefore cannot serve as a dating method, but since Palpa/Nasca geoglyphs are the UNESCO World Heritage Site, magnetometry suits best the purpose of protection, being an excellent tool for the fast location of underground structures without destruction.

References

Aitken, M. J. (1958), Magnetic prospecting I, *Archaeometry*, 1, 24-29

Aitken, M. J. (1974), *Physics and Archaeology*, Clarendon Press, Oxford

Alexandrov, E. B., and V. A. Bonch-Bruevich (1992), Optically pumped atomic magnetometers after three decades, *Optical Engineering* 31(4), 711-717

Angenheister, G., and H. Soffel (1971), *Gesteinsmagnetismus und Paläomagnetismus*, Bornträger-Schweizerbart-Verlag, Stuttgart

Andrianov, B. A. et al. (1976): Andrianov, B. A., I. E. Grin'ko, A. F. Lukoshin, and P. S. Ovcharenko, High-sensitivity Caesium Magnetometer, *Measurement Techniques*, Vol. 19, No. 10, 1519-1522, A translation of *Izmeritel'naya Tekhnika*, No. 10, 85-56

Aveling, E. (1997), "Archaeology: Magnetic tracing of giant henge", *Nature*, 390, 232-233

Aveni, A. F. (ed.) (1990), *The lines of Nazca* (Memoirs of the American Philosophical Society 183). American Philosophical Society, Philadelphia 1990.

Aveni, A. F. (2000), *Between the lines: the mystery of the giant ground drawings of ancient Nasca, Peru*. University of Texas Press, Austin 2000.

Aveni, A. F. (2000), *Nasca: eight wonder of the world?*, British Museum Press, London

Becker, H. (1982), Befestigungswerke auf dem Galgenberg bei Kopfham, *Arch. Jahr Bayern* 1981, 72-73

Becker, H. (1995), From Nanotesla to Picotesla – a new window for magnetic prospecting in archaeology, *Archaeological Prospection*, 2, 217-228

Becker, H. (1997), Entwicklung und Einsatz von Multi-Sensor-Konfigurationen zur magnetischen Prospektion archäologischer Denkmäler, *Arch. Jahr Bayern* 1996, 195-197

Becker, H. (1999), Duo- and quadro-sensor configuration for high speed/high resolution magnetic prospecting with caesium magnetometer, *Archaeological prospection: third international conference on archaeological prospection*, 100-105

Belshe, J. C. (1957), Recent magnetic investigations at Cambridge University, *Adv. Phys.*, 6, 193-193

- Berner, R. A.** (1967), Thermodynamic stability of sedimentary iron sulphides, *American Journal of Science*, 265, 773-785
- Bloom, A. L.** (1960), Optical Pumping, *Scientific American*, October 1960, 2-10
- Bloom, A. L.** (1962), Principles of operation of the rubidium vapour magnetometer, *Applied Optics*, 1: 61-68
- Breiner, S.** (1965), The Rubidium Magnetometer in Archaeological Exploration, *Science*, Vol. 150, 185-193
- Browne D.** (1992), Further archaeological reconnaissance in the province of Palpa, Department of Ica, Peru. In: Saunders, Nicholas J. (ed.), *Ancient America*.
- Campbell, W. H.** (1997), Introduction to geomagnetic fields, Cambridge University Press, 303 pp.
- Canti, M. G., and N. Linford** (2000), The effects of fire on archaeological soils and sediments: Temperature and colour relationships, *Proceedings of the Prehistoric Society* 66, 385-395
- Chwala et al.** (2001): Chwala, A., R. Stolz, R. IJsselsteijn, V. Schultze, N. Ukhansky, H.-G. Meyer and T. Schüler, SQUID gradiometers for archaeometry, *Supercond. Sci. Technol.* 14, 1111–1114
- Clark, A.** (1990), *Seeing Beneath the Soil: Prospecting Methods in Archaeology*, Butler & Tanner, London, ISBN: 0-7134-7994-9
- Clarkson P.** (1990), The archaeology of the Nazca pampa: environmental and cultural parameters. In: Aveni, Anthony F. (ed.), *The lines of Nazca* (Memoirs of the American Philosophical Society 183), 115-172. American Philosophical Society, Philadelphia 1990.
- Cornell, R. M., and U. Schwertmann** (1996), *The iron oxides: Structure, Properties, Reactions, Occurrences and Uses*, VCH Verlagsgesellschaft Weinheim, New York, 573 pp.
- Curry, A.** (2007), Digging Into a Desert Mystery, *Science*, Vol. 317, 446-447
- David, A.** (1995), *Geophysical survey in archaeological field evaluation*, Research & Professional Services Guideline No. 1, English Heritage, London
- Dell, C. I.** (1972), An Occurrence of greigite in Lake Superior sediments, *American Mineralogist*, 57, 1303-1304
- Dunlop, D. J., and Ö. Özdemir** (1997), *Rock Magnetism: Fundamentals and Frontiers*, Cambridge University Press, Cambridge UK, ISBN: 0-521-32514-5
- DW Consulting, D. Wilbourn** (2006), *Archeosurveyor User Manual program version 202X*.
- Eitel, B., B. Mächtle, and G. Schukraft** (2004), Geomorphologisch-bodenkundliche Untersuchungen zur Rekonstruktion der Klima- und Landschaftsentwicklung im Umfeld der ehemaligen Siedlungsflächen der Nasca-Kultur, *Neue naturwissenschaftliche Methoden und Technologien für die archäologische Forschung in Palpa, Peru; Feldkonferenz des Projektverbundes – NASCA: Entwicklung und Adaption archäometrischer Techniken zur Erforschung der Kulturgesichte*, 15-19

- Eitel et al.** (2005): Eitel, Bernhard, Stefan Hecht, Bertil Mächtle, Gerd Schukraft, Annette Kadereit, Günther Wagner, Bernd Kromer, Ingmar Unkel, Markus Reindel: Geoarchaeological evidence from desert loess in the Nazca-Palpa region, southern Peru: paleoenvironmental changes and their impact on pre-Columbian cultures. *Archaeometry* 47(1), 137-158. 2005.
- Ellwood et al.** (1986): Ellwood, B. B., W. Balsam, B. Burkart, G. J. Long, and M. L. Buhl, Anomalous magnetic properties in rocks containing the mineral siderite: Palaeomagnetic implications, *J. Geophys. Res.*, 91, 12779-12790
- Enfield, D.** (1987), The Intraseasonal Oscillation in Eastern Pacific Sea Level, How is it forced?, *J. Phys. Ocean.*, 17, 1860–1876,
- Evans, M. E., and F. Heller** (2005), *Environmental Magnetism – Principles and Applications of Enviromagnetics*, Academic Press, Elsevier Science, San Diego, ISBN: 0-12-243851-5
- Fassbinder, J. W. E., H. Stanjek, and H. Vali** (1990), Occurrence of magnetic bacteria in soil, *Nature*, 343, 161-163
- Fassbinder, J. W. E., and H. Stanjek** (1993), Occurrence of bacterial magnetite in soils from archaeological sites, *Archaeol. Polona*, 31, 117-128
- Fassbinder, J. W. E.** (1994), *Die magnetischen Eigenschaften und die Genese ferrimagnetischer Minerale in Böden, im Hinblick auf die magnetische Prospektion archäologischer Bodendenkmäler*, Verlag Marie L. Leidorf, Buch am Erlbach
- Fassbinder, J. W. E., and H. Stanjek** (1994), Magnetic properties of biogenic soil greigite (Fe₃Se₄), *Geophysical Research Letters* 21, 2349-2352
- Fassbinder, J. W. E., and W. E. Irlinger** (1999), Combining magnetometry and archaeological interpretation: a square enclosure in Bavaria, in *Archaeological prospection, Arbeitshefte des Bayerischen Landesamtes für Denkmalpflege* 108, 95-99
- Fassbinder, J. W. E., and H. Becker** (1999), Magnetic prospection of a megalithic necropolis at Ibbankatuwa (Sri Lanka), in Fassbinder, Irlinger (eds.) *Archaeological prospection, Arbeitshefte des Bayerischen Landesamtes für Denkmalpflege* 108, 106-109
- Fassbinder, J. W. E., and S. Hecht** (2004), Geophysikalische Untersuchungen zur Erforschung vorsepanischer Kulturen in Palpa, *Neue naturwissenschaftliche Methoden und Technologien für die archäologische Forschung in Palpa, Peru; Feldkonferenz des Projektverbundes – NASCA: Entwicklung und Adaption archäometrischer Techniken zur Erforschung der Kulturgeichte*, 19-22
- Fassbinder, J.W.E., and M. Reindel** (2005), Magnetometerprospektion as research for Pre-Spanish cultures at Nasca and Palpa, Peru. *Proc. 6th International Conference on Archaeological Prospection*. Vol. 6, 6-10.
- Fassbinder, J.W.E., and T. Gorka** (2007), Neue Methoden der Magnetometerprospektion für die Archäologie: Das Horizontalgradiometer, *Das Arch. Jahr in Bayern, 2006*, 183-185.
- Fassbinder, J.W.E., and T. Gorka** (2007), Magnetometry on the Geoglyphs of Palpa and Nasca (Peru), in *Nasca Symposium 2006, Dresdner Kartographische Schriften*, edited by Bernd Teichert and Christoph Rust, pp. 71-77.

- Fassbinder, J.W.E., T. Gorka, and K. Lambers** (2007), Magnetometry on the Geoglyphs of Palpa and Nasca (Peru), in *Computer Applications and Quantitative Methods in Archaeology CAA 2007, Berlin*, pp. 43-44.
- Fassbinder, J.W.E., I. Unkel, and K. Lambers** (2007), A tiny tool for a large line: magnetometry and dating of Nasca lines in Palpa, Southern Peru, In: Small samples big objects, Proc. EU-ARTEC Seminar, Mach. M. (ed.), 27-39, Munich
- Fassbinder, J.W.E., K. Berghausen, and T. Gorka** (2008), Neue geophysikalische Messungen am rætischen Limes, *Denkmalpflege Informationen*, 141, 15-20.
- Fassbinder, J.W.E., and T. Gorka** (2009), Beneath the desert soil - archaeological prospecting with a cesium magnetometer, in *New technologies for archaeology. Multidisciplinary investigations in Palpa and Nasca, Peru, First, Natural Science in Archaeology*, edited by M. Reindel and G.A. Wagner, pp. 49-69, Springer, Berlin, Heidelberg, doi:10.1007/978-3-540-87438-6_4, ISBN: 978-3-540-87437-9.
- Gorka, T., J.W.E. Fassbinder, and K. Lambers** (2007), Magnetometry on the Geoglyphs of Palpa and Nasca (Peru), in *Archaeological Prospection, Studijne Zvesti Archeologickeho Ustavu Slovenskej Akademie Vied*, vol. 41, edited by Ivan Kuzma, pp. 176-179, Nitra, ISBN: 978-80-89315-00-0.
- Greulich, S., B. Kromer, I. Unkel, and G. Wagner** (2004), Neue Ansätze der Chronometrie in der peruanischen Archäologie: Ortsaufgelöste Lumineszenz- und AMS-Radiokohlenstoff-Datierung, *Neue naturwissenschaftliche Methoden und Technologien für die archäologische Forschung in Palpa, Peru; Feldkonferenz des Projektverbundes – NASCA: Entwicklung und Adaption archäometrischer Techniken zur Erforschung der Kulturgesichte*, 19-22
- Grün et al.** (2000): Grün, A., S. Bär, S. Beutner: Signals in the sand: 3-D recording and visualization of the Nasca geoglyphs. *PFG Photogrammetrie - Fernerkundung – Geoinformation* 6/2000, 385-398. 2000.
- Grün A., and S. Beutner** (2001), The geoglyphs of San Ignacio - new results from the Nasca project. *International Archives of Photogrammetry, Remote Sensing and Spatial Information Sciences* XXXIV-5/W1, 18-23. 2001.
- Grün A., and K. Lambers** (2003), The geoglyphs of Nasca: 3-D recording with modern digital technologies. In: *Acts of the XIVth UISPP Congress, University of Liège, Belgium, 2-8 September 2001, section 1: theory and methods - general sessions and posters* (BAR International Series 1145), 95-103. Archaeopress, Oxford 2003.
- Hall, E. T.** (1962), Some notes on the design and manufacture of detector heads for proton magnetometers, *Archaeometry* 5, 139-145
- Hesse, R., and J. Baade** (2007), Palaeoenvironmental changes in the Nasca-Palpa Region, Southern Peru – Alternative interpretations of geoarchaeological evidence, *Archaeometry*, 49, 595-602
- Housen et al.** (1996): Housen B. A., S. K. Banerjee, and B. M. Moskowitz, Low-temperature magnetic properties of siderite and magnetite in marine sediments, *Geophys. Res. Lett.* 23, 2834-2846

- Isla et al.** (2003): Isla, Johny, Markus Reindel, Juan Carlos De La Torre: Jauranga: un sitio Paracas en el valle de Palpa. *Beiträge zur Allgemeinen und Vergleichenden Archäologie* 23, 227-275. 2003.
- Johnson et al.** (1990): Johnson, Gerald W., Douglas E. Meisner, William L. Johnson: Aerial photography of the Nazca lines. In: Aveni, Anthony F. (ed.), *The lines of Nazca* (Memoirs of the American Philosophical Society 183), 271-283. American Philosophical Society, Philadelphia 1990.
- Kadereit et al.** (2007): Kadereit A., S. Greulich, C. Woda, and G. Wagner: Kaltes Licht aus alten Steinen – Lumineszenzdatierung in der Archäologie, in G. Wagner (ed.) Einführung in die Archäometrie, Springer, Berlin
- Kearey, P., M. Brooks, and I. Hill** (2002), An Introduction to Geophysical Exploration, Blackwell Publishing, Oxford, ISBN-10: 0-632-04929-4
- Kosok, P.** (1965), *Life, land and water in ancient Peru*. Long Island University, Brooklyn 1965.
- Kosok, P., and M. Reiche** (1949), Ancient drawings on the desert of Peru. *Archaeology* 2(4).
- Kozera, A.** (1976), Geofizyka – metody grawimetryczne i magnetyczne. Wydawnictwa geologiczne, Warszawa
- Lagos et al.** (2008): P. Lagos, Y. Silva, E. Nickl, and K. Mosquera, El Nino – related precipitation variability in Peru, *Adv. Geosci.*, 14, 231–237
- Lambers, K., M. Sauerbier, and A. Grün** (2004), Einsatz von Photogrammetrie und Laserscanning zur Dokumentation von Geoglyphen und Ruinen in Palpa und Nasca, *Neue naturwissenschaftliche Methoden und Technologien für die archäologische Forschung in Palpa, Peru; Feldkonferenz des Projektverbundes – NASCA: Entwicklung und Adaption archäometrischer Techniken zur Erforschung der Kulturgesichte*, 23-27
- Lambers, K.** (2006), The Geoglyphs of Palpa, Peru: Documentation, Analysis, and Interpretation. Linden Soft Verlag, Aichwald, Germany, ISBN: 3-929290-32-4
- Le Borgne, E.** (1955), Susceptibilité magnétique anormale du sol superficiel, *Ann. Geophys.*, 11, 399-419
- Le Borgne, E.** (1960), Influence du feu sur les propriétés magnétiques du sol et sur celles du chiste et du granite, *Ann. Geophys.* 16, 159-195
- Le Borgne, E.** (1965), Les propriétés magnétiques du sol. Application a la prospection des sites archéologiques. *Archaeo-Physika* 1, 1-20
- Lenz, J. E.** (1990), A Review of Magnetic Sensors, *Proceedings of the IEEE*, Vol. 78, No. 6
- Linford, P.** (2003), Integrated use of caesium vapour total field and gradiometer magnetometer surveys to maximize data recovery and archaeological interpretation: field experiments from United Kingdom, *Archeologia Polona*, no. 41, 229-231.
- Linington, R. E.**, (1970), *Magnetic Surveying*, Leric Foundation, Milan Polytechnic School.
- Longworth, G., and M. S. Tite** (1977), Mössbauer and magnetic susceptibility studies of iron oxides in soils from archaeological sites, *Archaeometry* 19, 3-14

- Lowrie, W.** (1997), *Fundamentals of Geophysics*, Cambridge University Press, United Kingdom, ISBN: 0-521-46728-4
- Loveley, D. R., J. F. Stolz, E. J. P. Phillips, and G. L. Nord** (1987), Anaerobic production of magnetite by a dissimilatory iron-reducing microorganism, *Nature*, 330, 252-254
- Maher, B. A., and R. M. Taylor** (1988), Formation of ultrafine-grained magnetite in soils, *Nature*, 336, 368-370
- Maher, B. A., and R. M. Taylor** (1989), Origin of soil magnetite, *Nature* 340, 106
- Maki, D.** (2005), Lightning Strikes and Prehistoric Ovens: Determining the Source of Magnetic Anomalies Using Techniques of Environmental Magnetism, *Geoarchaeology: An International Journal*, Vol. 20, No. 5, 449-459
- Mächtle et al.** (2006), Holocene environmental changes in the northern Atacama desert, Southern Peru (14°30'S) and their impact on the rise and fall of pre-Columbian cultures, *Zeitschrift für Geomorphologie*, supplement 142, 47-62
- Mächtle B.** (2007), Geomorphologisch-bodenkundliche Untersuchungen zur Rekonstruktion der holozänen Umweltgeschichte in der nördlichen Atacama im Raum Palpa, Südperu. Diss. Heidelberger Geographische Arbeiten 123, Heidelberg
- Mächtle et al.** (2009), Built on the sand: Climatic Oscillation and Water Harvesting During the Late Intermediate Period, in *New technologies for archaeology. Multidisciplinary investigations in Palpa and Nasca, Peru, First, Natural Science in Archaeology*, edited by M. Reindel and G.A. Wagner, pp. 49-69, Springer, Berlin, Heidelberg
- McClellan, R. G., and W. F. Kean** (1993), Contributions of wood ash magnetism to archaeomagnetic properties fire pits and hearths, *Earth and Planetary Science Letters* 119, 387-394
- Milsom, J.** (1989), *Field geophysics*, Halsted Press, New York, ISBN: 0-470-21156-3
- Mullins, C. E.** (1974), The magnetic properties of the soil and their application to archaeological prospecting, *Archaeo-Physika* 5
- Mullins, C. E.** (1977), Magnetic susceptibility of soils and its significance in soil science – a review, *J. Soil Sci.*, 28, 223-246
- Neubauer, W.** (1990), Geophysikalische Prospektion in der Archäologie, *Mittl. Anthropol. Ges. Wien*, 120, 1-60.
- Neubauer, W.** (2001), Images of the invisible – Prospection methods for the documentation of threatened archaeological sites, *Naturwissenschaften*, No. 88, 13-24.
- Okrusch, M., and S. Matthes** (2005), *Eine Einführung in die spezielle Mineralogie, Petrologie und Lagerstättenkunde*, 7 Auflage, Springer Verlag, Berlin, Heidelberg, New York
- Reiche, M.**, (1976), *Geheimnis der Wüste / Mystery on the desert / Secreto de la pampa*. 6th ed. Stuttgart 1976.

Reindel, M., and G. Wagner (eds.) (2004), *Neue naturwissenschaftliche Methoden und Technologien für die archäologische Forschung in Palpa, Peru / Nuevos métodos y tecnologías para la investigación arqueológica en Palpa, Perú*. Companion volume, Nasca-Palpa project field conference, Palpa, Peru, 17-22 September 2004. Goethe Institut, Lima.

Reindel, M., K. Lambers, and A. Grün (2003), Photogrammetrische Dokumentation und archäologische Analyse der vorspanischen Bodenzeichnungen von Palpa, Südperu/ Documentación fotogramétrica y análisis arqueológico de los geoglifos prehispánicos de Palpa, costa sur del Perú. *Beiträge zur Allgemeinen und Vergleichenden Archäologie* 23, 183-226

Reindel, M., J. Isla, and K. Lambers (2003), Die Arbeiten des Archäologischen Projektes Nasca-Palpa, Peru, im Jahr 2002. *SLSA-Jahresbericht* 2002, 119-132

Reindel, M., J. Isla, and K. Lambers (2002), Abschliessende Untersuchungen zu Geoglyphen und Siedlungen in Palpa, Südperu: Ergebnisse der Feldkampagne 2001 des Archäologischen Projektes Nasca-Palpa. *SLSA-Jahresbericht* 2001, 37-54. 2002.

Reindel, M., and A. Grün (2006), The Nasca-Palpa Project: a cooperative approach of photogrammetry, archaeology and archaeometry. In: E. Baltasvias et al. (eds.), *Recording, modelling and visualisation of cultural heritage*, London 2006, 21-32

Reinhard, J. (1996), *The Nazca lines: a new perspective on their origin and meaning*. 6th ed. Editorial Los Pinos, Lima 1996.

Rodríguez, A. (1999), *Los campos de geoglifos en la costa central del Perú* (Cuadernos de Investigación 2/1997). Instituto Riva Agüero, Lima 1999.

Rostworowski, M. (1993), Origen religioso de los dibujos y rayas de Nasca. *Journal de la Société des Américanistes* LXXIX, 189-202. 1993.

Sauerbier, M., and K. Lambers (2003), A 3D model of the Nasca lines at Palpa (Peru). *International Archives of Photogrammetry, Remote Sensing and Spatial Information Sciences* XXXIV-5/W10.

Scollar, I. (1970), Magnetic Methods of Archaeological Prospecting – Advances in Instrumentation and Evaluation Techniques, *Phil. Trans. Roy. Soc. Lond. A.* 269, 109-119

Scollar I., and A. Lander (1972), A subtraction circuit for the differential operation of two commercial proton magnetometers, *Prospezioni Archeologiche*, 7, 93-98

Scollar et al. (1990): Scollar, I., A. Tabbagh, A. Hesse, I. Herzog, *Archaeological Prospecting and Remote Sensing*, in *Topics in Remote Sensing, 2*, edited by G. Hunt and M. Rycroft, Cambridge University Press, Cambridge UK, ISBN: 0-521-32050-X

Silverman, H. (1990), The early Nasca pilgrimage center of Cahuachi and the Nasca lines: anthropological and archaeological perspectives. In: Aveni, Anthony F. (ed.), *The lines of Nazca* (Memoirs of the American Philosophical Society 183), 207-244. American Philosophical Society, Philadelphia 1990.

Silverman, H. (1990), Beyond the pampa: the geoglyphs in the valleys of Nazca. *National Geographic Research* 6(4), 435-456. 1990.

- Silverman, H., and D. Browne** (1991), New evidence for the date of the Nazca lines. *Antiquity* 65, 208-220. 1991.
- Silverman, H., and D. Proulx** (2002), *The Nasca* (The Peoples of America). Blackwell, Malden, Oxford 2002.
- Soffel, H.** (1991), Paläomagnetismus und Archäomagnetismus, Springer Verlag, Berlin
- Stanjek et al.** (1994): Stanjek, H., J. W. E. Fassbinder, H. Vali, H. Wägele, and W. Graf, Evidence of biogenic greigite (ferrimagnetic Fe₃S₄) in soil. *European Journal of Soil Science*, 45, 97-103
- Stenz, E., and M. Mackiewicz** (1964), *Geofizyka ogólna*, PWN, Warszawa
- Stolz, W. A.** (1963), Rubidiumdampf-Magnetometer, *Z. Instr.* 71, Heft 10.
- Telford et al.** (1976): Telford, W. M., L. P. Geldart, R. E. Sheriff, and D. A. Keys, *Applied Geophysics*, Cambridge University Press, 860 pp.
- Thellier, E., and O. Thellier** (1938), Sur l'aimantation des terres cuites et ses applications géophysiques. *Annales de l'Institut de Physique du Globe*, 16, 157-302
- Thellier, E., and O. Thellier** (1959), Sur l'intensité du champ magnétique terrestre dans le passé historique et géologique. *Ann. Geophys.* 15, 285-376
- Tite, M.S.** (1966), Magnetic Prospecting Near the Geomagnetic Equator, *Archaeometry*, 9, 24-31
- Tite, M.S., and C. E. Mullins**, (1971), Enhancement of the magnetic susceptibility of soils on archaeological sites. *Archaeometry*, 13, 209-220
- Thompson, R., and F. Oldfield** (1986), *Environmental Magnetism*, Allen & Unwin, London, ISBN: 0-04-538003-1
- Trenberth, K. E.** (1997), The Definition of El Nino, *Bulletin of the American Meteorological Society*, Vol. 78, No. 12, 2771-2777
- Urton, G.** (1990), Andean social organization and the maintenance of the Nazca lines. In: Aveni, Anthony F. (ed.), *The lines of Nazca* (Memoirs of the American Philosophical Society 183), 173-206. American Philosophical Society, Philadelphia 1990.
- Wurm, M.** (1950), Beiträge zur Theorie und Praxis des Feldstärkedifferenzmessers für magnetische Felder nach Förster, *Zeitschrift für angewandte Physik*, Band 11, Heft 5, 210-219.
- Yapp, C. J.** (1983), Stable hydrogen isotopes in iron oxides isotope effects associated with the dehydration of a natural goethite, *Geochim. Cosmochim. Acta*, 47, 1277-1287

List of figures

Figure 1.1	Reloj Solar (Sun Dial) - geoglyph complex located on the southern slope of Cresta de Sacramento, north of Palpa; source – DAI: http://www.dainst.org/index_593_de.html	2
Figure 2.1	Geoglyph complex along the northern edge of the Nasca pampa; source Google Earth	6
Figure 3.1	Map of the Ica Region (Southern Peru) (http://www.dainst.org/index_593_de.html)	10
Figure 3.2	Satellite photograph of the Provinces of Palpa and Nasca (Southern Peru)	10
Figure 3.3	Shaded relief map of Peru (http://www.lib.utexas.edu/maps/peru.html on 15.02.2008); changed by the author; green circle – area of research	11
Figure 3.4	Area of research; red circles represent 5 measured geoglyph complexes surrounding the modern city of Palpa (green circle): A – PP01-36 Llipata, B – PV67A-15/16 Yunama, C – PV67A-47 Sacramento, D – PV67B-55 Carapo and E – PP01-49 San Ignacio; source Depto. Ica, Peru; SLSA Zürich, ETH Zürich; K. Lambers (2006); changed by the author ...	12
Figure 3.5	Geological map of the study area; red circles – prospected geoglyph locations; Carta Geologica del Peru (Mapa Geológico del Caudrángulo de Palpa) Ministerio de Energia y Minas, Instituto Geológico Minero y Metalúrgico, 1994 (source: http://www.ingemmet.gob.pe/form/plantilla01.aspx?opcion=27 on 24.04.2007); modified by the author	15
Figure 4.1	The elements of the Earth's magnetic field (left) and the dipole approximation of the geomagnetic field (right) (source http://radbelts.gsfc.nasa.gov/outreach/Radbelts0.html on 15.02.2009)	18
Figure 4.2	Idealized shape of anomaly in the total magnetic field intensity from a dipole source at different geomagnetic latitudes; left in Europe – the angle of dip is taken to be approx. 60°; right in Palpa at up to 3°, idealized to magnetic equator 0°. The horizontal scale represents a north – south traverse through the centre of anomaly in units of burial depth (violet square – anomaly source), vertical scale – anomaly strength as a deviation from the normal field strength (horizontal line of the coordinate system)	24
Figure 5.1	Caesium magnetometer sensor: caesium is pumped from a caesium-vapour lamp (far right) through the circular polarizer and a plastic condensing lens into an absorption cell (center). Coil around cell sets up a fluctuating magnetic field. Some of the energy of the beam is absorbed to pump atoms in cell to higher energy levels; the rest passes through the absorption cell and is measured by the photocell at far left (description after Bloom 1960; changed by the author)	31
Figure 5.2	The complete <i>Scintrex® SMARTMAG SM4G</i> gradiometer kit consisting of magnetometer sensors with cables, sensor electronics, readout unit (SMARTMAG console), battery belt and additional accessories (source: Scintrex, Ltd.)	32
Figure 5.3	The new SMARTMAG SM4G magnetometer frame construction providing effortless set-up in the field and unproblematic transportation to the measurement area	33
Figure 5.4	The new SMARTMAG SM4G magnetometer frame construction providing effortless set-up in the field and unproblematic transportation to the measurement area	33

Figure 5.5	Field measurement in Palpa, southern Peru; March 2006; magnetic sensors' correction 45°	34
Figure 5.6	Field measurement in Palpa in march 2006; walking along the survey lines	34
Figure 5.7	Simplified sketch of the measurement procedure; buried archaeological object generates the anomalous field producing the magnetic anomaly which can be measured by the sensitive magnetometer; field's inclination ca. 60°	34
Figure 5.8	Measurement grid and survey walking pattern	34
Figure 5.9	Temporal variations of the geomagnetic field; A - During a 60 second field measurement a linear decrease of about 0.3 nT is observed (top); while drift is removed (bottom), particular data present a 0.06 nT difference; B - in the gradiometer mode geomagnetic variations are reduced by the measurement of the difference between two magnetic sensors in the FM36 fluxgate gradiometer by Geoscan Research (top) and in the SM4 Gradiometer system by Scintrex (bottom) (Figure by Neil Linford, per. com)	36
Figure 5.10	Screenshot of the ArcheoSurveyor version 2200 (DW Consulting) during the processing of Peruvian test site Estequerilla (west of Palpa)	37
Figure 5.11	Scintrex SMARTMAG SM4G magnetometer data set. The XYZ data format is compatible with the processing software written by DW Consulting and Geoscan Research. This format contains a header section with the information about the job/grid/line numbers, date of survey, operator name, sampling rate, bandwidth and sensor separation. Data is placed into columns: X, Y, Total Field Sensor 1, Total Field Sensor 2, Time, Gradiometer	38
Figure 6.1	Orthophoto of the geoglyph site PP01-36 from the Pampa de Llipata, south of Palpa; K. Lambers, Institute of Geodesy and Photogrammetry, ETH Zürich, Switzerland	44
Figure 6.2	Detailed map of the geoglyph site PP01-36 from the Pampa de Llipata, south of Palpa; by K. Lambers, Institute of Geodesy and Photogrammetry, ETH Zürich, Switzerland	45
Figure 6.3	Magnetogram of the geoglyph complex on site PP01-36 "Llipata" located on Pampa de Llipata, south of Palpa; measurement in the Total Field Mode, SMARTMAG SM4G-Special in duo-sensor configuration; dynamics +/- 13 nT in 100 greyscale values from black to white, sampling density 50 x 12,5 cm, interpolated to 25 x 25 cm, resolution increased by 'Graduated Shade' function; Earth's magnetic field ca. 25000 nT; grid size 40 x 40 m	48
Figure 6.4	Magnetogram of the geoglyph complex on site PP01-36 "Llipata" located on Pampa de Llipata, south of Palpa; measurement in the Horizontal Gradiometer Mode, SMARTMAG SM4G-Special in duo-sensor configuration; dynamics +/- 13 nT in 100 greyscale values from black to white, sampling density 100 x 12,5 cm, interpolated to 25 x 25 cm, resolution increased by 'Graduated Shade' function; Earth's magnetic field ca. 25000 nT; grid size 40 x 40 m	49
Figure 6.5	Location of the LIRM structures (red circles) superimposed on the total field magnetogram of the geoglyph complex on site PP01-36 "Llipata", south of Palpa; Measurement with SMARTMAG SM4G-Special in duo-sensor configuration; dynamics +/- 13 nT in 100 greyscale values from black to white, sampling density 50 x 12,5 cm, interpolated to 25 x 25 cm, resolution increased by 'Graduated Shade' function; Earth's magnetic field ca. 25000 nT; grid size 40 x 40 m	50

Figure 6.6	Interpretation of the geoglyph complex on site PP01-36 “Llipata” plotted on the Horizontal Gradiometer Mode magnetogram; SMARTMAG SM4G-Special in duo-sensor configuration; dynamics +/- 13 nT in 100 greyscale values from black to white (with 50% of transparency applied), sampling density 100 x 12,5 cm, interpolated to 25 x 25 cm, resolution increased by ‘Graduated Shade’ function; Earth’s magnetic field ca. 25000 nT; grid size 40 x 40 m	51
Figure 6.7	Interpretation of the geoglyph complex on site PP01-36 “Llipata” located on Pampa de Llipata, south of Palpa; red, green and black lines represent ancient linear structures found by geophysical prospecting combined with aerial photography; grid size 40 x 40 m; numbers ① - ⑩ correspond to the documented set of lines (see description in text)	52
Figure 6.8	Magnetogram of the site PP01-36 “Llipata” superimposed on the orthophoto of the same area; Caesium SmartMag SM4G – Special applied in the duo-sensor configuration. Sampling rate 12,5 x 50 cm interpolated to 25 x 25 cm, grid size 40 x 40 meter, dynamics +/-20 nT, Earth’s magnetic field ca. 25.000 nT; orthoimage by K. Lambers, Institute of Geodesy and Photogrammetry, ETH Zürich, Switzerland	53
Figure 7.1	Orthophoto of the geoglyph site PV67A-15/16 from the Cresta de Sacramento, west of Palpa; K. Lambers, Institute of Geodesy and Photogrammetry, ETH Zürich, Switzerland ...	57
Figure 7.2	Detailed map of the geoglyph site PV67A-15/16 from the Cresta de Sacramento; the geoglyph assemblage with a strtigraphical sequence of different phases of construction and reworking drawn after an aerial photograph; K. Lambers, Institute of Geodesy and Photogrammetry, ETH Zürich, Switzerland	58
Figure 7.3	Magnetogram of the geoglyph complex on site PV67A-15/16 “Yunama” located on Cresta de Sacramento, west of Palpa; measurement in the Total Field Mode, SMARTMAG SM4G-Special in duo-sensor configuration; dynamics +/- 7 nT in 100 greyscale values from black to white, sampling density 50 x 12,5 cm, interpolated to 25 x 25 cm, resolution increased by ‘Graduated Shade’ function; Earth’s magnetic field ca. 24000 nT; grid size 40 x 40 m	61
Figure 7.4	Magnetogram of the geoglyph complex on site PV67A-15/16 “Yunama” located on Cresta de Sacramento, west of Palpa; measurement in the Gradiometer Mode, SMARTMAG SM4G-Special in duo-sensor configuration; dynamics +/- 5 nT in 100 greyscale values from black to white, sampling density 100 x 12,5 cm, interpolated to 25 x 25 cm, resolution increased by ‘Graduated Shade’ function; Earth’s magnetic field ca. 24000 nT; grid size 40 x 40 m	62
Figure 7.5	Interpretation of the geoglyph complex on site PV67A-15/16 “Yunama” plotted on the Total Field Mode magnetogram; SMARTMAG SM4G-Special in duo-sensor configuration; dynamics +/- 7 nT in 100 greyscale values from black to white (with 50% of transparency applied); sampling density 50 x 12,5 cm, interpolated to 25 x 25 cm, resolution increased by ‘Graduated Shade’ function; Earth’s magnetic field ca. 24000 nT; grid size 40 x 40 m; Red circle – location of the LIRM structure	63
Figure 7.6	Interpretation of the geoglyph complex on site PV67A-15/16 “Yunama” located on Cresta de Sacramento, west of Palpa; red, green and black lines represent ancient linear structures found by geophysical prospecting combined with aerial photography; ; grid size 40 x 40 m; numbers ① - ⑩ correspond to the documented set of lines (see description in text)	64
Figure 7.7	Magnetogram of the site PV67A-15/16 “Yunama” superimposed on the orthophoto of the same area; Caesium SmartMag SM4G – Special applied in the duo-sensor configuration. Sampling rate 12,5 x 50 cm interpolated to 25 x 25 cm, grid size 40 x 40 meter, dynamics +/- 7 nT, Earth’s magnetic field ca. 25.000 nT; orthoimage by K. Lambers, Institute of Geodesy and Photogrammetry, ETH Zurich, Switzerland	65

Figure 7.8	Magnetogram of the Total Field measurement on site PV67A-15/16 in a 3D-like visualisation seen from SW at the view angle 24°; Caesium SmartMag SM4G – Special applied in the duo-sensor configuration. Sampling rate 12,5 x 50 cm interpolated to 25 x 25 cm, grid size 40 x 40 meter, dynamics +/- 7 nT in colour spectrum values from green to blue; Earth's magnetic field ca. 25.000 nT; top of the image pointing NE	66
Figure 8.1	Orthophoto of the geoglyph site PV67A-47; Cresta de Sacramento, north of Palpa	71
Figure 8.2	Interpretation of geoglyphs on site PV67A-47; K. Lambers; Institute of Geodesy and Photogrammetry, ETH Zürich, Switzerland	71
Figure 8.3	Detailed map of the geoglyph site PV67A-47 from the Cresta de Sacramento; the geoglyph assemblage with a strtigraphical sequence of different phases of construction and reworking drawn after aerial photograph (Figure 8.1); K. Lambers, Institute of Geodesy and Photogrammetry, ETH Zürich, Switzerland	72
Figure 8.4	Magnetogram of the spiral structures on site PV67A-47 "Sacramento"; A – Total Field measurement with Caesium SmartMag SM4G – Special applied in the duo-sensor configuration; sampling density 12,5 x 50 cm interpolated to 25 x 25 cm, dynamics +/-10 nT; B – recalculated Gradiometer image of the same structure; sampling increment 12,5 x 100 cm interpolated to 25 x 25 cm; dynamics +/-18 nT; grid size 40 x 40 meter; Earth's magnetic field ca. 25.000 nT	73
Figure 8.5	Magnetogram of the geoglyph complex on site PV67A-47 "Sacramento" located on Cresta de Sacramento, north of Palpa; measurement in the Total Field Mode, SMARTMAG SM4G-Special in twin sensor configuration; dynamics approx. +/- 12 nT in 100 greyscale values from black to white, sampling density 50 x 12,5 cm, interpolated to 25 x 25 cm, resolution increased by 'Graduated Shade' function; Earth's magnetic field ca. 25000 nT; grid size 40 x 40 m	74
Figure 8.6	Magnetogram of the geoglyph complex on site PV67A-47 "Sacramento" located on Cresta de Sacramento, north of Palpa; measurement in the Gradiometer Mode, SMARTMAG SM4G-Special in twin sensor configuration; dynamics approx. +/- 13 nT in 100 greyscale values from black to white, sampling density 100 x 12,5 cm, interpolated to 25 x 25 cm, resolution increased by 'Graduated Shade' function; Earth's magnetic field ca. 25000 nT; grid size 40 x 40 m	75
Figure 8.7	Location of the LIRM structures (red circles) and possible LIRM structures (yellow circles) superimposed on the total field magnetogram of the geoglyph complex on site PV67A-47 "Sacramento", north of Palpa; SMARTMAG SM4G-Special in duo-sensor configuration; dynamics +/- 12 nT in 100 greyscale values from black to white, sampling density 50 x 12,5 cm, interpolated to 25 x 25 cm, resolution increased by 'Graduated Shade' function; Earth's magnetic field ca. 25000 nT; grid size 40 x 40 m	76
Figure 8.8	Interpretation of linear structures (red and green) on site PV67A-47 "Sacramento" plotted on the Total Field Mode magnetogram; SMARTMAG SM4G-Special in duo-sensor configuration; dynamics approx. +/- 12 nT in 100 greyscale values from black to white (with transparency factor 50%), sampling density 50 x 12,5 cm, interpolated to 25 x 25 cm, resolution increased by 'Graduated Shade' function; Earth's magnetic field ca. 25000 nT; grid size 40 x 40 m	77
Figure 8.9	Interpretation of additional linear structures (black) on site PV67A-47 "Sacramento" plotted on the Total Field Mode magnetogram; SMARTMAG SM4G-Special in duo-sensor configuration; dynamics approx. +/- 12 nT in 100 greyscale values from black to white (with transparency factor 50%), sampling density 50 x 12,5 cm, interpolated to 25 x 25 cm, resolution increased by 'Graduated Shade' function; Earth's magnetic field ca. 25000 nT; grid size 40 x 40 m	78

Figure 8.10	Interpretation of the geoglyph complex on site PV67A-47 “Sacramento” located on Cresta de Sacramento, north of Palpa; red lines represent ancient linear structures found by geophysical prospecting combined with aerial photography; grid size 40 x 40 m; numbers ① - ⑤ correspond to the documented set of lines (see description in text)	79
Figure 8.11	Interpretation of the geoglyph complex on site PV67A-47 “Sacramento” located on Cresta de Sacramento, north of Palpa; green and black lines represent ancient linear structures found exclusively by geophysical prospecting; grid size 40 x 40 m; numbers ⑥ - ⑩ and ② - ⑦ correspond to the documented set of lines (see description in text)	80
Figure 8.12	Magnetogram of the Total Field measurement on site PV67A-47 in a 3D-like visualisation seen from W at the view angle 20°; Caesium SmartMag SM4G – Special applied in the gradiometer mode. Sampling rate 12,5 x 100 cm interpolated to 25 x 25 cm, grid size 40 x 40 meter, dynamics +/- 13 nT in colour spectrum values from green to blue; Earth’s magnetic field ca. 25.000 nT; top of the image pointing E	82
Figure 8.13	Star-shaped magnetic anomaly from site PV67A-47 “Sacramento” caused by the lightning induced remanent magnetisation; Caesium SmartMag SM4G – Special applied in duo-sensor configuration; Sampling rate 12,5 x 50 cm interpolated to 25 x 25 cm, grid size 40 x 40 meter, dynamics +/- 250 nT in 99 greyscale values from black to white; Earth’s magnetic field ca. 24.000 nT	83
Figure 9.1	Orthophoto of the geoglyph site PV67B-55; Cerro Carapo, east of Palpa	88
Figure 9.2	Interpretation of drawings on site PV67B-55; after K. Lambers; ETH Zürich	88
Figure 9.3	Detailed map of the geoglyph site PV67B-55 from Cerro Carapo; geoglyph assemblage with a strtigraphical sequence of different phases of construction and reworking drawn after aerial photograph; by K. Lambers, Institute of Geodesy and Photogrammetry, ETH Zürich	89
Figure 9.4	Detailed map of the geoglyph site PV67B-55 from Cerro Carapo; geoglyph assemblage with a strtigraphical sequence of different phases of construction and reworking drawn after aerial photograph; by K. Lambers, Institute of Geodesy and Photogrammetry, ETH Zürich	89
Figure 9.5	Traverse layout and magnetometer grid arrangement on Peruvian geoglyph complexes Carapo and San Ignacio	90
Figure 9.6	Magnetograms of the site PV67B-55 “Carapo” located on Cerro Carapo east of Palpa; measurement in the Total Field Mode with dynamics approx. +/- 13 nT; SMARTMAG SM4G-Special in twin sensor configuration; sampling density 50 x 12,5 cm, interpolated to 25 x 25 cm, resolution increased by ‘Graduated Shade’ function; Earth’s magnetic field ca. 25000 nT; grid size 40 x 40 m	91
Figure 9.7	Magnetograms of the site PV67B-55 “Carapo” located on Cerro Carapo east of Palpa; measurement in the Gradiometer Mode with dynamics approx. +/- 17 nT; SMARTMAG SM4G-Special in twin sensor configuration; sampling density 100 x 12,5 cm, interpolated to 25 x 25 cm, resolution increased by ‘Graduated Shade’ function; Earth’s magnetic field ca. 25000 nT; grid size 40 x 40 m	91
Figure 9.8	Interpretation of linear structures (red, green and black) on site PV67B-55 “Carapo” plotted on the Gradiometer Mode magnetogram; SMARTMAG SM4G-Special in duo-sensor configuration; dynamics approx. +/- 12 nT in 100 greyscale values from black to white (with transparency factor 50%), sampling density 100 x 12,5 cm, interpolated to 25 x 25 cm, resolution increased by ‘Graduated Shade’ function; Earth’s magnetic field ca. 25000 nT; grid size 40 x 40 m	92

Figure 9.9	Interpretation of linear structures (red, green and black) on site PV67B-55 “Carapo” plotted on the Gradiometer Mode magnetogram; SMARTMAG SM4G-Special in duo-sensor configuration; dynamics approx. +/- 12 nT in 100 greyscale values from black to white (with transparency factor 50%), sampling density 100 x 12,5 cm, interpolated to 25 x 25 cm, resolution increased by ‘Graduated Shade’ function; Earth’s magnetic field ca. 25000 nT; grid size 40 x 40 m	92
Figure 9.10	Interpretation of the geoglyph complex on site PV67B-55 “Carapo” located on Cerro Carapo, east of Palpa; red and green lines represent ancient linear structures found by geophysical prospecting combined with aerial photography; grid size 40 x 40 m; numbers ① - ⑩ correspond to the documented set of lines (see description in text)	93
Figure 9.11	Interpretation of the geoglyph complex on site PV67B-55 “Carapo” located on Cerro Carapo, east of Palpa; red and black lines represent ancient linear structures found by geophysical prospecting combined with aerial photography; grid size 40 x 40 m; numbers ① - ⑩ correspond to the documented set of lines (see description in text)	93
Figure 10.1	Orthophoto of the geoglyph site PP01-49 from the Pampa de San Ignacio, south of Palpa; K. Lambers, Institute of Geodesy and Photogrammetry, ETH Zürich, Switzerland ..	97
Figure 10.2	Orthophoto of the survey area on site PP01-49 from the Pampa de San Ignacio, south of Palpa; K. Lambers, Institute of Geodesy and Photogrammetry, ETH Zürich, Switzerland ...	98
Figure 10.3	Magnetogram of the site PP01-49 “San Ignacio” located on Pampa de San Ignacio; south of Palpa; measurement in the Total Field Mode with dynamics approx. +/- 19 nT; SMARTMAG SM4G-Special in twin sensor configuration; sampling density 50 x 12,5 cm, interpolated to 25 x 25 cm, resolution increased by ‘Graduated Shade’ function; Earth’s magnetic field ca. 25000 nT; grid size 40 x 40 m	99
Figure 10.4	Magnetogram of the site PP01-49 “San Ignacio” located on Pampa de San Ignacio; south of Palpa; measurement in the Gradiometer Mode with dynamics approx. +/- 18 nT; SMARTMAG SM4G-Special in twin sensor configuration; sampling density 100 x 12,5 cm, interpolated to 25 x 25 cm, resolution increased by ‘Graduated Shade’ function; Earth’s magnetic field ca. 25000 nT; grid size 40 x 40 m	99
Figure 10.5	Interpretation of linear structures (red, green and black) on site PP01-49 “San Ignacio” plotted on the Gradiometer Mode magnetogram; SMARTMAG SM4G-Special in duo-sensor configuration; dynamics approx. +/- 18 nT in 99 greyscale values from black to white (with transparency factor 50%), sampling density 100 x 12,5 cm, interpolated to 25 x 25 cm, resolution increased by ‘Graduated Shade’ function; Earth’s magnetic field ca. 25000 nT; grid size 40 x 40 m	100
Figure 10.6	Interpretation of linear structures (red, green and black) on site PP01-49 “San Ignacio” plotted on the Gradiometer Mode magnetogram; SMARTMAG SM4G-Special in duo-sensor configuration; dynamics approx. +/- 18 nT in 99 greyscale values from black to white (with transparency factor 50%), sampling density 100 x 12,5 cm, interpolated to 25 x 25 cm, resolution increased by ‘Graduated Shade’ function; Earth’s magnetic field ca. 25000 nT; grid size 40 x 40 m	100
Figure 10.7	Interpretation of the geoglyph complex on site PP01-49 “San Ignacio” located on Pampa de San Ignacio, south of Palpa; red and green lines represent ancient linear structures found by geophysical prospecting combined with aerial photography; grid size 40 x 40 m; numbers ① - ⑩ correspond to the documented set of lines (see description in text)	101
Figure 10.8	Interpretation of the geoglyph complex on site PP01-49 “San Ignacio” located on Pampa de San Ignacio, south of Palpa; red and black lines represent ancient linear structures found by geophysical prospecting combined with aerial photography; grid size 40 x 40 m; numbers ① - ⑩ correspond to the documented set of lines (see description in text)	101

List of tables

Table 2.1	Chronology and the cultural history of the Nasca basin (dates based on preliminary results of the Nasca – Palpa Project); after Lambers (2006)	7
Table 3.1	The geoglyph nomenclature within the area of research	13

Acknowledgements

First and foremost I would like to thank Dr. Jörg Fassbinder, who guided me throughout the whole work on the thesis and all over these years of my employment at the Bavarian State Department of Monuments and Sites (BLfD). Thank you for the precious suggestions to my work, fruitful advice and useful discussions. Many thanks for giving me the chance to join the Nasca/Palpa project and for showing me the exciting and humorous approach to the field of geophysical prospection and the whole science in general. Thanks for always being ready to help me solve all those bureaucratic problems with “some troublemaking” institutions and for having me in the field here in Bavaria and in all those places worldwide.

I am also very grateful to Prof. Dr. Valerian Bachtadse for making the cooperation between BLfD and the Institute of Geophysics, LMU Munich possible, for the supervision, support and the most valuable comments on the original text. I would also like to express my sincere gratitude to Prof. Dr. Heinrich C. Soffel for the patronage and for the careful revision of the final manuscript.

I am especially thankful to prof. zw. dr hab. Wojciech Stankowski from the Institute of Geology, Adam Mickiewicz University of Poznań, for the engagement, direction and the enormous support during the first stage of the work.

I thank Dr. Karsten Lambers from the University of Konstanz (former KAAK Bonn and IGP ETH Zurich) for providing the most valuable comparative material in the form of high resolution orthoimages and for corrections of the archaeological part of the thesis.

Thanks to my dear colleagues and co-workers at BLfD (especially J. Fassbinder, K. Berghausen, J. Lichtenauer, T. Deller and R. Linck) for the fruitful cooperation both during the numerous field trips and in the office, for the pleasant and amusing atmosphere at work and for the priceless influence on the constant improvement of my German.

Thanks all my friends and colleagues I got to know in Munich, from the university and outside, not mentioned by names but not forgotten. Without you my stay here would be dull and samey. Thanks for bringing colours to my everyday life.

Thanks to all the good people that helped me carry on when I came to Munich. It would be a great deal harder for the guy with the hard-gained visa valid for 3 months, with no job perspectives and no knowledge of German, to survive here for such a long time without an aid of the local hero. These are particularly to you Peter, for your unconditional help and the constant willingness to lend a hand.

I thank my family for their permanent and unlimited support. It's been mightily good to know I can come back anytime I want and always be most welcome.

Last but not least ... the most sincere thanks to Renata, for ups and downs we've been through here, emotions we've shared, hurdles we've got over ... together ...

... a najbardziej za Pszczółkę ... z całego serca ... Dziękuję.

Curriculum Vitae

TOMASZ GÓRKA

Born on 21.09.1979 in Krosno Odrzańskie, Poland
tomasz.gorka@geophysik.uni-muenchen.de

EDUCATION

V 2005 – X 2009

Ludwig Maximilian University, Munich, Germany
Department of Earth and Environmental Sciences
Institute of Geophysics

PhD position: Geophysics

X 1998 - VII 2003

Adam Mickiewicz University, Poznań, Poland
Faculty of Geographical and Geological Sciences
Institute of Geology

MSc diploma: Geology

WORK EXPERIENCE

I 2006 - present

Bavarian State Department of Monuments and Sites, Munich, Germany
(**Bayerisches Landesamt für Denkmalpflege**)

Geophysicist:

Acquisition, processing and interpretation of geophysical survey data acquired with magnetic, electric and ground penetrating radar techniques

VII 2004 - VII 2005

Ludwig Maximilian University, Munich, Germany
Institute of Mineralogy, Petrology and Geochemistry

Laboratory employee:

High temperature density measurements of silicate melts

XI 2003 - IV 2004

Ludwig Maximilian University, Munich, Germany
Institute of Crystallography and Applied Mineralogy

Laboratory employee:

Atomic Force Microscope measurements of mineral grains' surfaces in micro- and nanoscale